POLITECNICO
MILANO 1863

POLITECNICO DI MILANO

School of Civil, Environmental and Land Management Engineering

MASTER OF SCIENCE IN CIVIL ENGINEERING FOR RISK MITIGATION

THESIS TITLE:

Analysis of Pedestrian Flows in an Open Space

Supervisor: Prof. Lorenzo Mussone

Co-supervisor: Prof. Roberto Notari

Student: Waleed Ahmed Hikal

Person code : 10792169

Matricula : 245561

Academic Year: 2025/2026

Acknowledgement

I would like to express my sincere gratitude to Prof. Lorenzo Mussone, my supervisor, for his guidance, availability, and valuable feedback throughout the development of this thesis. His critical insights and methodological advice were fundamental in shaping the structure, scope, and scientific rigor of the work.

I am also grateful to Prof. Roberto Notari, my co-supervisor, for his support and constructive comments, which contributed to refining both the methodological approach and the interpretation of the results.

I would like to thank the academic and technical staff of Politecnico di Milano for providing a stimulating research environment and the resources necessary to carry out this study.

I also thank my colleagues and peers for the discussions and exchanges that supported the research process and helped improve several aspects of this work.

Finally, I would like to express my deepest appreciation to my family for their continuous encouragement, patience, and support throughout my academic journey.

Contents

List of figures

List of Tables

Abstract

Understanding pedestrian movement at an aggregate level is essential for the analysis, planning, and management of urban spaces and transport facilities. In many practical applications, interest lies not in individual walking behavior, but in macroscopic demand patterns describing how pedestrians move between spatial zones. Origin–Destination (OD) modeling provides a compact and interpretable framework for representing such demand, while deliberately abstracting away detailed trajectory geometry and interaction dynamics.

This thesis investigates macroscopic pedestrian OD modeling using empirical trajectory data extracted from video observations. An empirical OD benchmark is first constructed by spatially aggregating observed trajectory origins and destinations into a fixed set of zones. Two complementary OD modeling approaches are then developed and evaluated under consistent conditions: a stochastic Monte Carlo model that reproduces demand through probabilistic sampling, and a data-driven neural network model that predicts destination zones at the trip level based on origin information and geometric features. Both models are assessed using out-of-sample data and compared using macroscopic performance metrics applied to reconstructed OD matrices.

In addition to predictive OD modeling, the thesis presents a descriptive analysis of pedestrian trajectory geometry and temporal crowd context. Metrics such as trajectory linearity, concavity, and crowd count over time are computed post hoc to characterize intra-OD variability that OD matrices necessarily abstract away. These analyses are not used for prediction, but provide contextual insight into geometric and temporal characteristics of pedestrian movement.

The results demonstrate that both stochastic and data-driven approaches can robustly reproduce macroscopic pedestrian OD structures, with distinct strengths reflecting their underlying modeling philosophies. By combining transparent OD modeling with descriptive trajectory analysis, this work establishes a robust and interpretable foundation for macroscopic pedestrian demand estimation and supports future extensions toward geometry-aware and flow-dynamics–oriented pedestrian modeling.

1 Introduction

1.1 Background and Motivation

Pedestrian movement is a fundamental component of urban systems, transport facilities, and public spaces. Understanding how pedestrians move and how aggregate flows are distributed across space is essential for mobility planning, infrastructure design, safety assessment, and crowd management. In many applications, the primary interest lies not in individual walking behavior, but in macroscopic movement patterns at a system level.

Modeling pedestrian movement is inherently challenging due to variability in individual behavior, the influence of spatial layout, and the presence of local interactions. These factors give rise to complex collective dynamics that are difficult to represent deterministically, particularly in open environments where movement is not constrained by predefined paths.

Origin–Destination (OD) modeling provides a macroscopic abstraction of pedestrian demand by describing where pedestrians travel between spatial zones, while deliberately omitting the geometric details of individual paths. OD models offer a compact and interpretable representation of demand that is well suited for system-level analysis, especially in contexts where detailed behavioral assumptions or interaction modeling are difficult to justify.

At the same time, OD models necessarily abstract away trajectory geometry, local movement variability, and temporal context. While fully dynamic and interaction-based pedestrian models aim to capture these aspects, they typically require strong assumptions, extensive calibration, and high-resolution data, which may exceed the scope of a single study.

Recent advances in video-based sensing and data-driven modeling have created new opportunities for pedestrian flow analysis. Trajectory data extracted from real-world observations enable empirical OD estimation, while machine learning techniques provide flexible tools for learning demand patterns directly from data. These developments

motivate a systematic evaluation of different macroscopic OD modeling approaches under consistent empirical conditions.

The primary motivation of this thesis is therefore to establish and compare robust and interpretable methods for pedestrian OD modeling using both stochastic and data-driven techniques. Rather than attempting to predict full pedestrian flow dynamics, the focus is placed on constructing a transparent macroscopic OD modeling framework that can serve as a foundation for future extensions.

In addition, descriptive analysis of trajectory geometry and crowd presence is considered as a complementary perspective. While not used for prediction, these analyses provide insight into intra-OD variability and contextual characteristics of pedestrian movement, supporting longer-term research toward integrated flow-dynamics modeling.

1.1.1 Applications of Pedestrian Origin–Destination Modeling

Pedestrian Origin–Destination (OD) modeling is applied across a wide range of built environments to support planning, design, and operational decision-making. By representing pedestrian demand as aggregated flows between spatial zones, OD models provide a macroscopic description of movement patterns that is particularly suitable when detailed individual behavior is difficult to observe or unnecessary for the intended application.

In transport terminals and complex public facilities, pedestrian OD models are commonly used to quantify demand between entrances, platforms, concourses, and service areas. In such environments, pedestrian movement is influenced by spatial layout, signage, and time-dependent demand, while individual route choices may vary significantly. Macroscopic OD representations enable planners to identify dominant flow patterns, assess capacity utilization, and evaluate alternative spatial configurations without relying on detailed assumptions about individual decision-making. Although many studies in this domain focus on evacuation or emergency conditions, similar OD-based representations are also applicable under normal operating conditions, where demand estimation rather than behavioral realism is the primary objective.

In campus environments and large institutional settings, pedestrian OD modeling supports mobility planning and space management. University campuses, hospitals, and office complexes typically exhibit heterogeneous pedestrian flows generated by scheduled activities, distributed destinations, and mixed user groups. OD matrices allow these flows to be summarized in a compact form, facilitating comparisons across time periods or spatial configurations. When trajectory data are available, empirical OD estimation provides an evidence-based foundation for understanding how pedestrians utilize space at a system level, complementing traditional counting or survey-based approaches.

Event management and crowd monitoring constitute another important application domain. During planned events such as exhibitions, concerts, or sports gatherings, pedestrian demand is often highly directional and temporally concentrated. OD modeling enables the identification of dominant origin–destination pairs and the assessment of how demand redistributes over time. In these contexts, OD matrices support high-level operational decisions, such as access management and crowd dispersion strategies, without requiring full simulation of pedestrian interactions or route choices.

Pedestrian OD modeling is also relevant in safety-oriented analyses, particularly as a descriptive or preparatory tool. A large body of literature has investigated exit choice, wayfinding, and pre-evacuation behavior using experiments, virtual reality, and serious gaming approaches (e.g., Kobes et al., 2010; Fang et al., 2010; Heliövaara et al., 2012; Lovreglio et al., 2014, 2021). While these studies often aim to model behavioral responses under emergency conditions, they also highlight the importance of understanding aggregate movement patterns between functional zones. In this sense, OD modeling can serve as a macroscopic abstraction of pedestrian demand that complements more detailed behavioral analyses, without explicitly modeling evacuation dynamics or individual decision processes.

Recent advances in data-driven and machine learning approaches further expand the applicability of pedestrian OD modeling. Trajectory data extracted from video recordings or immersive virtual environments enable empirical estimation of OD demand under controlled or real-world conditions (Feng et al., 2021; Lin et al., 2019). Data-driven models, including supervised learning techniques, have been increasingly used to infer

movement patterns and decision outcomes from observed data (Zhao et al., 2020; Wang et al., 2019). In this context, OD matrices provide a natural macroscopic target representation that allows different modeling approaches to be compared consistently using aggregate performance metrics.

Across these application domains, a common characteristic is the need for robust, interpretable, and scalable representations of pedestrian demand. Pedestrian OD modeling satisfies this requirement by abstracting individual trajectories into a system-level description that is compatible with limited data availability and exploratory analysis. For these reasons, OD-based approaches remain a central component of pedestrian flow analysis and provide a suitable foundation for the modeling framework developed in this thesis.

1.2 Research Problem and Scope

The research problem addressed in this thesis concerns the estimation and reproduction of pedestrian Origin–Destination (OD) demand at a macroscopic level using empirical trajectory data. Specifically, the objective is to infer how pedestrians move between spatial zones within a given environment and to assess how accurately this demand structure can be reproduced using different modeling paradigms.

Pedestrian movement can be modeled at varying levels of detail, ranging from microscopic behavior-based simulations to macroscopic demand representations. While microscopic approaches aim to capture individual decision-making, local interactions, and dynamic flow evolution, they typically rely on strong behavioral assumptions, high-resolution data, and extensive calibration. Such requirements often limit their applicability in data-constrained or exploratory settings.

This thesis therefore focuses explicitly on macroscopic OD modeling, which aggregates individual trajectories into flows between predefined spatial zones. The central research question is formulated as follows: given a set of observed pedestrian trajectories, how robustly and accurately can the underlying OD demand structure be estimated and reproduced using stochastic and data-driven approaches?

The scope of this work is intentionally constrained. The proposed framework does not attempt to model pedestrian decision-making, route choice, local interactions, or density-dependent behavior. OD matrices are treated as static demand representations over the observation period, and dynamic flow evolution, congestion formation, and feedback mechanisms are not explicitly represented.

Trajectory geometry and crowd presence are analyzed only in a post hoc and descriptive manner. These analyses do not influence OD estimation or prediction, but instead provide contextual insight into intra-OD variability without extending the modeling framework beyond macroscopic demand representation.

By clearly defining these boundaries, the thesis establishes a focused and methodologically coherent problem setting. The results should therefore be interpreted as contributions to macroscopic pedestrian OD modeling rather than as comprehensive pedestrian flow or behavior prediction.

1.3 Research Objectives and Contributions

Within the scope defined above, this thesis pursues the following research objectives.

The first objective is to construct an empirical pedestrian OD representation from real-world trajectory data. By spatially aggregating trajectory origins and destinations into a fixed set of zones, a normalized OD matrix is derived to serve as a reference benchmark for demand estimation and model evaluation.

The second objective is to develop and evaluate a stochastic Monte Carlo OD modeling approach. This model reproduces pedestrian demand through probabilistic sampling from empirical OD frequencies, explicitly representing uncertainty and variability across realizations. Performance is assessed using out-of-sample data, repeated simulations, and bootstrap analysis.

The third objective is to implement a data-driven OD modeling approach based on a neural network. The network predicts destination zones at the trip level by conditioning on origin information and geometric features, and predicted destinations are aggregated to

reconstruct OD matrices. Performance is evaluated on held-out test data and compared directly with the Monte Carlo approach using consistent macroscopic evaluation metrics.

In addition, the thesis aims to provide a descriptive characterization of pedestrian trajectory geometry and temporal crowd context. Metrics such as trajectory linearity, concavity, and crowd count over time are computed independently of the OD models to quantify intra-OD variability that OD matrices necessarily abstract away.

The main contributions of this thesis are:

- An empirical benchmark for pedestrian OD demand derived from observed trajectory data.
- A stochastic Monte Carlo OD modeling framework serving as a transparent probabilistic baseline.
- A neural network–based OD modeling approach evaluated under consistent empirical conditions.
- A systematic comparison between stochastic and data-driven OD models using macroscopic performance metrics.
- A descriptive analysis of trajectory geometry and crowd context that complements OD-based demand modeling and supports future research directions.

Together, these contributions establish a robust and interpretable foundation for macroscopic pedestrian OD modeling, providing a clear basis for future extensions toward geometry-aware and flow-dynamics–oriented models.

1.3.1 Methodological Positioning

The methodology adopted in this thesis follows a data-driven yet macroscopic perspective on pedestrian movement. The work combines empirical observation, probabilistic modeling, and supervised learning within a unified analytical framework, while deliberately avoiding detailed behavioral or interaction-based modeling.

Rather than proposing a fully integrated pedestrian simulation model, the thesis emphasizes methodological transparency and empirical validation. Trajectory data extracted from real-world video recordings are treated as the primary source of information, from which macroscopic demand representations are derived and evaluated. This approach allows the analysis to remain closely grounded in observed data while maintaining a clear separation between measurement, modeling, and interpretation.

The modeling approaches considered in this study are intentionally modular. A stochastic Monte Carlo framework is employed as a probabilistic baseline that directly reflects empirical Origin–Destination (OD) demand distributions and explicitly represents uncertainty through repeated sampling. In parallel, a neural network–based model is developed as a data-driven alternative capable of learning non-linear relationships at the trip level. Both approaches are evaluated using consistent macroscopic performance metrics, enabling a direct and transparent comparison of their predictive behavior and limitations.

Descriptive analyses of trajectory geometry and crowd presence are included to contextualize macroscopic demand patterns but are not integrated into the predictive modeling process. This separation reflects a deliberate methodological choice aimed at preserving clarity of scope, avoiding overfitting, and ensuring that the results can be interpreted as contributions to macroscopic pedestrian OD modeling rather than to comprehensive flow-dynamics or behavioral prediction.

1.4 Thesis Structure

This thesis is structured to reflect a clear and coherent progression from problem formulation to modeling, results, and interpretation, consistent with the macroscopic perspective adopted for pedestrian Origin–Destination (OD) analysis.

Chapter 1 introduces the research background and motivation, defines the research problem and scope, and presents the objectives and contributions of the thesis. It establishes a macroscopic perspective on pedestrian movement based on Origin–Destination (OD) modeling and positions the work within the broader context of pedestrian flow analysis.

Chapter 2 reviews relevant literature on pedestrian flow modeling and OD estimation. The chapter discusses macroscopic OD approaches, stochastic simulation methods, and data-driven modeling techniques, with particular attention to their assumptions, scope, and applicability. It also reviews trajectory-based geometric analyses and walking-side behavior. This review situates the proposed framework within existing research and highlights gaps related to the joint use of empirical trajectory data for OD modeling and descriptive geometric analysis.

Chapter 3 describes the data acquisition and preprocessing procedures. It presents the video data source, the pedestrian detection and multi-object tracking pipeline, and the trajectory reconstruction process. The chapter details filtering, smoothing, temporal resampling, and trajectory merging steps, as well as the approximate conversion from image coordinates to metric space. The resulting trajectory dataset provides the empirical foundation for subsequent OD modeling and descriptive analyses.

Chapter 4 presents the methodological framework adopted in the thesis. It defines the representation of pedestrian trajectories and introduces geometric descriptors such as linearity, tortuosity, and concavity, including the alignment of concavity by walking direction. The chapter also describes the computation of crowd context indicators and statistical descriptors. Finally, it introduces the macroscopic OD modeling framework, including spatial clustering of origins and destinations, the Monte Carlo OD model, and the neural network–based OD model, together with their respective training, validation, and evaluation procedures.

Chapter 5 reports the results of the OD modeling and descriptive analyses. Results from the Monte Carlo and neural network models are presented and evaluated using consistent macroscopic performance metrics, followed by a comparative assessment of their behavior. Descriptive results on trajectory geometry, concavity, and crowd context are reported separately to provide contextual insight into intra-OD variability, without influencing predictive evaluation.

Chapter 6 discusses the results in relation to the research objectives and the broader context of pedestrian flow modeling. The chapter interprets the strengths and limitations of the

stochastic and data-driven OD models, examines the implications of trajectory geometry and crowd context, and reflects on methodological choices and limitations. Directions for future research toward geometry-aware and flow-dynamics–oriented modeling are also outlined.

Finally, Chapter 7 concludes the thesis by summarizing the main findings and contributions, highlighting their significance, and emphasizing the role of macroscopic OD modeling as a robust and extensible foundation for future pedestrian flow research.

2 Literature review

2.1 Introduction to Human Motion and Trajectory Analysis

Understanding pedestrian dynamics has become increasingly important in urban planning, architectural design, and safety engineering, particularly as cities grow denser and public spaces host larger and more diverse crowds. Pedestrian dynamics examine how individuals and groups move within open and bounded environments, identifying the physical constraints, social interactions, and behavioral factors that shape collective mobility patterns (Duives et al., 2021). Empirical studies conducted in transportation facilities and large railway stations have demonstrated how pedestrian route choice and movement behavior influence congestion formation and spatial performance (Daamen et al., 2003). Such work provides quantitative foundations for evaluating walking speeds, route selection behavior, and flow capacity in complex infrastructures.

A major application domain of pedestrian dynamics lies in safety engineering and evacuation modeling. For example, Helbing et al. (2002) developed simulation-based models of pedestrian crowds using the Social Force framework to analyze both normal circulation and emergency evacuation scenarios. Their work did not design specific evacuation procedures, but rather introduced a physics-inspired modeling tool capable of reproducing collective phenomena such as clogging at exits, panic-induced instabilities, and faster-is-slower effects. These simulation models provide designers and safety engineers with analytical tools to test evacuation configurations, assess bottleneck risks, and evaluate alternative layout strategies under controlled assumptions. Similarly, empirical evacuation studies have investigated exit choice behavior and pre-movement times to improve understanding of human response during emergencies (Heliövaara et al., 2012; Kobes et al., 2010).

Beyond emergency scenarios, pedestrian dynamics also contribute to accessibility and comfort evaluation. Research in wayfinding and spatial cognition has shown how environmental complexity, signage, and spatial configuration influence route selection and movement efficiency (Kuliga et al., 2019; Tzeng & Huang, 2009). These studies combine behavioral experiments and environmental analysis to examine how individuals interpret

and navigate built environments. Such findings inform architectural layout decisions and contribute to inclusive design strategies.

At the methodological level, pedestrian trajectory prediction represents a focused research direction concerned with forecasting short-term motion based on observed trajectory histories. A comprehensive survey by Rudenko et al. (2019) systematically reviews classical physics-based models, probabilistic methods, and modern deep learning approaches for trajectory prediction. Their work does not propose a new evacuation model, but rather provides a taxonomy and critical evaluation of prediction methods, highlighting limitations in long-horizon forecasting and generalization to complex scenes. The survey emphasizes that human motion is inherently multimodal and uncertain, making deterministic prediction insufficient in many real-world scenarios.

Historically, trajectory prediction evolved from analytical and rule-based formulations toward data-driven systems capable of learning from observed trajectories. For instance, Moussaïd et al. (2011) analyzed how simple local interaction rules between pedestrians can generate emergent collective patterns at the crowd level, demonstrating how microscopic behavioral assumptions scale to macroscopic crowd phenomena. More recently, deep learning–based approaches have leveraged recurrent neural networks, generative adversarial networks, and attention mechanisms to capture nonlinear interaction effects and multimodal future paths. Recent surveys categorize these models into classical analytical models, stochastic simulation approaches, and deep neural architectures, providing structured comparisons of their strengths and limitations (Korbmacher et al., 2023).

These findings indicate that trajectory-level modeling is particularly effective for short-term forecasting and interaction analysis in structured environments. However, for large-scale planning and system-level evaluation—especially in open or semi-open spaces—macroscopic representations such as aggregated flow models and Origin–Destination (OD) matrices provide complementary advantages by abstracting individual variability while preserving overall movement structure.

Understanding the contributions and limitations of each modeling family is therefore critical for selecting appropriate tools in urban design applications.

2.2 Pedestrian Behavior in Open and Bounded Spaces

Understanding how pedestrians behave within different spatial configurations is fundamental for modeling crowd movement, designing circulation systems, and developing accurate prediction and simulation tools (Hoogendoorn & Bovy, 2004). Open environments support high variability in route choice and self-organization, whereas confined spaces impose restrictions that increase interaction intensity and magnify the effects of density (Helbing et al., 2002). These differences become even more pronounced during emergencies, where urgency and stress alter movement strategies and risk accumulation.

2.2.1 Spatial Typologies: Open vs. Bounded Spaces

Pedestrian environments are commonly classified into open and bounded spaces, a distinction that fundamentally shapes movement dynamics (Hoogendoorn & Bovy, 2004). Open spaces—such as plazas, squares, parks, and wide sidewalks—are characterized by limited geometric constraints, allowing pedestrians substantial freedom in selecting direction and speed based on visibility, preference, and destination intent. Movement in these environments is weakly channelized and spatially distributed.

In contrast, bounded environments—such as corridors, passageways, station platforms, stairwells, and enclosed facilities—impose geometric restrictions that constrain lateral maneuverability and channel movement along predefined directions. Confinement concentrates density within narrower spatial envelopes, increasing the sensitivity of flow performance to local interactions and geometric bottlenecks (Helbing et al., 2002). Consequently, queuing, speed reduction, and congestion formation become structurally more likely than in open settings.

This classification establishes a structural basis for analyzing how geometry regulates trajectory variability, interaction intensity, and flow stability. Open configurations permit greater spatial redistribution and higher trajectory diversity, whereas bounded geometries compress movement and amplify density-dependent feedback effects. These differences directly influence predictability and determine the suitability of microscopic versus aggregate modeling abstractions.

2.2.2 Behavior in Open Spaces

Open public spaces function as low-constraint environments in which pedestrian movement is governed primarily by visual perception, interpersonal interaction, and destination intent rather than strict geometric channeling (Hoogendoorn & Bovy, 2004). Because lateral movement is largely unrestricted, individuals retain a high degree of freedom in selecting direction, speed, and intermediate waypoints. This structural openness increases variability in trajectory geometry and amplifies the role of anticipatory collision avoidance and self-organization mechanisms.

Empirical and modeling studies have shown that even in unconstrained areas, pedestrians do not move randomly. Instead, local interaction rules—such as maintaining personal space and adjusting direction based on neighboring motion—generate emergent collective patterns. Moussaïd et al. (2011) demonstrated that simple interaction mechanisms can reproduce spontaneous lane formation and adaptive path selection in bidirectional flows, even in environments without fixed physical guidance. These findings indicate that ordered collective structures can arise from decentralized decision-making, without external coordination or imposed routing.

The absence of rigid boundaries in open spaces also increases trajectory multimodality. Multiple feasible paths typically connect any origin–destination pair, and small perturbations in local density or social grouping can redirect movement substantially. As a result, trajectory prediction in open environments is inherently more uncertain than in corridor-like settings, where geometry constrains motion. From a modeling perspective, this flexibility challenges deterministic routing assumptions and supports the use of probabilistic or aggregate representations when analyzing large-scale flows.

Open spaces further allow rapid redistribution of pedestrians in response to localized congestion. When density increases in one region, individuals can adjust direction and disperse laterally, preventing sustained bottleneck formation under moderate demand levels. This adaptive redistribution mechanism reduces the persistence of high-density clusters compared to confined geometries. However, during very high demand conditions, the same openness can produce complex crossing flows and multi-directional conflicts,

increasing the dimensionality of interaction effects and complicating microscopic prediction.

Recent developments in video-based tracking and trajectory extraction (Duives et al., 2021) have enabled high-resolution empirical observation of these adaptive behaviors, supporting quantitative analysis of dispersion patterns, lane emergence, and spatial utilization in open environments. These empirical advances reinforce the importance of distinguishing between geometrically constrained and unconstrained contexts when selecting appropriate modeling scales and abstractions.

2.2.3 Behavior in Bounded or Confined Spaces

Pedestrian behavior in bounded or confined environments—such as corridors, station platforms, stadium concourses, and enclosed facilities—is strongly shaped by geometric constraints that limit lateral freedom and channel movement along predefined directions. Unlike open spaces, where route flexibility is high, confined environments impose spatial boundaries that compress trajectories into narrow flow corridors. As a result, density increases more rapidly, and interaction effects become dominant determinants of system performance (Hoogendoorn & Bovy, 2004).

In these settings, walking speed and flow stability are highly sensitive to corridor width, obstacle placement, and exit geometry. Even minor geometric irregularities—such as columns or partial obstructions—can alter local density distributions and induce asymmetric flow patterns. Empirical and simulation-based research has shown that under increasing density, confined flows transition from free movement to coordinated lane formation and eventually to unstable regimes characterized by stop-and-go waves and oscillatory motion (Helbing et al., 2002). These phenomena emerge from local interaction forces and anticipation dynamics rather than centralized coordination.

Because lateral redistribution is restricted, congestion in bounded spaces tends to accumulate near bottlenecks such as doorways, staircases, and narrow passages. At these locations, competitive interactions intensify and throughput becomes limited by geometric capacity rather than behavioral preference. Helbing et al. (2002), through simulation studies using force-based modeling, demonstrated that high-density conditions at exits can

generate arching structures, intermittent clogging, and the “faster-is-slower” effect, where increased desired speed paradoxically reduces evacuation efficiency. These findings highlight that bounded geometries amplify nonlinear interaction effects and can destabilize otherwise orderly flows.

Behavioral heterogeneity further complicates confined environments. Group cohesion, social spacing preferences, and differential walking speeds interact with spatial constraints, influencing both microscopic coordination and macroscopic throughput. In high-density regimes, voluntary control may partially give way to physical crowd pressure, producing collective dynamics that resemble compressible flow systems. This transition underscores the need for modeling approaches capable of capturing strong interaction coupling and density-dependent feedback mechanisms.

From a modeling standpoint, confined spaces are particularly suitable for microscopic or agent-based formulations, where collision avoidance, anisotropic perception, and local coordination rules can be explicitly represented. However, as spatial scale increases, aggregate flow representations may become more computationally efficient while still capturing capacity limitations and congestion propagation. The pronounced sensitivity of bounded environments to geometry and density thus makes them critical test cases for validating pedestrian models and evaluating evacuation performance.

2.2.4 Semi-Bounded and Mixed-Use Pedestrian Environments

Many real-world pedestrian environments cannot be strictly categorized as fully open or fully bounded. Semi-bounded or mixed-use spaces—such as university campuses, transit concourses, atriums, shopping galleries, and institutional courtyards—combine areas of geometric freedom with localized spatial constraints. These hybrid environments generate heterogeneous movement regimes within the same spatial domain.

In semi-bounded contexts, pedestrians typically alternate between free-flow movement in open zones and channelized behavior when approaching entrances, corridors, staircases, or service facilities. This transition creates spatially non-uniform interaction intensities:

density and coordination effects remain moderate in open regions but increase sharply near access points and functional bottlenecks. The resulting flow structure is therefore piecewise, characterized by locally constrained subspaces embedded within globally flexible circulation areas.

Visibility, spatial legibility, and environmental cognition play a decisive role in such environments. Studies in wayfinding and spatial cognition (Kuliga et al., 2019; Tzeng & Huang, 2009) show that navigation performance depends strongly on environmental clarity, landmark visibility, and decision-point structure. In semi-bounded spaces, route selection is influenced not only by geometric shortest paths but also by perceived accessibility, familiarity, and visual guidance cues. This introduces additional variability beyond purely physical interaction effects.

From a modeling perspective, semi-bounded environments present a structural challenge. Purely microscopic models must account for abrupt transitions between low-density dispersion and high-density coordination, increasing calibration complexity. Conversely, purely macroscopic continuum models may smooth out localized congestion effects near entrances and vertical circulation elements. As highlighted in the state-of-the-art review by Duives et al. (2021), no single modeling paradigm captures all scales of behavior equally well in heterogeneous environments.

In this context, Origin–Destination (OD) modeling provides a pragmatic intermediate abstraction. By representing aggregate movement between functional zones rather than simulating continuous trajectories across the entire domain, OD frameworks preserve large-scale demand structure while remaining agnostic to fine-grained interaction details. Dynamic assignment approaches within network-based simulations (von Sivers et al., 2014) further demonstrate how aggregate demand can be distributed across spatial connections while incorporating congestion feedback. This abstraction is particularly suitable for campuses and large public facilities, where pedestrian flows are distributed across multiple destinations and interaction intensity varies spatially.

Semi-bounded environments therefore highlight the need for modeling approaches that balance geometric realism with computational scalability. They form a natural bridge

between microscopic interaction models and macroscopic demand representations, reinforcing the relevance of aggregate OD-based frameworks for large-scale pedestrian analysis.

2.2.5 Normal vs. Emergency Behavior Across Spatial Typologies

Under everyday conditions, pedestrian movement is typically smooth, cooperative, and adaptive. Individuals maintain personal space, avoid collisions through anticipatory adjustments, and follow visually clear, socially acceptable paths (Hoogendoorn & Bovy, 2004; Moussaïd et al., 2011). In emergencies, however, behavioral patterns change sharply: urgency, heightened stress, and risk perception trigger more abrupt, competitive, and less coordinated movements. In open spaces, emergency conditions may lead to rapid dispersal or strong herding behavior depending on the visibility of exits and clarity of environmental cues. In bounded or confined spaces, urgency produces more severe effects, including sudden density spikes, breakdowns of orderly queues, and pressure buildup near bottlenecks where limited geometry restricts escape options. At extreme densities, pedestrians can experience loss of voluntary control as physical forces dominate intentional movement, leading to dangerous turbulence and instability (Helbing et al., 2002).

2.3 Analytical and Mathematical Models of Pedestrian Flows

This section reviews the principal modeling paradigms used to represent pedestrian dynamics, emphasizing analytical formulations, discrete simulation approaches, probabilistic frameworks, and network-based methods (Hoogendoorn & Bovy, 2004). Each modeling family offers distinct advantages and limitations depending on the intended level of resolution, computational constraints, and behavioral complexity. Together, these formulations contribute to the theoretical foundation for the methodological framework developed in this thesis, which integrates OD matrices with Monte Carlo sampling to describe aggregate flow structures in open and bounded environments.

2.3.1 Analytical Modeling Foundations

Analytical and mathematical models constitute some of the earliest and most influential approaches to pedestrian dynamics (Hoogendoorn & Bovy, 2004; Helbing & Molnár,

1995). They aim to describe movement through formal mathematical relationships that capture how individuals react to goals, obstacles, and neighboring pedestrians. These models operate at either a microscopic or macroscopic scale. Microscopic analytical models describe individuals explicitly, focusing on their decision-making mechanisms and interactions. In contrast, macroscopic models treat the crowd as a continuous medium governed by variables such as density, speed, and flow.

The main strength of analytical models lies in their interpretability: because behavioral rules are explicitly formulated, the resulting dynamics are transparent and mathematically tractable. They also facilitate rigorous calibration and validation against empirical field measurements. At the same time, analytical models necessarily simplify complex human behaviors and may struggle in environments with heterogeneous populations or irregular spatial constraints. Nevertheless, they form a conceptual foundation for more advanced modeling paradigms, including agent-based, discrete, probabilistic, and data-driven approaches.

2.3.2 Social Force Model (SFM)

The Social Force Model (SFM) is one of the most influential microscopic frameworks for modeling pedestrian dynamics (Helbing & Molnár, 1995). The model conceptualizes pedestrian motion as the outcome of internal behavioral motivations expressed mathematically in a form analogous to physical forces. These "social forces" are not mechanical forces in the Newtonian sense, but rather represent psychological and behavioral tendencies that cause individuals to accelerate, decelerate, or change direction in response to goals and surrounding stimuli.

Formally, pedestrian motion is described by:

$$\boldsymbol{m_i}\frac{\boldsymbol{dv_i}}{\boldsymbol{dt}} = \boldsymbol{m_i}\frac{\boldsymbol{v_i^0 - v_i}}{\boldsymbol{\tau}} + \sum_{\boldsymbol{j}} \boldsymbol{f_{ij}} + \sum_{\boldsymbol{W}} \boldsymbol{f_{iW}} \qquad \textit{Equation 2-1}$$

where $m_i$denotes the mass of pedestrian i, $\mathbf{v}_i$the current velocity, $\mathbf{v}_i^0$the desired velocity, and $\tau$the relaxation time representing how quickly the pedestrian adapts to the desired state. The terms $\mathbf{f}_{ij}$and $\mathbf{f}_{iW}$represent interaction effects with other pedestrians and with obstacles,

respectively. This formulation captures the assumption that pedestrians continuously regulate their motion toward a goal-oriented state while responding to nearby stimuli.

Each pedestrian is therefore modeled as a self-driven agent attempting to move in a desired direction at a preferred walking speed. Deviations from this intended state generate corrective acceleration over a characteristic relaxation time. This mechanism reflects adaptive regulation of movement in response to both internal intention and environmental context.

Interactions with other pedestrians are represented as distance-dependent repulsive effects that increase as interpersonal distance decreases. These interaction terms model personal space preservation and collision avoidance. The influence of another pedestrian decays with distance, ensuring that nearby individuals exert stronger effects than distant ones. Similar repulsive formulations account for interactions with fixed obstacles such as walls or barriers. Some model extensions introduce attractive components to represent movement toward points of interest or social companions, although the core model emphasizes repulsive dynamics.

A distinctive feature of the SFM is anisotropic perception. Pedestrians respond more strongly to stimuli within their primary field of view than to those located behind them. This directional weighting reflects empirical evidence that visual attention is not uniformly distributed. Interactions outside the main field of vision are attenuated but not ignored, enabling realistic modeling of reduced responsiveness to rearward intrusions.

To capture natural variability in human motion, a small stochastic component is incorporated. This term represents behavioral heterogeneity, perception errors, and spontaneous adjustments. Its inclusion prevents perfectly deterministic trajectories and improves realism, particularly in heterogeneous crowd conditions.

Despite being defined at the individual level, the SFM reproduces several empirically observed collective phenomena, including spontaneous lane formation in bidirectional streams, oscillatory flow at bottlenecks, and temporary directional dominance at narrow exits. In bidirectional flow, pedestrians self-organize into lanes aligned with walking direction once density exceeds a critical threshold, reducing friction between opposing

flows. At bottlenecks, alternating passing sequences emerge from competing interaction forces. These macroscopic patterns arise from simple local behavioral rules without centralized coordination.

Empirical calibration suggests desired walking speeds of approximately 1.3 m/s under low-density conditions (Helbing & Molnár, 1995), relaxation times around 0.5 seconds, and visual fields approaching 200 degrees. However, parameter values are context-dependent and vary across demographics, environments, and cultural settings. Later studies report lower average speeds in mixed-age or high-density scenarios, emphasizing the need for context-specific calibration.

A key limitation of the SFM is its sensitivity to parameter selection. Small variations in interaction strength, relaxation time, or perception weighting can significantly affect system stability and emergent behavior. Under extreme densities, improper calibration may lead to unrealistic accelerations or numerical instability (Helbing et al., 2002). Furthermore, while the model captures reactive local interactions effectively, it does not explicitly represent higher-level cognitive processes such as route planning or strategic decision-making.

Although the Social Force Model provides a powerful microscopic description of pedestrian interaction mechanics, its detailed agent-level formulation makes it computationally intensive for large-scale applications and heavily dependent on fine-grained calibration data. Moreover, it models how pedestrians move locally but does not directly address aggregate travel demand or origin–destination structure. For these reasons, while the SFM serves as an important theoretical reference in pedestrian dynamics, it operates at a different level of abstraction from the macroscopic demand modeling framework developed in this thesis.

2.3.3 Cellular Automata (CA) Models

Cellular Automata (CA) models represent pedestrian movement in a fully discrete framework (Burstedde et al., 2001; Blue & Adler, 2001), where both space and time are discretized. The walking domain is modeled as a two-dimensional lattice composed of cells, each of which may be either empty or occupied by at most one pedestrian. A typical

cell dimension of approximately $0.4 \times 0.4\ \mathrm{m}^2$ corresponds to the minimum personal space in high-density conditions, while the time step $\Delta t \approx 0.3$ s reflects an empirical free-flow walking speed of approximately 1.3 m/s . Under this discretization, pedestrians are restricted to move to one of the neighboring cells per time step, imposing a maximum velocity constraint of one cell per update. This simplification enables computationally efficient synchronous updates across the lattice.

Movement decisions are governed by local transition probabilities. For each pedestrian j, the possible moves are encoded in a 3×3 preference matrix $M^{(j)} = [M_{ik}]$, where the indices $(i, k) \in \{-1,0,1\} \times \{-1,0,1\}$ represent relative displacements to neighboring cells. The central element $(0, 0)$ corresponds to the probability of remaining stationary. These preference weights define directional tendencies before environmental and interaction effects are incorporated.

In the floor-field formulation introduced by Burstedde et al. (2001), local transition probabilities are influenced by two scalar fields defined over the lattice: a static floor field S, which encodes invariant environmental features such as exits or walls, and a dynamic floor field D, which evolves over time according to pedestrian movement. The probability of moving from cell x to a neighboring cell in direction (i, k) is given by

$$p_{ik} = N\, M_{ik}\, D_{ik}\, S_{ik}\, (1 - n_{ik}) \qquad \textit{Equation 2-2}$$

where n_{ik} indicates occupancy of the target cell (0 if empty, 1 if occupied), and N is a normalization constant ensuring that

$$\sum_{i,k} \boldsymbol{p_{ik}} = \mathbf{1}. \qquad \textit{Equation 2-3}$$

This multiplicative structure ensures that movement decisions depend simultaneously on intrinsic direction preference, environmental attraction, and local occupancy constraints. The exclusion term $(1-n_{ik})$ enforces collision avoidance at the lattice level.

The dynamic floor field evolves according to a discrete diffusion–decay process:

$$\boldsymbol{D(x,t+1) = (1-\delta)D(x,t) + \alpha \sum_{y \in \mathcal{N}(x)} [D(y,t) - D(x,t)] + \rho_{\text{deposit}}(x,t)}$$

Equation 2-4

where δ is a decay parameter, α is a diffusion coefficient, and ρ_{deposit} represents the increment deposited by pedestrians occupying cell $x$at time t. This formulation constitutes a lattice-based reaction–diffusion system (Burstedde et al., 2001). Pedestrians bias their movement toward cells with higher D values, producing an interaction mechanism analogous to chemotaxis

Despite the simplicity of its local rules, the CA framework reproduces several empirically observed collective phenomena. In bidirectional corridors, lane formation emerges spontaneously as pedestrians preferentially follow predecessors moving in the same direction. At bottlenecks, alternating passage patterns and clogging behavior arise from stochastic competition for limited cells. Evacuation times decrease with exit width but exhibit sublinear scaling due to increased clogging probability at narrow doors. Sensitivity to the dynamic floor field parameter can intensify herding effects, accelerating evacuation but also increasing the risk of congestion concentration at specific exits.

A principal strength of CA models lies in their computational efficiency and scalability. The discrete structure permits parallel updates and stable behavior at very high densities, where continuous force-based models may require small integration steps or encounter numerical instability. The lattice formulation also guarantees collision-free motion through the exclusion rule.

However, the discretization of space introduces structural artifacts. Trajectories are constrained to grid directions, limiting smoothness and realism in low-density or open environments. Velocity is quantized, and fine-grained variations in speed or direction cannot be represented continuously. Moreover, although the floor-field mechanism captures collective effects such as herding, it does not explicitly model physical forces or cognitive decision processes. The realism of the model depends strongly on parameter selection for diffusion, decay, and preference weighting.

In contrast to the Social Force Model, which operates in continuous space and represents interactions through distance-dependent forces, the CA framework relies on stochastic local transition rules defined over a discrete lattice. Both approaches are microscopic in nature, but they differ fundamentally in mathematical structure and numerical behavior. While CA models are particularly well suited for evacuation and high-density simulations due to their stability and speed, they remain less appropriate for applications requiring geometrically precise trajectories or continuous kinematic realism.

2.3.4 Continuum and Fluid-Dynamic Models

Continuum or fluid-dynamic models describe pedestrian crowds at a macroscopic scale by treating them as a continuous compressible medium characterized by density and velocity fields. Instead of tracking individual pedestrians, these models represent collective motion through spatially distributed variables such as pedestrian density $\rho(x,t)$ and mean velocity $v(x,t)$. The density field satisfies $0 \leq \rho(x,t) \leq \rho_{\max}$, where $\rho_{\max}$ denotes the jam density corresponding to maximum packing conditions. This formulation is conceptually analogous to fluid mechanics, where conservation principles govern the evolution of mass; in the present context, this corresponds to conservation of pedestrian number (mass in the continuum sense).

Early macroscopic formulations treated pedestrian crowds as compressible continua governed by conservation principles (Helbing, 1992; Duives et al., 2021). A more comprehensive continuum framework was later developed by Hughes (2002), who formulated pedestrian motion as a density-driven flow coupled with route-choice potentials. In this formulation, pedestrians move along gradients of a potential field representing the locally optimal path to exits, thereby coupling conservation laws with a dynamic route-choice mechanism that depends on crowd density.

The fundamental equation underlying continuum crowd models is the conservation law expressed through the continuity equation:

$$\frac{\partial \boldsymbol{\rho}}{\partial \boldsymbol{t}} + \boldsymbol{\nabla} \cdot (\boldsymbol{\rho v}) = \mathbf{0} \qquad \textit{Equation 2-5}$$

This equation ensures that pedestrian number is neither created nor destroyed, and that changes in local density are governed by the divergence of the flow field. It provides the core macroscopic constraint linking density and velocity dynamics.

To close the system, a constitutive relationship is required to determine pedestrian velocity as a function of density and environmental influences. In first-order models, velocity is typically derived from an empirical fundamental diagram relating speed to density (Hoogendoorn & Bovy, 2004), such as:

$$\boldsymbol{v} = \boldsymbol{V}(\boldsymbol{\rho})\, \boldsymbol{e} \qquad \textit{Equation 2-6}$$

where $V(\rho)$ represents a density-dependent speed function satisfying $V(0) = V_{\text{free}}$ and $V(\rho_{\max}) = 0$, and $e = e(x,t)$ denotes the desired walking direction, which may vary spatially and temporally depending on environmental geometry and destination choice. As density increases, walking speed decreases, capturing congestion effects observed in empirical studies.

More advanced second-order formulations introduce a momentum balance equation analogous in structure to compressible Navier–Stokes dynamics:

$$\frac{\partial(\boldsymbol{\rho v})}{\partial \boldsymbol{t}} + \boldsymbol{\nabla} \cdot (\boldsymbol{\rho v} \otimes \boldsymbol{v}) = -\boldsymbol{\nabla P}(\boldsymbol{\rho}) + \boldsymbol{\mu \nabla^2 v} + \boldsymbol{F_{ext}} \qquad \textit{Equation 2-7}$$

Here, $P(\rho)$represents a density-dependent pressure term modeling behavioral repulsive effects arising at high crowd densities rather than thermodynamic pressure; typically $P'(\rho) > 0$ensures increasing resistance with density. The parameter $\mu$is a viscosity-like coefficient that introduces internal momentum diffusion and numerical regularization, rather than representing physical fluid viscosity. The term F_{ext}represents environmental driving forces or desired-direction fields. In some formulations, additional relaxation terms toward a desired velocity are included; the present form focuses on density-driven interactions.

This formulation allows the model to capture macroscopic wave propagation phenomena and, under appropriate parameter regimes, reproduce stop-and-go behavior and transitions between free-flow and congested states.

One of the primary strengths of continuum models is computational efficiency at large spatial scales. Because they operate on aggregate fields rather than individual agents, they are well suited for simulating large transport hubs, stadiums, or evacuation scenarios involving thousands of pedestrians. They naturally capture macroscopic phenomena such as density waves, congestion buildup, and global capacity limits. Moreover, their mathematical structure allows analytical investigation of stability conditions and wave propagation characteristics.

However, the macroscopic abstraction comes at the cost of individual-level realism. Continuum models cannot explicitly represent discrete decision-making, local collision avoidance, or heterogeneous behavioral differences. Fine-scale phenomena such as small-group coordination, overtaking maneuvers, or detailed interpersonal spacing cannot be resolved. Additionally, the assumption of a continuous density field may become less valid in low-density environments where pedestrian motion is sparse and discrete.

For this reason, continuum models are often embedded within hybrid frameworks, where macroscopic formulations describe large-scale flow while microscopic models are applied in localized high-interaction regions. In contrast to Social Force Model and Cellular Automata approaches, which resolve individual trajectories explicitly, continuum formulations operate at a higher level of abstraction focused on aggregate density evolution. They are therefore conceptually closer to the macroscopic Origin–Destination modeling perspective adopted in this thesis, although they emphasize dynamic flow evolution rather than static demand representation.

2.3.5 Network-Based and Graph Models

Network-based pedestrian models represent the walking environment as a directed or undirected graph $G = (V, E)$, where nodes V correspond to spatial zones, intersections, entrances, exits, or decision points, and edges E represent feasible pedestrian connections between these locations (von Sivers et al., 2014). Such graph-based abstractions are widely used in pedestrian simulation and route-choice modeling to represent structured environments such as railway stations and multi-level buildings (Daamen et al., 2003; Hoogendoorn & Bovy, 2004). Unlike microscopic models that track continuous

trajectories, network formulations abstract movement into discrete path choices along graph edges.

Each edge $e \in E$ is assigned a generalized cost function C_e, which may depend on geometric length, travel time, slope, congestion level, or perceived effort (Hoogendoorn & Bovy, 2004). In its simplest static form, route choice is formulated as a shortest-path problem:

$$\min_{p \in \mathcal{P}_{od}} \sum_{e \in p} C_e \qquad \textit{Equation 2-8}$$

where P_{od} denotes the set of feasible paths between origin o and destination d. This deterministic formulation corresponds to classical shortest-path assignment and has been applied in passenger route-choice studies in large railway stations (Daamen et al., 2003).

More realistic formulations incorporate stochastic route choice, often expressed through discrete choice theory. In this case, the probability that a pedestrian selects path p between origin o and destination d may be represented using a logit model:

$$P_{od}(p) = \frac{exp\,(-\theta C_p)}{\sum_{q \in \mathcal{P}_{od}} exp\,(-\theta C_q)} \qquad \textit{Equation 2-9}$$

where C_p is the total generalized cost of path p, and θ is a sensitivity parameter governing the degree of rationality or dispersion in decision-making. This probabilistic formulation follows the random utility framework widely used in transportation science (Ben-Akiva & Bierlaire, 2006) and has been applied to pedestrian exit and route choice modeling in evacuation contexts (Lovreglio et al., 2014; Feng et al., 2021).

Dynamic network models extend this framework by allowing edge costs to depend on time and density:

$$C_e(t) = L_e / V(\rho_e(t)) \qquad \textit{Equation 2-10}$$

where L_e is edge length and $V(\rho_e(t))$ is a density-dependent speed derived from empirical pedestrian flow relationships (Hoogendoorn & Bovy, 2004; Duives et al., 2021). This

coupling introduces feedback between flow and travel time, enabling congestion-sensitive routing and dynamic assignment (von Sivers et al., 2014).

From a demand perspective, Origin–Destination (OD) matrices provide aggregate trip volumes T_{od}, which are assigned to the network through either path-based or link-based assignment procedures (von Sivers et al., 2014; Nishino et al., 2015). The resulting link flows must satisfy flow conservation constraints at each node:

$$\sum_{e \in \delta^-(v)} \boldsymbol{f_e} = \sum_{e \in \delta^+(v)} \boldsymbol{f_e} \qquad \textit{Equation 2-11}$$

where $\delta^-(v)$and $\delta^+(v)$denote incoming and outgoing edges at node v. Such assignment mechanisms are particularly relevant in structured facilities such as train stations, where OD demand is inferred and distributed across predefined pedestrian corridors (Daamen et al., 2003; Nishino et al., 2015).

One of the primary strengths of network-based models lies in their scalability and computational efficiency. Because pedestrians are not simulated individually in continuous space, large facilities such as railway stations, campuses, or event venues can be analyzed with modest computational resources (Duives et al., 2021). These models are particularly well suited for strategic planning, accessibility studies, and scenario testing.

However, the abstraction inherent in graph representations introduces limitations. Continuous spatial variability is discretized into predefined nodes and edges, potentially oversimplifying open areas where pedestrians do not follow clearly defined corridors (Hoogendoorn & Bovy, 2004). Local interaction phenomena, such as collision avoidance and lane formation, are not resolved explicitly but instead approximated through aggregate impedance functions or capacity constraints (Duives et al., 2021). Consequently, network models are best interpreted as mesoscopic or macroscopic representations of movement rather than detailed behavioral simulators.

Conceptually, network-based formulations form a bridge between microscopic pedestrian models and fully aggregate demand representations. They provide a natural framework for integrating OD matrices with flow assignment procedures (von Sivers et al., 2014; Nishino

et al., 2015), and therefore align closely with the macroscopic modeling philosophy adopted in this thesis.

2.3.6 Stochastic and Probabilistic Models (Monte Carlo Framework)

Stochastic and probabilistic models introduce randomness into pedestrian motion in order to represent behavioral variability and uncertainty in movement decisions. Unlike deterministic formulations—where pedestrian trajectories are uniquely determined by initial conditions and fixed rules—stochastic models acknowledge that real pedestrian behavior is inherently variable. Differences in perception, reaction time, walking speed, personal preferences, and local interpretation of space lead to non-identical outcomes even under similar environmental conditions (Robin et al., 2009; Duives et al., 2021).

In pedestrian dynamics, stochasticity is commonly incorporated through probabilistic decision rules governing speed adaptation, direction choice, or local interactions. Rather than prescribing a single trajectory, these models allow multiple plausible realizations of motion. Such variability becomes particularly important in high-density or evacuation scenarios, where small perturbations can significantly influence global flow organization. As shown in empirical and simulation studies (Helbing et al., 2002), stochastic fluctuations can trigger instabilities, stop-and-go waves, clogging at bottlenecks, and sudden transitions between stable and unstable flow regimes. Deterministic models may fail to reproduce these abrupt changes because they lack the perturbations necessary to initiate them.

Monte Carlo methods provide a systematic computational framework for implementing stochastic pedestrian modeling (Duives et al., 2021). The central idea of Monte Carlo simulation is repeated random sampling from predefined probability distributions that characterize uncertain parameters or behavioral choices. In the context of pedestrian dynamics, such distributions may describe walking speed variability, departure times, path selection tendencies, or response delays. By generating a large number of independent realizations under identical macroscopic conditions, Monte Carlo simulation produces a distribution of possible outcomes rather than a single deterministic result.

This repeated-sampling approach enables estimation of variability in aggregate performance indicators such as evacuation time, flow rate, or density distribution (Duives

et al., 2021). It also allows identification of extreme or rare scenarios that may not appear in a single deterministic run but are critical for safety analysis. Probabilistic route and exit choice modeling based on random utility theory further demonstrates how stochasticity can be integrated into pedestrian decision-making processes (Lovreglio et al., 2014).

A key advantage of probabilistic approaches is their flexibility: stochastic components can be integrated into microscopic models, mesoscopic network representations, or macroscopic flow models (Duives et al., 2021). When the focus is on trajectory-level realism, stochasticity typically affects local interactions. When the focus is on aggregate demand representation, randomness may instead govern origin–destination assignment, departure timing, or route selection at a higher level.

Despite their strengths, stochastic models depend on the specification of appropriate probability distributions. Poorly chosen distributions may introduce unrealistic variability or bias results. Moreover, Monte Carlo simulation can become computationally demanding when a large number of realizations is required to achieve statistical stability. Nevertheless, compared to high-resolution deep learning approaches, Monte Carlo–based stochastic frameworks remain computationally efficient and conceptually transparent, particularly when applied at a macroscopic level (Duives et al., 2021).

For these reasons, stochastic and Monte Carlo methods occupy an important position within pedestrian modeling research. They provide a principled way to represent uncertainty without abandoning interpretability. In the context of this thesis, Monte Carlo simulation is employed not to model microscopic interactions directly, but to reproduce aggregate Origin–Destination demand under probabilistic sampling, thereby linking stochastic variability with macroscopic flow representation.

2.4 Data-Driven and Deep Learning Approaches for Pedestrian Trajectory Prediction

2.4.1 Introduction to Data-Driven Trajectory Prediction

The rapid growth of large-scale pedestrian trajectory datasets has enabled a shift from classical analytical and rule-based modeling toward data-driven prediction. Traditional

models, including force-based formulations or cellular automata, offer interpretability but often struggle to generalize across diverse environments or capture subtle interpersonal cues. In contrast, data-driven approaches learn movement patterns directly from recorded trajectories, allowing them to represent collision-avoidance strategies, behavioral variability, and context-dependent decisions that are difficult to encode analytically. Deep learning, in particular, has expanded the capabilities of trajectory prediction by leveraging architectures such as recurrent neural networks (RNNs), convolutional neural networks (CNNs), graph neural networks (GNNs), and transformers to represent social interactions and environmental influences (Alahi et al., 2016; Rudenko et al., 2019). These models are designed to extract high-level features from complex urban scenes and to represent the multimodal nature of human mobility.

While these data-driven trajectory prediction models represent the state of the art at the individual-motion level, their complexity, data requirements, and focus on microscopic behavior place them outside the scope of the macroscopic OD-based demand modeling framework adopted in this thesis.

2.4.2 Deep Learning Architectures for Trajectory Prediction

Recurrent neural networks, especially Long Short-Term Memory (LSTM) models, were among the earliest deep learning methods applied to pedestrian forecasting (Alahi et al., 2016). Their ability to represent temporal dependencies made them naturally suited for sequential trajectory data. Extensions such as Social-LSTM introduced spatial pooling mechanisms to account for interactions between nearby pedestrians (Alahi et al., 2016).

Convolutional neural network (CNN)-based formulations were later explored to improve computational efficiency and exploit parallelizable convolutional operations for encoding temporal and spatial features, particularly in scene-aware and interaction-based settings (Rudenko et al., 2019; Korbmacher et al., 2023). Generative Adversarial Networks (GANs) further expanded the field by enabling multimodal trajectory generation through adversarial training objectives (Gupta et al., 2018). More recently, transformer-based architectures have become prominent due to their self-attention mechanisms, which allow

modeling of long-range temporal dependencies and complex interaction structures (Rudenko et al., 2019; Korbmacher et al., 2023).

Together, these architectures represent the major families of deep learning models used today:

- RNN/LSTM-based,
- CNN-based,
- GAN and variational models, and
- Transformer-based encoders and decoders.

Each class offers different strengths in modeling temporal dynamics, social interactions, context, and uncertainty.

2.4.3 Social Interaction Learning Models

A key advancement in deep learning–based pedestrian prediction is the explicit modeling of social interactions. The seminal Social-LSTM introduced a social pooling module that aggregates hidden states of neighboring agents, enabling each pedestrian's LSTM to encode local interactions (Alahi et al., 2016). Social-GAN later extended this idea using a GAN framework and proximity-aware pooling, improving flexibility in multi-agent environments (Gupta et al., 2018). These pooling approaches represent how pedestrians adjust motion based on nearby individuals, but remain limited in capturing long-range dependencies.

To address this limitation, attention mechanisms have been increasingly integrated into interaction models. Soft and hard attention schemes selectively weight the influence of neighboring pedestrians, enabling models to represent which agents are most relevant at each timestep (Rudenko et al., 2019). Beyond attention pooling, graph neural networks (GNNs) represent interactions explicitly through nodes and edges, enabling dynamic spatio-temporal reasoning (Rudenko et al., 2019). Overall, social interaction models aim to represent interpersonal dependencies that are difficult to encode explicitly in analytical formulations, though they may still underrepresent environmental context.

2.4.4 Scene-Aware and Context-Based Models

Although social interaction plays a critical role in shaping pedestrian motion, many deep learning models show degraded performance when environmental context is ignored (Rudenko et al., 2019). Real-world movement is strongly influenced by static and dynamic scene elements such as sidewalks, roads, crosswalks, obstacles, vegetation, and building geometry. Scene-aware approaches therefore incorporate semantic and spatial features derived from maps or imagery to constrain predictions to physically feasible walking areas (Rudenko et al., 2019; Korbmacher et al., 2023).

These approaches integrate scene information using semantic segmentation masks, attention mechanisms, or hybrid spatio-temporal representations that jointly encode agents and environment. Despite these developments, their applicability remains limited in large-scale or data-constrained simulation contexts due to high computational costs, dependence on specialized sensing setups, and limited transferability across environments (Rudenko et al., 2019).

2.4.5 Attention and Transformer-Based Models

Recent research has increasingly adopted attention-based and transformer-based architectures for pedestrian trajectory prediction (Rudenko et al., 2019; Korbmacher et al., 2023). Self-attention mechanisms allow models to compute relationships across entire sequences, supporting the representation of long-range temporal dependencies and complex interaction structures. Transformer variants have been adapted to capture spatial relationships, agent-to-agent interactions, and scene context through hybrid attention and graph-based formulations (Korbmacher et al., 2023).

These models are capable of modeling complex dependencies and producing diverse trajectory predictions, but they are computationally demanding and require large annotated datasets (Rudenko et al., 2019). Their complexity and data requirements limit their suitability for macroscopic modeling or large-scale simulation tasks where interpretability and scalability are central concerns.

2.4.6 Probabilistic Deep Learning and Generative Models

Pedestrian motion is inherently uncertain and multimodal, with multiple futures often plausible given the same observed history (Rudenko et al., 2019). Generative models are designed to address this by producing distributions of possible outcomes rather than single deterministic trajectories. Conditional Variational Autoencoders (CVAEs) and Generative Adversarial Networks (GANs) represent the dominant classes of generative approaches in trajectory prediction (Gupta et al., 2018; Rudenko et al., 2019).

CVAEs encode past motion into latent representations from which future trajectories are sampled, enabling explicit modeling of uncertainty through latent variables. GAN-based methods, such as Social-GAN, use adversarial training to encourage realistic and diverse predictions (Gupta et al., 2018). Together, these approaches model pedestrian behavior as non-deterministic and multimodal, but they introduce significant computational overhead and rely heavily on high-quality training data.

2.4.7 Limitations of Deep Learning Models

Despite substantial progress, deep learning methods face several limitations that restrict their applicability to large-scale simulation and planning tasks (Rudenko et al., 2019). They require extensive labeled datasets covering diverse environments, crowd densities, and spatial configurations; without such data, performance degrades sharply. Models trained in one environment often generalize poorly to new locations due to scene and behavioral differences. Many approaches also depend on high-resolution visual inputs or top-view camera arrangements that are not always feasible in practice.

Furthermore, deep models may violate physical or kinematic constraints, producing implausible trajectories when environmental structure or interaction rules are not explicitly enforced (Rudenko et al., 2019). Although generative models improve multimodal reasoning, evaluating predictive uncertainty and comparing multimodal outputs remain challenging problems. These limitations highlight the need for complementary modeling approaches—particularly in applications focused on macroscopic flow analysis, interpretability, and scalable simulation.

2.5 Origin–Destination (OD) Matrices and Monte Carlo Simulation in Pedestrian Modeling

2.5.1 Introduction

Modeling pedestrian flows at the macroscopic and mesoscopic scales requires tools that can describe aggregate travel demand without relying on dense trajectory datasets. Origin–Destination (OD) matrices serve this purpose by summarizing how many individuals travel from each origin zone to each destination zone during a given time period. In transportation systems—particularly train stations, transit hubs, and major public facilities—OD matrices form the foundation for understanding pedestrian demand, capacity usage, bottlenecks, and infrastructure performance (Nishino et al., 2015). Unlike individual trajectory data, OD matrices represent aggregate movement patterns, making them especially valuable in environments where comprehensive pedestrian tracking is unavailable or impractical. Because pedestrian flows are highly variable and influenced by external factors such as train arrivals, environmental structure, and temporal fluctuations, supplementary stochastic methods are required to capture behavioral uncertainty. For this reason, Monte Carlo simulation provides a natural complement to OD modeling, enabling repeated random sampling of pedestrian behaviors based on probabilistic assumptions about speed, route choice, and temporal variability (Duives et al., 2021). By integrating OD matrices with Monte Carlo sampling, this thesis develops a flexible framework to model pedestrian flows in both open and bounded spaces, capturing realistic variability without the computational overhead of deep learning models. This section therefore reviews the theoretical foundations of OD matrices and Monte Carlo sampling as applied in pedestrian modeling.

2.5.2 Defining Origin–Destination Matrices

An Origin–Destination matrix is a tabular representation that specifies the number of pedestrians traveling from each defined origin zone to each destination zone within a given period (von Sivers et al., 2014). These zones may represent entrances and exits, platforms, corridors, commercial areas, or functional regions within a facility. In contrast to vehicular OD matrices—where movement is constrained by roadway networks—pedestrian OD matrices inherently capture more flexible and continuous routing possibilities because

pedestrians are not restricted to fixed lanes. OD matrices can also be time-dependent, with separate matrices for peak hours, off-peak periods, or event conditions to reflect temporal variations in demand. For example, a train station may exhibit sharp increases in flows immediately after train arrivals or shortly before departures, requiring OD matrices with high temporal resolution (Duives et al., 2021). By reducing complex pedestrian behavior into a structured OD table, researchers and planners can efficiently simulate high-level flow patterns, evaluate system capacity, and test the impact of design or operational changes. This aggregation also facilitates computational tractability, making OD matrices a practical input for simulations where fine-grained trajectory data are unavailable.

2.5.3 Data Sources and OD Estimation Methods

Estimating pedestrian OD matrices in real-world environments poses significant challenges due to the free-flow nature of pedestrian movement and the difficulty of obtaining complete trajectory datasets (Duives et al., 2021). Unlike vehicular traffic, pedestrians do not move within fixed lanes and may change direction freely, complicating sensor placement and reducing detection accuracy. Additional challenges include occlusion, varying crowd densities, and the need to distinguish individuals travelling in groups.

To address these issues, OD estimation often relies on a combination of heterogeneous data sources. Manual observation remains a traditional method, though it is labor-intensive and prone to sampling bias. Automated approaches include camera-based tracking, WiFi and Bluetooth sniffers, LiDAR sensors, and smart-card entry/exit logs (Nishino et al., 2015). Ticketing and faregate data can reveal inflow and outflow patterns, while computer vision techniques can extract pedestrian trajectories when camera coverage exists.

Indirect estimation methods, such as gravity models, statistical inference, or entropy-maximization approaches, are used when only partial information is available (von Sivers et al., 2014). For example, link flow counts from corridor entrances or stairways can provide indirect signals of OD demand. Train timetable and ridership data are especially valuable in rail stations, where pedestrian demand oscillates sharply based on train arrivals and departures.

Spatial zoning plays a central role in OD definition, with zones designed to reflect entrance areas, platforms, corridors, and open spaces. However, each of these data sources introduces uncertainty—through missing paths, partial coverage, sampling errors, or aggregation—necessitating careful integration and calibration during OD estimation.

2.5.4 Use of OD Matrices in Pedestrian Simulation

OD matrices serve as the primary demand input for a wide range of pedestrian simulation models (Duives et al., 2021). In evacuation modeling, OD matrices specify how many people must move from hazard zones to safety areas, enabling planners to evaluate clearance times and identify congestion points. In large event planning, OD demand defines expected flows between entrances, amenities, and exits, supporting crowd management strategies. Transport hubs—such as railway stations and airports—use OD-based simulations to assess platform crowding, circulation efficiency, and transfer patterns (Nishino et al., 2015). In urban design and public-space planning, OD matrices underpin spatial flow analysis, helping determine whether walkways, corridors, or public squares have sufficient capacity.

Within simulation engines, OD matrices may integrate with either path-based assignment—where predefined routes are selected based on cost—or link-based assignment, where flows are distributed across network links according to equilibrium principles (von Sivers et al., 2014). Although pedestrians move in continuous two-dimensional space, constructing abstract graphs or potential fields allows OD-based routing to approximate realistic movement patterns. This makes OD matrices particularly suitable for macroscopic and mesoscopic modeling, where the primary objective is to capture overall flow structures rather than detailed agent-level interactions. Their simplicity, interpretability, and scalability make them essential tools for studying pedestrian systems at an aggregate level.

2.5.5 Monte Carlo Simulation in Pedestrian Modeling

Monte Carlo simulation is a probabilistic technique based on repeated random sampling from defined probability distributions. In the context of pedestrian modeling, Monte Carlo methods introduce variability that reflects natural human differences in walking speed,

route choice, reaction times, and social behavior (Duives et al., 2021). Randomness is fundamental to realistic pedestrian movement: individuals do not behave identically, even under similar conditions. For example, speed distributions vary by age, intent, and personal preference; route choices differ due to spatial awareness or local crowding; and micro-level interactions introduce stochastic fluctuations. Studies such as Helbing et al. (2002) and Robin et al. (2009) highlight how stochasticity influences crowd dynamics, especially under evacuation conditions or high-density scenarios. By repeatedly sampling pedestrian characteristics and movement decisions, Monte Carlo simulation generates multiple plausible outcomes from the same OD matrix. This allows researchers to study uncertainty, analyze risk, and understand variability in system performance—particularly in safety-critical contexts.

2.5.6 Integration of OD Matrices with Monte Carlo Simulation

Previous research has explored the integration of OD matrices with stochastic simulation techniques to represent uncertainty in pedestrian demand (Duives et al., 2021; von Sivers et al., 2014). In such approaches, the OD matrix specifies aggregate movement volumes between zones, while stochastic sampling is used to introduce variability in individual attributes and decision processes within the simulation environment.

Monte Carlo methods are typically applied by repeatedly sampling behavioral parameters—such as walking speed, departure time, and route choice—from predefined probability distributions (Duives et al., 2021). Through multiple realizations, these simulations generate distributions of system-level outcomes rather than single deterministic results. This enables evaluation of variability in evacuation times, density patterns, and congestion formation.

Stochastic OD-based simulation is particularly valuable in contexts where empirical OD estimates contain uncertainty or where demand fluctuates across time periods (von Sivers et al., 2014). By combining aggregate demand representation with probabilistic variability, such approaches provide a compromise between computational efficiency and behavioral realism in large-scale pedestrian modeling (Duives et al., 2021).

2.5.7 Advantages and Limitations

The OD–Monte Carlo framework offers several notable advantages for pedestrian modeling. Its structure is simple, interpretable, and scalable, enabling efficient simulations even in large open or bounded spaces. Because it operates at an aggregate level, the method does not require millions of trajectories or deep-learning-scale datasets, making it practical for environments where sensing is limited (Duives et al., 2021). Monte Carlo sampling effectively captures variability in human behavior, producing realistic distributions of outcomes. The approach aligns well with macroscopic and mesoscopic flow modeling and is computationally lightweight compared to agent-based or deep learning methods.

However, this methodology also has limitations. It cannot replicate detailed interaction dynamics, such as collision avoidance, group behaviors, or nuanced social cues, with the precision of modern deep learning models. The approach depends on assumed probability distributions for speed, timing, or path choices, making model accuracy sensitive to distribution selection. Furthermore, OD matrices do not capture individual-level heterogeneity unless supplemented by Monte Carlo sampling, and even then, the realism is constrained by the abstraction level. This makes the method less suitable for fine-grained robotics, autonomous navigation, or high-fidelity simulation tasks that require trajectory-level precision. Nonetheless, for large-scale flow analysis and design evaluation, OD–Monte Carlo remains a robust and efficient solution.

For these reasons, OD–Monte Carlo frameworks are particularly well suited for comparative modeling studies and exploratory analyses, where transparency, robustness, and scalability are prioritized over microscopic behavioral realism. By operating at an aggregate level, such frameworks enable consistent evaluation of different modeling paradigms under identical empirical conditions, facilitating direct comparison without confounding effects introduced by complex interaction modeling. This makes the OD–Monte Carlo approach especially appropriate for data-driven studies aimed at understanding demand structure and variability in real pedestrian environments.

2.6 Summary of Findings and Transition to Methodology

The literature reviewed in this chapter demonstrates the breadth and evolution of research on pedestrian dynamics, spanning behavioral observation, analytical modeling, probabilistic simulation, and modern data-driven approaches. Together, these bodies of work provide a comprehensive foundation for understanding how individuals move in open and bounded environments, how interactions and spatial constraints influence behavior, and how movement patterns vary under routine and emergency conditions.

Analytical and mathematical modeling frameworks introduced structured representations of pedestrian motion at different levels of granularity. Microscopic models capture interpersonal interactions and emergent phenomena, while macroscopic formulations describe aggregate crowd behavior through density and flow relationships. These approaches offer interpretability and theoretical clarity but are constrained by simplifying assumptions.

More recent data-driven methods have expanded trajectory-level modeling capabilities by learning directly from observational data. Deep learning architectures incorporating social interactions, scene context, and probabilistic reasoning have demonstrated strong performance at the individual-trajectory level in data-rich settings. However, these approaches remain computationally demanding, data-intensive, and limited in generalizability, reducing their suitability for large-scale or macroscopic applications.

Parallel to these developments, research on pedestrian flow modeling has emphasized the importance of aggregate demand representation through Origin–Destination (OD) matrices. OD matrices provide a compact and interpretable description of pedestrian demand but abstract away individual variability. Monte Carlo simulation has therefore been adopted as a complementary approach, introducing stochastic sampling to represent behavioral uncertainty and variability in flow outcomes.

Table 2-1 Comparison of Pedestrian Movement Modeling

Model Type	Core Representation	Key References	Main Features	Strengths	Limitations
Empirical / Fundamental Diagram Models	Data-driven relationships between density, speed, and flow	Daamen et al., 2003; Weidmann, 1993	Density–velocity and flow–density relationships derived from observations	Simple, interpretable, calibration-friendly	Descriptive only; no predictive spatial dynamics; no interaction modeling
Social Force Model (Microscopic, Continuous)	Individuals modeled as self-driven particles governed by interaction forces	Helbing & Molnár, 1995; Helbing et al., 2000	Goal-directed acceleration, repulsive pedestrian–pedestrian and pedestrian–obstacle forces, anisotropic perception	Captures lane formation, oscillations at bottlenecks, local avoidance; interpretable physics analogy	Parameter-sensitive; computationally expensive; limited cognitive modeling; unstable at extreme densities
Cellular Automata (Microscopic, Discrete)	Grid-based discrete lattice with probabilistic transition rules	Burstedde et al., 2001; Blue & Adler, 2001	Discrete time/space; local transition matrix; static and dynamic floor fields; synchronous updates	Computationally efficient; scalable; robust at high densities; good for evacuation modeling	Grid artifacts; limited trajectory smoothness; simplified movement kinematics
Continuum / Fluid-Dynamic Models (Macroscopic)	Density and velocity fields governed by conservation equations	Hoogendoorn & Bovy, 2004; Treiber & Kesting, 2013	PDE-based conservation laws; fundamental diagrams; pressure-like terms	Efficient for large-scale flows; analytical tractability; captures congestion waves	No individual behavior; no discrete interactions; limited at low densities
Network / Graph-Based Models	Nodes (zones) and edges (connections) with cost-based routing	von Sivers et al., 2014; Zheng et al., 2021	Route choice via cost minimization; capacity constraints; OD assignment	Scalable; integrates naturally with OD matrices; strategic planning tool	Ignores local interactions; path realism depends on network design
Stochastic / Monte Carlo OD Models	Aggregate OD demand with probabilistic sampling	Helbing et al., 2002; Duives et al., 2021	Random sampling of speeds, routes, departure times; scenario variability	Represents uncertainty; simple; interpretable; computationally light	No detailed interaction mechanics; depends on assumed distributions
Deep Learning / Data-Driven Trajectory Models	Neural networks predicting individual future trajectories	Alahi et al., 2016; Gupta et al., 2018; Rudenko et al., 2019	LSTM, GNN, GAN, Transformer architectures; social pooling; scene encoding	High predictive accuracy; models nonlinear dependencies; multimodal outputs	Data-intensive; low interpretability; poor transferability; computationally heavy

Table 2.1 synthesizes the principal pedestrian modeling paradigms discussed in this chapter, highlighting their scale of representation, mathematical structure, strengths, and limitations. The comparison reveals a structural trade-off between microscopic behavioral

realism and macroscopic scalability. Force-based and cellular automata models capture detailed interaction dynamics but require fine-grained calibration, while continuum and network formulations prioritize aggregate flow efficiency and computational tractability. Data-driven approaches achieve strong trajectory-level prediction performance but depend heavily on large training datasets and computational resources. In contrast, OD-based stochastic frameworks operate at a demand level of abstraction, emphasizing interpretability, robustness, and scalability for large-scale environments.

Overall, the comparison reveals a conceptual gap between high-fidelity trajectory prediction models and scalable macroscopic flow representations. While microscopic and deep learning approaches prioritize behavioral realism and trajectory precision, macroscopic and network-based models emphasize computational efficiency and aggregate flow structure.

This thesis addresses this gap by evaluating stochastic and neural-network-based OD models under a common empirical benchmark and by complementing OD analysis with descriptive trajectory geometry and crowd-context characterization. By focusing on macroscopic OD demand representation combined with probabilistic variability through Monte Carlo sampling, the present work positions itself between detailed microscopic interaction models and high-complexity data-driven prediction frameworks. The following chapter introduces the empirical data and methodological framework used to implement and evaluate this approach.

3 Data Acquisition and Preprocessing

3.1 Overview

This chapter describes the data source and preprocessing steps used to extract pedestrian trajectories from raw video recordings. The objective is to transform unstructured video data into clean, consistent trajectory representations suitable for subsequent analysis. No modeling or analysis results are presented in this chapter.

The preprocessing pipeline consists of four main stages: video acquisition, pedestrian detection, multi-object tracking, and trajectory reconstruction. The resulting trajectories form the empirical foundation for all analyses and models developed in the following chapters. Figure 3.1 summarizes the adopted data acquisition and preprocessing pipeline.

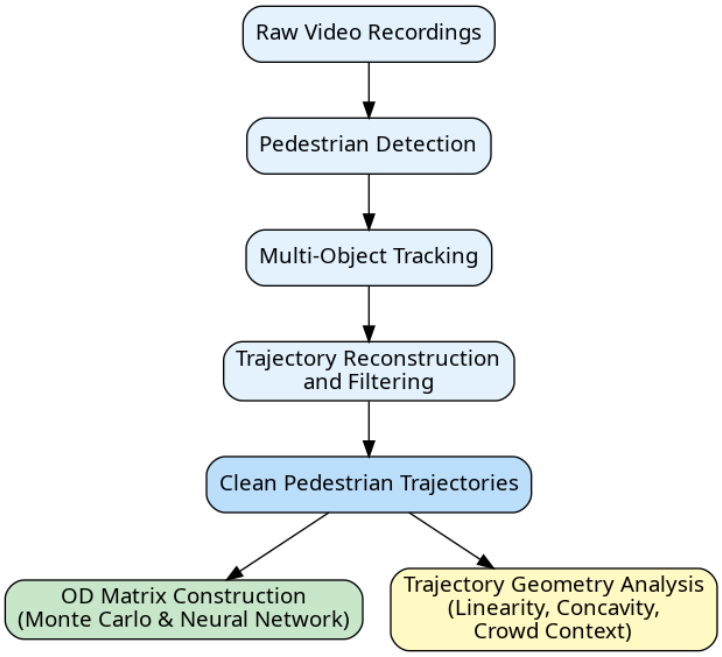

Figure 3-1 Data acquisition and preprocessing pipeline .

3.2 Video Data Description

The video dataset used in this study was recorded at the Leonardo Campus of Politecnico di Milano. A fixed, stationary camera was installed at an elevated position, providing a

wide field of view of an open pedestrian area with natural walking paths and unconstrained movement. The setup allows observation of pedestrian entry and exit behavior, crossing flows, and local interactions without enforcing predefined routes.

The recording was captured at a resolution of 478 × 850 pixels and a frame rate of 30 frames per second (fps). The camera remained static throughout the recording period, ensuring spatial consistency across frames. No identifiable personal information was collected; the analysis relies exclusively on anonymous bounding boxes and centroid positions extracted through automated processing. Figure 3.2 illustrates the camera field of view and provides a visual reference for the observed environment.

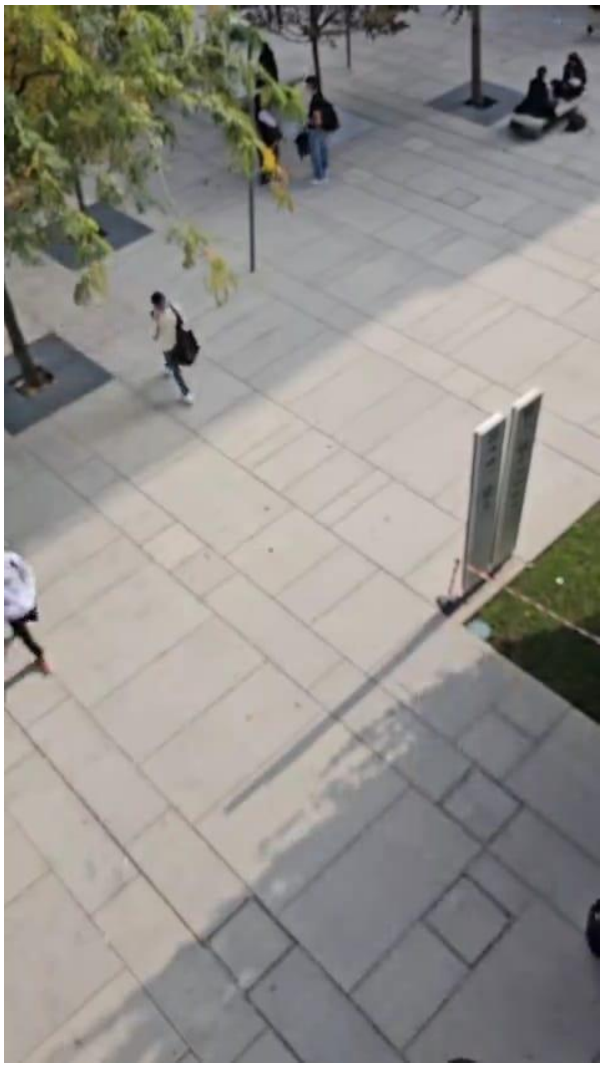

Figure 3-2 Camera setup and field of view of the observed pedestrian area.

3.3 Recording Conditions and Data Limitations

The video was recorded in October 2025 during the afternoon under clear, sunny conditions. The dataset consists of a single continuous recording lasting 6 minutes and 36 seconds (396 seconds). Since only one recording session was conducted, no averaging across multiple recordings is applicable.

Due to the oblique viewing geometry, perspective distortion is present, particularly for pedestrians located farther from the camera. As a result, apparent pedestrian size and displacement vary across the field of view, affecting the accuracy of geometric measurements derived from pixel coordinates.

Several practical limitations are inherent to the data collection setup. Temporary occlusions occur when pedestrians overlap in the camera view, particularly during crossing flows or when small groups form. Prolonged occlusions may lead to fragmented trajectories or identity switches, which are subsequently handled during trajectory filtering and merging.

Lighting-related effects also influence detection quality. Strong sunlight produces shadows that vary in shape and intensity over time. These shadows can occasionally interfere with pedestrian detection, leading to false positives or missed detections in localized regions of the scene. Confidence filtering and track validation procedures are therefore applied to ensure robustness of the extracted trajectories.

Trajectory coordinates are converted from pixel space to approximate metric units using a fixed pixel-to-meter scaling factor. This approach does not fully correct for perspective distortion and therefore limits the precision of absolute distance and speed measurements. The subsequent analysis therefore emphasizes relative and aggregate movement patterns rather than fine-grained kinematic accuracy.

Finally, the use of a single fixed camera restricts observation to a two-dimensional projection of pedestrian movement and does not capture vertical motion, head orientation, or gaze behavior. Despite these limitations, the dataset provides an empirically grounded representation of pedestrian movement suitable for trajectory-based analysis.

3.4 Video Preprocessing

To enable efficient and robust pedestrian detection and tracking, the raw video stream is preprocessed prior to analysis. The video is loaded frame-by-frame using MATLAB's VideoReader, allowing sequential access without loading the entire recording into memory.

To reduce computational load, frames may be downscaled using a fixed scaling factor while preserving spatial proportions. Detection is performed at regular frame intervals to balance accuracy and efficiency, while tracking is maintained at every frame to preserve temporal continuity. For long recordings, the video is processed in fixed-length segments to avoid memory saturation and ensure stable execution.

The original recording was acquired at 30 frames per second (fps), and pedestrian tracking is performed at the native frame rate to preserve motion continuity. For trajectory-level analysis, the tracked positions are subsequently resampled to a uniform temporal resolution of $\Delta t = 1$ second (one position per second). This resampling reduces high-frequency noise introduced by detection and tracking uncertainty while maintaining sufficient temporal detail for origin–destination identification and geometric trajectory analysis.

These preprocessing steps ensure a consistent and reproducible input stream for the detection and tracking stages.

3.5 Pedestrian Detection and Tracking

Pedestrian detection is performed using a deep-learning-based object detector (YOLOv4 or Tiny-YOLOv4, depending on computational availability). Detected bounding boxes are filtered using confidence thresholds and non-maximum suppression to eliminate false positives and overlapping detections.

Detected pedestrians are tracked across frames using a multi-object tracking framework based on a constant-velocity Kalman filter. Data association is handled through a Global Nearest Neighbor (GNN) strategy, ensuring that detections are consistently linked to the correct pedestrian identity over time. Track confirmation and deletion rules are applied to remove short-lived or unstable tracks.

Each pedestrian is assigned a unique identifier, and identity consistency is maintained across video segments by applying ID offsets at segment boundaries. The output of this stage consists of time-stamped pedestrian centroids with persistent track IDs.

3.6 Trajectory Reconstruction and Filtering

Pedestrian trajectories are reconstructed by grouping centroid positions belonging to the same tracked identity over time. Each trajectory represents the planar movement of a single pedestrian within the observed scene. Trajectories are smoothed using a moving-average filter.

Short or fragmented trajectories are filtered out to retain only meaningful pedestrian movements. Fragmented segments are merged when their temporal and spatial gaps fall below predefined thresholds, resulting in continuous and stable trajectories. Only trajectories containing a sufficient number of valid observations are retained for further analysis.

After reconstruction, trajectories have variable lengths because pedestrians enter and exit the camera field of view at different times and may stop or change speed. To exclude short-lived detections and unstable track fragments, a minimum threshold of four valid observations is enforced after temporal resampling ($\Delta t = 1$ s), corresponding to a minimum duration of approximately 4 seconds. Trajectories shorter than this threshold are often dominated by detection noise, brief edge appearances, or temporary tracking artifacts and typically provide insufficient displacement to reliably infer directionality or assign consistent origins and destinations. Therefore, the threshold is used as a practical quality-control criterion, while longer trajectories are retained with their full number of observations.

3.7 Trajectory Validation and Quality Control

The raw output of the pedestrian detection and tracking process includes trajectories of varying length and quality. These trajectories may contain noise, short-lived detections, or fragmented segments resulting from temporary occlusions, missed detections, or pedestrians entering and exiting the scene. To ensure the reliability of subsequent analyses,

a systematic trajectory validation and quality control procedure is applied prior to modeling.

A minimum trajectory duration threshold is enforced to exclude spurious or non-representative movements. Only trajectories containing at least four valid observations—corresponding to a minimum duration of approximately four seconds after temporal resampling—are retained. This criterion removes short detections that do not reflect meaningful pedestrian motion, such as brief appearances at the edge of the scene or transient false positives generated by the detector. By enforcing a minimum duration, the retained trajectories are more likely to represent intentional pedestrian movement with a clearly defined origin and destination.

Trajectory fragmentation is addressed through a merging procedure based on temporal and spatial continuity. When multiple trajectory segments exhibit small temporal gaps and limited spatial separation, they are merged and treated as a single pedestrian trajectory. This step reduces artificial fragmentation caused by brief occlusions or intermittent detection failures and improves the consistency of origin–destination identification. Trajectories that cannot be reliably merged or that remain highly fragmented after this process are excluded from further analysis.

To reduce high-frequency noise introduced by detection uncertainty and tracking jitter, trajectories are smoothed using a moving-average filter. This operation preserves the overall shape and direction of pedestrian motion while attenuating small-scale fluctuations that are not representative of true movement. Following smoothing, trajectories are temporally downsampled to one position per second, ensuring uniform temporal resolution across all pedestrians. This resampling facilitates consistent geometric analysis and simplifies comparison between trajectories with different original frame lengths.

Quality control also includes the removal of trajectories with missing or inconsistent time ordering, as well as those exhibiting implausible spatial jumps that exceed reasonable pedestrian displacement between consecutive observations. These checks further ensure that retained trajectories are physically plausible and suitable for geometric interpretation.

The combined application of minimum duration filtering, fragmentation handling, smoothing, and temporal normalization results in a curated trajectory dataset characterized by consistent temporal resolution, reduced noise, and stable identity assignment. This validated dataset provides a robust empirical foundation for both macroscopic Origin–Destination modeling and descriptive trajectory analysis presented in the subsequent chapters.

3.8 Coordinate Conversion and Representation

Trajectory coordinates are initially expressed in pixel space. To allow geometric interpretation and approximate distance computation, pixel coordinates are converted to an approximate world coordinate system using a fixed pixel-to-meter ratio. While full perspective correction is not applied, this conversion is sufficient to distinguish origins, destinations, and relative path geometry.

Each trajectory is represented as an ordered sequence of time-stamped planar coordinates:

$$\boldsymbol{T_i} = \{(\boldsymbol{t_1}, \boldsymbol{x_1}, \boldsymbol{y_1}), (\boldsymbol{t_2}, \boldsymbol{x_2}, \boldsymbol{y_2}), \dots, (\boldsymbol{t_N}, \boldsymbol{x_N}, \boldsymbol{y_N})\} \qquad \textit{Equation 3-1}$$

where $\boldsymbol{t_k}$denotes the discrete time index and $(\boldsymbol{x_k}, \boldsymbol{y_k})$the pedestrian's position at time $\boldsymbol{t_k}$.

The first and last valid points of each trajectory define its geometric origin and destination. These representations form the basis for OD matrix construction and trajectory-level geometric analysis in subsequent chapters.

3.9 Ethical and Privacy Considerations

The data collection and analysis conducted in this study were designed to comply with ethical standards and privacy protection principles applicable to observational research in public spaces. The video recordings were obtained in an open campus environment where pedestrian movement occurs in a public setting, without any form of interaction or intervention by the researchers.

All data processing was performed in a fully anonymized manner. No personally identifiable information was collected, stored, or analyzed at any stage of the workflow.

Pedestrians were represented exclusively through automatically detected bounding boxes and derived centroid positions, and each individual was assigned a numerical track identifier solely for the purpose of trajectory reconstruction. These identifiers have no association with real-world identities and are not preserved beyond the scope of the analysis.

The analysis does not involve facial recognition, biometric identification, or inference of sensitive personal attributes. Only aggregated trajectory information, geometric descriptors, and macroscopic flow representations are used in subsequent chapters. Individual trajectories are analyzed solely in terms of spatial and temporal movement patterns and are not examined at an individual or behavioral profiling level.

The resulting outputs—such as Origin–Destination matrices, statistical distributions of trajectory metrics, and aggregate flow indicators—are reported exclusively in aggregated form. This ensures that no individual pedestrian can be identified directly or indirectly from the published results. The study therefore aligns with the principles of data minimization and purpose limitation, as defined in applicable data protection frameworks.

By restricting the analysis to anonymized and aggregated data derived from observations in a public environment, this study ensures that ethical considerations and privacy protection are maintained throughout the research process, while still enabling meaningful analysis of pedestrian movement at a macroscopic level.

3.10 Reproducibility and Implementation Considerations

Reproducibility is a key requirement for empirical research and is particularly important in data-driven studies involving automated detection, tracking, and preprocessing pipelines. The procedures adopted in this study are designed to ensure that trajectory extraction and preprocessing can be reproduced consistently under the same experimental conditions.

All preprocessing steps—including video loading, frame sampling, pedestrian detection, tracking, trajectory reconstruction, filtering, and resampling—are applied using fixed and explicitly defined parameters. The use of deterministic algorithms for detection

thresholding, track confirmation and deletion, and trajectory filtering ensures that repeated executions of the preprocessing pipeline on the same video data yield consistent results. Where stochastic components are present in downstream modeling stages, they are explicitly controlled through fixed random seeds; however, the preprocessing pipeline itself remains deterministic.

To support stable execution and scalability, long video recordings are processed in fixed-length segments. Segment boundaries are handled carefully by applying track identifier offsets to preserve identity uniqueness across segments. This design prevents memory saturation while maintaining continuity and consistency in trajectory representation. Intermediate results, including reconstructed trajectories and filtered datasets, are stored in structured tabular formats, enabling transparent inspection and reuse in subsequent analysis stages.

The final trajectory dataset is exported in a standardized comma-separated values (CSV) format, containing time indices, planar coordinates, and trajectory identifiers. This format facilitates interoperability with different analysis tools and ensures that the same dataset can be used consistently across macroscopic Origin–Destination modeling, neural network training, and descriptive trajectory analysis. The clear separation between data preprocessing and modeling stages further enhances reproducibility by allowing each component of the workflow to be independently validated.

By explicitly defining processing steps, parameter choices, and data formats, the methodology adopted in this chapter supports transparent, reproducible, and extensible analysis. This design enables future researchers to replicate the preprocessing pipeline, apply alternative modeling approaches to the same data, or extend the framework to additional datasets and environments.

3.11 Summary

This chapter presented the data acquisition and preprocessing pipeline used to extract pedestrian trajectories from video recordings. Starting from raw video data, pedestrians are detected, tracked, and reconstructed into clean and consistent trajectories through a series of automated processing steps.

The resulting trajectory dataset provides the empirical foundation for both macroscopic Origin–Destination modeling and descriptive trajectory analysis developed in the remainder of this thesis. By clearly separating data preparation from modeling and results, the chapter establishes transparency and reproducibility while maintaining a focused methodological scope.

4 Methodology

4.1 Overview of the Proposed Modeling Framework

This chapter presents the methodological framework adopted to model pedestrian Origin–Destination (OD) demand using empirically extracted trajectory data. Building on the data acquisition and preprocessing pipeline described in Chapter 3, the methodology defines a structured and reproducible approach for representing, modeling, and evaluating macroscopic pedestrian movement patterns in open spaces.

The framework starts from cleaned pedestrian trajectories obtained through video-based detection and tracking, which constitute the sole empirical input to the modeling process. From these trajectories, a spatially aggregated OD representation is constructed. The OD matrix is selected as the central abstraction because it provides a compact and interpretable description of pedestrian demand while remaining suitable for both probabilistic simulation and data-driven prediction.

Two complementary OD modeling approaches are developed. The first is a probabilistic Monte Carlo (MC) model, which generates synthetic OD demand through stochastic sampling from an empirical OD distribution estimated from observed trajectories. The second is a neural network (NN) model, which formulates OD prediction as a supervised destination-choice problem and learns conditional destination probabilities based on origin-related and geometric trip features. Both models operate on the same spatial zoning system, rely on the same trajectory-derived inputs, and are evaluated under identical conditions, ensuring methodological fairness and isolating differences attributable solely to the modeling approach.

Model evaluation is conducted exclusively at the OD-matrix level using a common set of macroscopic performance metrics that assess structural similarity, distributional agreement, and aggregate flow consistency between predicted and observed OD matrices. No interpretation of individual pedestrian decisions or trajectory dynamics is introduced at this stage.

In addition to OD demand modeling, the chapter includes a complementary trajectory-level analysis that quantifies geometric properties of pedestrian paths and their temporal context. Measures of trajectory linearity, concavity, and crowd count are computed post hoc from the extracted trajectories. These descriptors are strictly descriptive: they are not used as inputs to either the Monte Carlo or neural network models and do not influence OD estimation or evaluation. Their purpose is to characterize intra-OD variability that cannot be captured by OD matrices alone.

Figure 4.1 summarizes the overall methodological pipeline, illustrating the sequential flow from trajectory extraction to OD modeling, macroscopic evaluation, and independent trajectory characterization. This modular structure emphasizes a clear separation between data preparation, OD demand modeling, and descriptive analysis, supporting transparency, reproducibility, and methodological clarity.

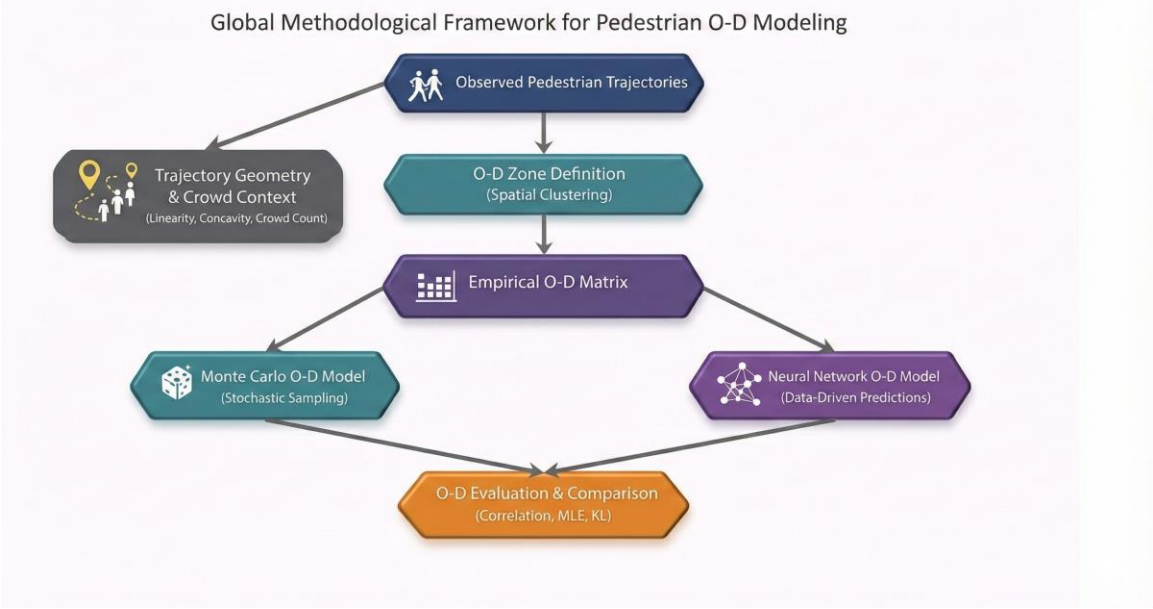

Figure 4-1 Overview of the methodological framework .

4.2 Origin–Destination Matrix Construction

4.2.1 Conceptual Basis of Origin–Destination Representation

The Origin–Destination (OD) representation provides a structured way to summarize pedestrian movement by mapping each observed trip to an ordered pair indicating its starting and ending spatial zones. Rather than relying on full trajectory time series, the OD framework reduces each pedestrian path to a discrete transition (o, d), significantly simplifying the structure of demand while preserving the core behavioral information needed for macroscopic modeling. This compact representation is widely used in pedestrian-flow analysis because it is interpretable, scalable, and compatible with both probabilistic simulation and data-driven learning. In this thesis, the OD matrix serves as the unified demand input for both the Monte Carlo and neural network models, ensuring that their outputs are directly comparable under a common movement abstraction.

4.2.2 Defining Origins and Destinations from Trajectories

Each extracted trajectory corresponds to a single pedestrian trip. Given a trajectory represented as a sequence of timestamped positions

$$\boldsymbol{T} = \{(\boldsymbol{t_1}, \boldsymbol{x_1}), (\boldsymbol{t_2}, \boldsymbol{x_2}), \dots, (\boldsymbol{t_N}, \boldsymbol{x_N})\}, \qquad \textit{Equation 4-1}$$

the origin is defined as the first valid coordinate

$$\boldsymbol{x_{orig}} = \boldsymbol{x_1}, \qquad \textit{Equation 4-2}$$

and the destination is defined as the last valid coordinate

$$\boldsymbol{x_{dest}} = \boldsymbol{x_N}. \qquad \textit{Equation 4-3}$$

Because trajectories are downsampled to one point per second and filtered for stability, these endpoints reliably represent true entry and exit positions within the scene. Only trajectories with sufficient valid samples are retained to ensure that each OD pair reflects genuine movement rather than artifacts. The result is a set of origin–destination coordinate pairs derived consistently from the cleaned trajectory dataset.

4.2.3 Spatial Clustering into OD Zones

OD matrices require a discrete zoning system rather than continuous coordinates. To define these zones, the set of all origin and destination points is clustered using the k-means algorithm. Let

$$\boldsymbol{P} = \{\boldsymbol{x}_{orig}(\boldsymbol{i}), \boldsymbol{x}_{dest}(\boldsymbol{i})\}_{\boldsymbol{i=1}}^{\boldsymbol{N}} \qquad \textit{Equation 4-4}$$

be the combined set of start and end points. K-means partitions these points into K spatial clusters by solving

$$\underset{\{\boldsymbol{c_k}\},\{\boldsymbol{z_i}\}}{\boldsymbol{min}} \sum_{\boldsymbol{i=1}}^{|\boldsymbol{P}|} \| \boldsymbol{p_i} - \boldsymbol{c_{z_i}} \|^{\boldsymbol{2}}, \qquad \textit{Equation 4-5}$$

where c_k are cluster centroids and $z_i \in \{1, \dots, K\}$ is the assigned cluster index. This produces:

- a set of zone centroids $\{c_1, \dots, c_K\}$,
- an origin zone label o_i for each trajectory,
- a destination zone label d_i for each trajectory.

Clustering origins and destinations jointly ensures a consistent spatial zoning structure, allowing the OD matrix to reflect meaningful transitions between well-defined spatial regions.

Figure 4.2 illustrates the spatial clustering of trajectory start and end points into five Origin–Destination zones, together with the corresponding cluster centroids. The clustering is applied jointly to all origin and destination points and defines the fixed spatial zoning used for all OD matrices and models developed in this study.

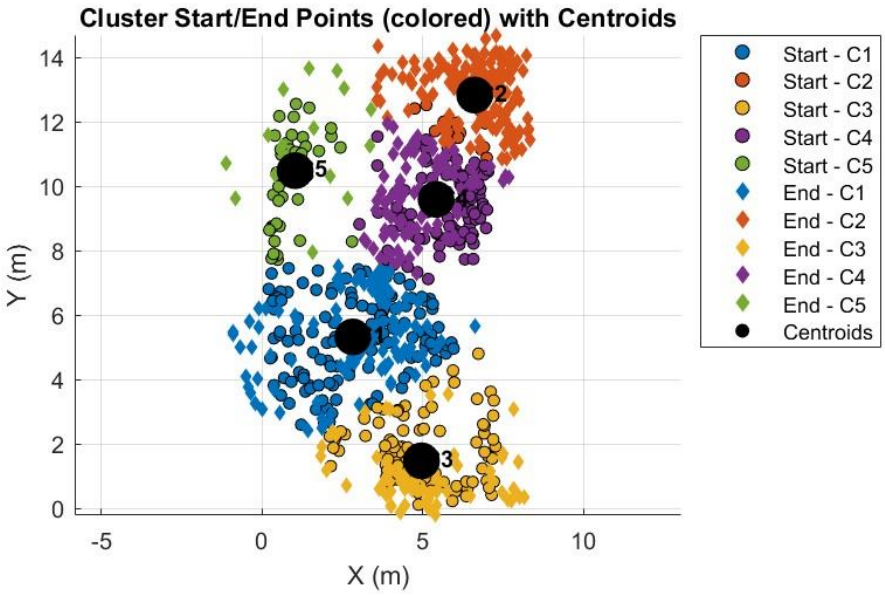

Figure 4-2 Spatial clustering of trajectory start and end points into Origin–Destination zones.

The clustering procedure was applied to a total of 418 validated pedestrian trajectories, corresponding to 836 spatial points (origins and destinations combined). The number of clusters K in k-means is not determined automatically and must be specified a priori. In this study, several values of K were explored, including K = 4, 5, and 6. Increasing K improved spatial granularity but led to smaller and spatially fragmented zones, reducing interpretability of the resulting OD matrix. Conversely, lower values merged distinct entry and exit areas into broader zones, limiting spatial resolution. The choice K = 5 was therefore retained as a compromise between spatial resolution and interpretability, ensuring coherent zone delineation without excessive segmentation. The selected zoning structure was kept fixed for all subsequent OD matrix constructions.

4.2.4 Constructing the OD Matrix

With each trajectory assigned an origin zone $o_i$and destination zone d_i, the OD matrix is constructed by counting transitions.

The raw OD count matrix $M \in \mathbb{R}^{K\times K}$ is defined as

$$\boldsymbol{M_{ij}} = \sum_{n=1}^{N} \mathbf{1}(o_n = i \; and \; d_n = j), \qquad \textit{Equation 4-6}$$

where $\mathbf{1}(\cdot)$ is the indicator function.

To transform this into a probability-based matrix suitable for both modeling approaches, the matrix is normalized:

$$\boldsymbol{P_{ij}} = \frac{M_{ij}}{\sum_{a=1}^{K}\sum_{b=1}^{K} M_{ab}}. \qquad \textit{Equation 4-7}$$

The resulting matrix $\boldsymbol{P}$ satisfies

$$\sum_{i=1}^{K}\sum_{\boldsymbol{j=1}}^{\boldsymbol{K}} \boldsymbol{P_{ij}} = 1, \qquad \textit{Equation 4-8}$$

and represents the empirical OD distribution derived from the full dataset. Heatmaps and flow diagrams of P provide intuitive visualizations of movement intensity and directional patterns.

The OD matrix $\boldsymbol{P}$ constitutes the fundamental demand representation for the predictive modeling developed in Sections 4.3 and 4.4. Both the Monte Carlo simulation and the neural network predictor operate on this identical zonal OD structure, ensuring that their outcomes can be compared directly and without confounding differences in input representation. Using the same OD foundation allows the evaluation to isolate differences in modeling approach—probabilistic simulation versus learned inference—thus strengthening the methodological validity of the comparison.

4.3 Monte Carlo Methodology

4.3.1 Conceptual Role of Monte Carlo in OD Prediction

Monte Carlo simulation is employed as a probabilistic baseline for Origin–Destination (OD) prediction in pedestrian systems. The method generates alternative realizations of demand through repeated sampling from an empirical probability distribution. This

formulation is appropriate for pedestrian movement, where aggregate flow structures emerge from heterogeneous and decentralized individual decisions rather than deterministic optimization (Helbing et al., 2002; Duives et al., 2021).

In this study, the OD matrix is interpreted as a discrete probability distribution over zone-to-zone transitions. Each element represents the empirical likelihood of observing a trip between two zones. This interpretation aligns with aggregate demand modeling traditions in transportation research, where OD matrices summarize spatial trip distributions without explicitly modeling individual utility functions (von Sivers et al., 2014; Ben-Akiva & Bierlaire, 2006).

The model is purely empirical and parameter-free. Synthetic trips are generated directly from the observed distribution, making the approach transparent and suitable as a statistical benchmark against which more complex predictive models can be evaluated.

4.3.2 Monte Carlo OD Model Formulation and Data Partitioning

Let Ddenote the full trajectory dataset of size N. To evaluate generalization, the data are partitioned into disjoint training and testing subsets:

$$\boldsymbol{D = D_{train} \cup D_{test},\ |\ D_{train}\ | = 0.8N,} \qquad \textit{Equation 4-9}$$

where $D_{\text{train}} \cap D_{\text{test}} = \emptyset$.

Each trajectory contributes a single OD pair defined by its origin and destination zones. The training subset is used exclusively to estimate the empirical OD distribution, while the test subset is reserved for out-of-sample evaluation.

From the training data, OD counts are computed. Let M_{ij}^{train} denote the number of trajectories traveling from zone $i$to zone j. The empirical probability matrix is defined as

$$\boldsymbol{\widehat{P}_{ij} = \frac{M_{ij}^{train}}{\sum_{a,b} M_{ab}^{train}}.} \qquad \textit{Equation 4-10}$$

This matrix represents the observed distribution of zone-to-zone transitions in the training data.

4.3.3 Stochastic Sampling Procedure

Synthetic OD realizations are generated by sampling from the categorical distribution defined by $\hat{P}$:

$$(\boldsymbol{o}, \boldsymbol{d}) \sim \boldsymbol{Categorical}(\widehat{\boldsymbol{P}}), \qquad \textit{Equation 4-11}$$

For each simulation run, the number of sampled trips is set equal to N_{test}, ensuring consistency with the scale of the observed test demand.

Let (o_s, d_s) denote the OD pair drawn at sample s. The simulated count matrix is constructed as

$$\widetilde{\boldsymbol{M}}_{\boldsymbol{ij}} = \sum_{\boldsymbol{s=1}}^{\boldsymbol{N_{test}}} \mathbf{1}(\boldsymbol{o_s = i, d_s = j}), \qquad \textit{Equation 4-12}$$

where $\mathbf{1}(\cdot)$is the indicator function.

The corresponding simulated probability matrix is obtained by normalization:

$$\widetilde{\boldsymbol{P}}_{\boldsymbol{ij}} = \frac{\widetilde{\boldsymbol{M}}_{\boldsymbol{ij}}}{\sum_{\boldsymbol{a,b}} \widetilde{\boldsymbol{M}}_{\boldsymbol{ab}}}. \qquad \textit{Equation 4-13}$$

Because sampling is stochastic, the procedure is repeated multiple times to estimate expected performance and quantify variability. The ensemble of simulated OD matrices provides the basis for statistical comparison with the observed test distribution in the subsequent evaluation stage.

4.3.4 Evaluation Metrics and Validation Strategy

This subsection defines the evaluation framework used to compare simulated Origin–Destination (OD) matrices with observed OD matrices. The purpose of the evaluation is to assess macroscopic agreement in terms of structural patterns, probability distributions, and aggregated flows, rather than to interpret or rank model performance. Accordingly, this

section specifies how validation is conducted and which metrics are employed, while deferring all quantitative results and interpretations to the Results chapter.

The evaluation is performed by comparing simulated OD matrices $\tilde{P}$ with empirical OD matrices P, both normalized such that their elements sum to one. Identical spatial zoning, clustering definitions, and aggregation rules are applied throughout, allowing direct cell-wise and matrix-wise comparisons.

Correlation is used as a global structural similarity metric. Let $\bar{P}$ and $\bar{\tilde{P}}$ denote the mean values of the respective OD matrices. Correlation is computed as

$$\boldsymbol{Corr} = \frac{\sum_{i,j}(\boldsymbol{P_{ij}} - \bar{\boldsymbol{P}})(\widetilde{\boldsymbol{P}}_{\boldsymbol{ij}} - \bar{\widetilde{\boldsymbol{P}}})}{\sqrt{\sum_{i,j}(\boldsymbol{P_{ij}} - \bar{\boldsymbol{P}})^2}\sqrt{\sum_{i,j}(\widetilde{\boldsymbol{P}}_{\boldsymbol{ij}} - \bar{\widetilde{\boldsymbol{P}}})^2}}. \qquad \textit{Equation 4-14}$$

Mean Absolute Error (MAE) is employed to quantify average cell-wise deviations between simulated and observed OD probabilities:

$$\boldsymbol{MAE} = \frac{\mathbf{1}}{\boldsymbol{K^2}}\sum_{i,j} | \boldsymbol{P_{ij}} - \widetilde{\boldsymbol{P}}_{\boldsymbol{ij}} |, \qquad \textit{Equation 4-15}$$

where K denotes the number of spatial zones.

Kullback–Leibler (KL) divergence is used to assess distributional mismatch between simulated and observed OD matrices (Kullback & Leibler, 1951). The divergence is defined as

$$\boldsymbol{D_{KL}}(\boldsymbol{P} \parallel \widetilde{\boldsymbol{P}}) = \sum_{i,j} \boldsymbol{P_{ij}}\, \boldsymbol{log}\, \frac{\boldsymbol{P_{ij}}}{\widetilde{\boldsymbol{P}}_{\boldsymbol{ij}}}. \qquad \textit{Equation 4-16}$$

For numerical stability, a small positive constant ε is added to all matrix entries during implementation to avoid undefined values due to zero probabilities.

In addition to full matrix comparisons, marginal flow validation is conducted. Origin and destination marginals are defined as

$$\boldsymbol{P_i^{orig}} = \sum_j \boldsymbol{P_{ij}}\,, \boldsymbol{P_j^{dest}} = \sum_i \boldsymbol{P_{ij}}, \qquad \textit{Equation 4-17}$$

with analogous definitions for simulated matrices. Comparing these marginals allows evaluation of aggregate departure and arrival consistency.

Because Monte Carlo simulation is inherently stochastic, all evaluation metrics are computed across multiple independent realizations. Bootstrap resampling with replacement is further applied to assess robustness under data variability.

Finally, it is emphasized that this subsection defines the evaluation protocol only. All reported metrics serve as methodological tools for comparison, and no interpretation of model performance is provided here. The same evaluation framework is later applied to both the Monte Carlo model and the neural network model, ensuring methodological consistency and fair comparison in the Results chapter.

4.4 Neural Network Methodology

4.4.1 Conceptual Role of Neural Networks in Origin–Destination Prediction

The neural network is introduced as a supervised multi-class classification model for predicting pedestrian destination zones at the trip level. Given origin-related and geometric features, the model estimates the conditional probability distribution over destination clusters.

Each trajectory is treated as an independent sample, where engineered spatial and geometric features form the input and the destination zone serves as the output label. In this way, Origin–Destination (OD) estimation is expressed as a statistical learning task that infers conditional destination probabilities from explanatory variables.

Unlike frequency-based approaches that reproduce aggregate OD structure directly, the neural network captures nonlinear relationships between input features and destination choice. The predicted probabilities are subsequently aggregated across trips to reconstruct OD matrices, ensuring compatibility with the macroscopic representation adopted throughout the study.

The model therefore operates at the individual-trip level during learning but is evaluated at the aggregate OD level.

4.4.2 Input Feature Design and Dataset Construction

The dataset is defined at the trajectory level, with each trajectory contributing one feature vector and one destination label. Intermediate trajectory points are not used, preserving consistency with OD-based modeling rather than time-series forecasting.

The input vector includes both categorical and continuous variables:

- Origin cluster (one-hot encoded)
- Origin x-coordinate
- Origin y-coordinate
- Straight-line trip distance
- Movement direction (angle computed via arctangent of displacement)

One-hot encoding allows the model to capture zone-specific destination patterns without imposing ordinal relationships. Continuous features provide global spatial context and trip geometry. All variables are directly derived from observed trajectory data and remain interpretable.

The target variable is the destination cluster. Self-loops (origin equals destination) are retained to preserve the empirical OD structure.

The dataset is partitioned into training (70%), validation (15%), and test (15%) subsets. Numerical features are normalized using statistics computed on the training set and applied consistently to validation and test subsets to avoid information leakage. One-hot encoded features are not normalized.

4.4.3 Neural Network Architecture and Training Procedure

The model is a fully connected feedforward neural network for multi-class classification. The architecture consists of:

An input layer receiving the engineered feature vector

Multiple hidden layers with ReLU activation

Dropout layers to reduce overfitting

Layer normalization for training stability

A SoftMax output layer with dimensionality equal to the number of destination zones

The SoftMax output produces conditional destination probabilities:

$$\boldsymbol{P(d = j \mid x) = \frac{e^{z_j}}{\sum_{k=1}^{K} e^{z_k}}} \qquad \textit{Equation 4-18}$$

Training minimizes the categorical cross-entropy loss:

$$\boldsymbol{\mathcal{L} = -\sum_{j=1}^{K} y_j \, log \, (P_j),} \qquad \textit{Equation 4-19}$$

To account for class imbalance in destination frequencies, class weights are incorporated into the loss function. Optimization is performed using the Adam algorithm with mini-batch gradient descent. Training proceeds until convergence or early stopping based on validation performance.

After training, predicted probabilities for the test set are aggregated by origin zone to construct OD matrices. Resulting counts are normalized to ensure comparability with alternative modeling approaches.

Model performance and comparative evaluation are presented in the Results chapter.

4.4.4 Neural Network Evaluation and OD Reconstruction

The purpose of this evaluation stage is to assess the ability of the neural network to reproduce observed Origin–Destination (OD) demand patterns in an out-of-sample setting. Evaluation is conducted at the OD-matrix level rather than at the level of individual trajectories, reflecting the macroscopic modeling perspective adopted throughout this

study. The objective of this subsection is to define the evaluation procedure, not to interpret predictive performance.

Evaluation is performed using the held-out test set, which constitutes 15% of the available trajectories and is never used during training or validation. For each test trajectory, the trained neural network outputs a probability vector over all destination zones through the SoftMax layer. A predicted destination label is obtained by selecting the destination class with the highest predicted probability:

$$\widehat{\boldsymbol{d}}_{\boldsymbol{i}} = \boldsymbol{arg}\ \boldsymbol{\max_{k}}\ \ \boldsymbol{p}(\boldsymbol{d} = \boldsymbol{k} \mid \boldsymbol{x}_{\boldsymbol{i}}). \qquad \textit{Equation 4-20}$$

To reconstruct the neural-network-based OD matrix, predicted destinations are aggregated together with the known origin zones of the test trajectories. Each test trip contributes one unit count to the OD cell corresponding to its origin zone and predicted destination zone. Self-loops, where origin and destination belong to the same zone, are explicitly retained. The resulting OD count matrix is normalized so that the sum of all entries equals one:

$$\boldsymbol{P}_{\boldsymbol{ij}}^{\boldsymbol{NN}} = \frac{\boldsymbol{M}_{\boldsymbol{ij}}^{\boldsymbol{NN}}}{\sum_{\boldsymbol{a}=\boldsymbol{1}}^{\boldsymbol{K}} \sum_{\boldsymbol{b}=\boldsymbol{1}}^{\boldsymbol{K}} \boldsymbol{M}_{\boldsymbol{ab}}^{\boldsymbol{NN}}}, \qquad \textit{Equation 4-21}$$

where M_{ij}^{NN} denotes the number of predicted trips from origin zone i to destination zone j.

The neural-network-based OD matrix is evaluated using the same macroscopic metrics adopted for the Monte Carlo model. These include correlation, mean absolute error (MAE), and Kullback–Leibler (KL) divergence, as well as comparisons of origin and destination marginals. These metrics are defined solely as evaluation tools, without ranking models or interpreting numerical values at this stage.

As a secondary diagnostic indicator, classification accuracy at the individual-trip level is also reported. This measure reflects the proportion of test trajectories for which the predicted destination matches the observed destination. However, classification accuracy is not used as the primary criterion for OD prediction quality, as the central evaluation focus remains on aggregated OD structures and probability distributions.

4.5 Quantification of Trajectory Linearity and Crowd Context

4.5.1 Motivation and Conceptual Role

Origin–Destination (OD) models adopted in this study describe pedestrian movement at an aggregated level by representing transitions between spatial zones. By design, this abstraction captures where pedestrians travel while omitting the geometric details of how they move between zones. Such macroscopic representations are appropriate for demand analysis but do not reflect variability in path shape within the same OD pair (Duives et al., 2021; von Sivers et al., 2014).

To characterize this intra-OD variability, trajectory linearity is introduced as a geometric descriptor. Linearity quantifies the deviation of an observed path from the straight segment connecting its origin and destination. It measures geometric efficiency only and does not imply optimality, behavioral intent, or decision-making mechanisms. Comparable indicators—often termed straightness index, detour index, or tortuosity—are widely used in transportation and spatial movement analysis to evaluate route deviation independently of behavioral modeling assumptions (Duives et al., 2021).

Two trajectories sharing the same origin and destination zones may differ substantially in curvature, displacement length, or directional stability. Because OD matrices aggregate trips at the zone level, they cannot represent this geometric heterogeneity. Linearity metrics therefore provide a complementary descriptive layer that reveals structural differences within aggregated OD flows.

Pedestrian movement is also embedded in a temporal context shaped by the simultaneous presence of other pedestrians. To acknowledge this contextual dimension without introducing explicit interaction modeling, a simple crowd count is used as an auxiliary indicator. Crowd count reflects the number of pedestrians present in the scene at a given time and serves as a coarse proxy for collective presence. Similar aggregate intensity measures are frequently employed in pedestrian studies as indicators of interaction potential (Helbing et al., 2002; Duives et al., 2021). In this study, the measure is used descriptively rather than causally.

No explicit density modeling is introduced. Estimating spatial density fields would require additional discretization choices and interaction assumptions that fall outside the scope of the present work. The objective here is geometric characterization rather than behavioral inference.

Trajectory linearity and crowd context metrics are therefore computed independently of OD modeling. They do not serve as inputs to predictive models and do not modify OD estimation. Instead, they provide complementary descriptors that enrich interpretation while preserving a clear methodological separation between demand modeling and trajectory geometry analysis.

4.5.2 Trajectory Representation and Preprocessing

The trajectory analysis in this section relies on the pedestrian trajectories extracted during the video processing stage described in Chapter 3. No additional tracking or reconstruction is performed here; previously validated trajectories are reused for geometric characterization.

Each trajectory is represented as an ordered sequence of planar coordinates:

$$\boldsymbol{T_i} = \{(\boldsymbol{t_1}, \boldsymbol{x_1}, \boldsymbol{y_1}), (\boldsymbol{t_2}, \boldsymbol{x_2}, \boldsymbol{y_2}), \dots, (\boldsymbol{t_N}, \boldsymbol{x_N}, \boldsymbol{y_N})\}, \qquad \textit{Equation 4-22}$$

where $t_k$denotes discrete time and $(x_k, y_k)$the spatial position at that instant.

For geometric analysis, only trajectories containing at least three valid observations are retained, ensuring that path shape can be meaningfully defined. Origin and destination points correspond to the first and last valid coordinates of each trajectory and are treated purely as geometric anchors, independent of OD zone clustering used elsewhere in the thesis.

Coordinates are expressed in the approximate metric system obtained during preprocessing. Although full perspective correction is not applied, the geometric indicators computed in this section are ratio-based or comparative in nature, making them robust to uniform scaling effects.

To mitigate tracking noise, a mild spatial smoothing is applied using a moving-average filter. This operation reduces high-frequency positional fluctuations while preserving overall path geometry and endpoints. No trajectory interpolation, rescaling, density filtering, or artificial modification of path length is introduced. Each trajectory retains its original temporal structure and geometric form.

This representation provides a consistent basis for computing linearity and deviation metrics while avoiding methodological duplication of the preprocessing procedures already described in Chapter 3.

4.5.3 Linearity and Path Deviation Metrics

This subsection introduces quantitative geometric metrics to describe how closely pedestrian trajectories follow the straight-line segment connecting their origin and destination. Such measures are commonly used in transportation geography and movement analysis under terms such as straightness index, detour index, or path tortuosity, where they quantify deviation from shortest-path geometry without implying behavioral optimality (Duives et al., 2021). Similar geometric efficiency indicators are widely adopted in spatial network analysis and pedestrian modeling to characterize route structure independently of decision-making assumptions.

All deviation-based metrics are computed relative to the same straight-line reference vector

$$\boldsymbol{v} = (\boldsymbol{x_N} - \boldsymbol{x_1}, \boldsymbol{y_N} - \boldsymbol{y_1}), \qquad \textit{Equation 4-23}$$

which represents the minimal geometric connection between origin and destination in the adopted coordinate system.

Two fundamental distance measures are computed. The straight-line distance is

$$\boldsymbol{D_{straight}} = \sqrt{(\boldsymbol{x_N} - \boldsymbol{x_1})^2 + (\boldsymbol{y_N} - \boldsymbol{y_1})^2}, \qquad \textit{Equation 4-24}$$

while the path length is computed as

$$\boldsymbol{D_{path}} = \sum_{k=1}^{N-1} \sqrt{(\boldsymbol{x_{k+1}} - \boldsymbol{x_k})^2 + (\boldsymbol{y_{k+1}} - \boldsymbol{y_k})^2}. \qquad \textit{Equation 4-25}$$

The straight-line distance represents minimal geometric separation, whereas the path length reflects the actual displacement along the observed trajectory.

Linearity is defined as the ratio

$$\boldsymbol{L} = \frac{\boldsymbol{D_{straight}}}{\boldsymbol{D_{path}}}. \qquad \textit{Equation 4-26}$$

with $0 < L \leq 1$. Values close to one indicate trajectories that closely approximate straight-line motion. The complementary measure of tortuosity is defined as

$$\boldsymbol{\tau} = \frac{\boldsymbol{D_{path}}}{\boldsymbol{D_{straight}}}. \qquad \textit{Equation 4-27}$$

Both indicators are dimensionless and robust to uniform spatial scaling, making them suitable for comparative analysis.

These indicators are computed for descriptive analysis only and are not used as inputs to the predictive OD models.

4.5.4 Concavity and Directional Bias Metrics

Building on the linearity and deviation measures introduced previously, this subsection presents geometric metrics that characterize the directional asymmetry of pedestrian trajectories with respect to the straight-line reference connecting their origin and destination. While linearity quantifies the magnitude of deviation from a straight path, concavity metrics capture the direction of deviation. Similar signed deviation and curvature indicators are commonly used in trajectory analysis, movement ecology, and spatial path analysis to characterize bending behavior and lateral bias without embedding behavioral assumptions (Duives et al., 2021).

For each pedestrian trajectory, a straight-line reference is defined as the line segment connecting the first valid point $(x_1, y_1)$and the last valid point $(x_N, y_N)$of the trajectory.

For every intermediate point (x_k, y_k), with $k = 2, \ldots, N-1$, the signed perpendicular deviation from this reference line is computed. The signed deviation is defined as

$$\boldsymbol{\delta_k} = \frac{(x_k - x_1)(y_N - y_1) - (y_k - y_1)(x_N - x_1)}{\sqrt{(x_N - x_1)^2 + (y_N - y_1)^2}}. \qquad \textit{Equation 4-28}$$

The magnitude of $\delta_k$represents the lateral distance from the straight-line reference, while its sign indicates on which side of the reference line the trajectory point lies. This sign convention is determined by the cross-product formulation and allows deviations on opposite sides of the reference path to be distinguished consistently. The resulting sequence of signed deviations provides a geometric description of directional curvature along the trajectory.

Based on these signed deviations, a raw concavity index is defined for each trajectory as the mean signed deviation across all interior points:

$$\boldsymbol{C} = \frac{\mathbf{1}}{\boldsymbol{N-2}} \sum_{\boldsymbol{k=2}}^{\boldsymbol{N-1}} \boldsymbol{\delta_k}. \qquad \textit{Equation 4-29}$$

Averaging signed deviations to characterize directional curvature is consistent with geometric trajectory descriptors used in movement and path-shape analysis (Duives et al., 2021). Positive values indicate systematic bending toward one side of the reference line, negative values indicate bending toward the opposite side, and values near zero indicate approximate symmetry. This index is purely geometric and does not imply optimization or intent.

To enable comparison between trajectories moving in opposite directions, a geometric reference walking direction is defined from the sign of horizontal displacement:

$$\boldsymbol{w} = \begin{cases} \mathbf{+1}, & \textbf{if } \boldsymbol{x_N - x_1 \geq 0}, \\ \mathbf{-1}, & \textbf{if } \boldsymbol{x_N - x_1 < 0}. \end{cases} \qquad \textit{Equation 4-30}$$

This definition does not assume compliance with any walking rules or conventions; it simply establishes a common geometric orientation. Using this reference, the concavity index is aligned as

$$\boldsymbol{C_{aligned} = w \cdot C.} \qquad \textit{Equation 4-31}$$

The aligned concavity index removes sign ambiguity caused by opposite movement directions, allowing trajectories traveling in different directions to be analyzed within a unified concavity framework. After alignment, positive values consistently indicate deviation toward the same relative side of the walking direction, while negative values indicate deviation toward the opposite side.

In addition to the mean concavity index, directional bias indicators are computed as the proportion of interior points with positive and negative signed deviations. Such proportion-based asymmetry indicators are frequently used in movement analysis to characterize lateral preference or curvature dominance along a path (Duives et al., 2021). These measures complement the mean concavity index by capturing distributional asymmetry rather than relying solely on an average value.

Concavity-related metrics are aggregated across all trajectories to examine the overall distribution of directional curvature. Both raw and aligned concavity indices are analyzed to assess symmetry, skewness, and dispersion, and summary statistics are used to characterize their distributional properties. These analyses provide descriptive insight into directional variability of pedestrian movement patterns within identical OD pairs.

The concavity and directional bias metrics introduced in this subsection do not model pedestrian decision-making, do not infer intent, and do not serve as inputs to the Monte Carlo or neural network models. They are applied exclusively as post hoc geometric descriptors, with the sole purpose of characterizing directional aspects of trajectory shape and enriching the interpretation of observed pedestrian movement without modifying the OD-based demand representations.

4.5.5 Crowd Count Estimation and Temporal Context

Crowd context is introduced in this study as a temporal descriptor rather than a spatial or interaction-based variable. The objective is to quantify how many pedestrians are simultaneously present in the scene over time, providing contextual information for interpreting trajectory geometry. This approach deliberately focuses on crowd count rather than pedestrian density, thereby avoiding assumptions about occupied area, local interactions, or behavioral responses. Crowd count is used strictly as a descriptive indicator of scene occupancy, not as a behavioral or predictive variable.

Crowd count is defined as the number of pedestrians present in the scene at a given time instant. A pedestrian is considered present at time t if their trajectory contains a valid observation at that time. Formally, the crowd count at time t can be expressed as

$$\boldsymbol{N(t) = \sum_{i=1}^{N_{traj}} 1(t \in T_i)}, \qquad \textit{Equation 4-32}$$

where $N(t)$ denotes the number of pedestrians present at time t, T_i is the set of timestamps associated with trajectory i, and $1(\cdot)$ is the indicator function.

The crowd count is computed directly from the extracted trajectories by identifying all unique timestamps and counting the number of trajectories that include each timestamp. No temporal interpolation, smoothing, or spatial subdivision is applied. The resulting crowd count represents a global scene-level measure, aggregated over the entire observed area, and is independent of spatial zoning or trajectory geometry.

To relate crowd context to individual trajectories, each trajectory is associated with the mean crowd count experienced over its active duration. This enables trajectory-level comparison while preserving the temporal nature of the measure. The average crowd count for trajectory i is defined as

$$\boldsymbol{\bar{N}_i = \frac{1}{|T_i|} \sum_{t \in T_i} N(t)}, \qquad \textit{Equation 4-33}$$

where $|T_i|$ denotes the number of time instants associated with trajectory i. This aggregated measure provides a compact summary of the temporal crowd environment in which each trajectory occurs.

Crowd count is analyzed jointly with the linearity and concavity metrics introduced in Sections 4.5.3 and 4.5.4. While linearity captures the magnitude of geometric deviation and concavity captures its directional asymmetry, crowd count provides the temporal context in which these geometric properties are observed. No causal relationship is assumed or inferred between crowd count and trajectory shape, and no predictive modeling is performed.

Finally, clear methodological boundaries are maintained. Pedestrian density is not estimated, as this would require reliable area measurement and local interaction modeling. No force-based, interaction-based, or behavioral interpretations are introduced, and crowd count is not used as an input to the Monte Carlo or neural network models. The role of crowd count is strictly descriptive, supporting the interpretation of geometric trajectory variability without extending beyond the scope of the present methodological framework.

4.5.6 Positioning Within the Overall Framework

The methodological framework developed in Chapter 4 follows a sequential pipeline that begins with video-based pedestrian detection and trajectory extraction, proceeds through macroscopic Origin–Destination (OD) modeling using Monte Carlo simulation and neural networks, and is subsequently complemented by trajectory-level geometric and temporal analysis. Within this pipeline, the analyses presented in Section 4.5 are explicitly positioned after the construction and evaluation of OD demand models, and therefore do not influence any stage of OD estimation or prediction.

The trajectory descriptors introduced in Section 4.5—including linearity metrics, concavity and directional bias measures, and crowd count indicators—are computed independently of both the Monte Carlo and neural network models. These quantities are not used as model inputs, do not modify OD matrices, and do not affect prediction outcomes. Their computation is fully decoupled from the OD modeling stages, ensuring that the

probabilistic and data-driven demand representations developed earlier remain methodologically uncontaminated and internally consistent.

The analytical role of Section 4.5 is therefore descriptive rather than predictive. By characterizing geometric deviation, directional asymmetry, and temporal crowd context at the trajectory level, this section provides additional insight into intra-OD variability that cannot be captured by OD matrices alone. These analyses enrich the interpretation of observed pedestrian movement patterns without introducing behavioral assumptions, causal claims, or decision-making models. As such, they complement the OD-based framework by adding contextual understanding while preserving the macroscopic abstraction central to this study.

Finally, the methodological choices adopted in Section 4.5—such as the exclusion of pedestrian density estimation, local interaction modeling, and causal inference—reflect deliberate scope boundaries rather than analytical omissions. These boundaries naturally motivate the discussion presented in the following section, which addresses the methodological limitations of the proposed framework and identifies directions for future research**.** While the analyses in Section 4.5 are intentionally descriptive and decoupled from OD prediction, they establish geometric and contextual descriptors that are relevant to the broader objective of future predictive pedestrian flow modeling, in which both trajectory geometry and flow characteristics may ultimately be integrated.

4.6 Methodological Limitations

This section discusses the methodological boundaries of the proposed framework. The limitations identified here arise from deliberate modeling choices made to ensure clarity, reproducibility, and analytical robustness, rather than from shortcomings of the methodology. The objective is to explicitly define the scope within which the results of this thesis should be interpreted and to clarify how the adopted approach fits into a broader research agenda.

A first limitation concerns the macroscopic nature of the Origin–Destination (OD) modeling framework. Both the Monte Carlo model (Section 4.3) and the neural network model (Section 4.4) operate at the OD level, capturing where pedestrians travel between

spatial zones without predicting the specific routes or paths taken within the environment. As a result, the models describe aggregate demand patterns rather than detailed spatial trajectories. This abstraction is consistent with established OD modeling principles but necessarily excludes route-level and path-level prediction.

The proposed framework also does not aim to model dynamic flow evolution. Time-dependent phenomena such as congestion formation, transient interactions, and feedback between pedestrian density and movement behavior are not explicitly represented. Predicting the full dynamics of pedestrian flows under varying geometrical and operational conditions is a broader research objective that extends beyond the scope of a single thesis. In line with this perspective, the present work focuses on static demand representations and post-hoc trajectory characterization, acknowledging that fully predictive flow-dynamics modeling remains a longer-term research goal.

With respect to crowd effects, the analysis considers pedestrian presence through a global crowd count measure rather than through spatially resolved density estimation. Pedestrian density modeling typically requires accurate area measurement, fine-grained spatial partitioning, and explicit interaction modeling, which introduce additional assumptions and complexity. For this reason, crowd count is used in this thesis as a descriptive temporal context indicator rather than as a behavioral or causal variable, as discussed in Section 4.5.

Another important limitation is that trajectory geometry metrics—such as linearity, path deviation, and concavity—are not fed back into the OD models. These metrics are computed independently and applied post hoc to characterize geometric variability within observed trajectories. They do not influence OD estimation or prediction and are not used as explanatory variables in either the Monte Carlo or neural network models. This separation is intentional and ensures a clear conceptual distinction between demand modeling and trajectory characterization.

The spatial scale adopted in the trajectory analysis also introduces limitations. While an approximate pixel-to-meter conversion is applied to allow geometric interpretation, full perspective correction is not performed. Consequently, absolute distance values should be interpreted as approximate. However, the primary geometric measures employed—such as

ratios, relative deviations, and normalized indices—are comparative in nature and therefore robust to uniform scaling effects. The analysis emphasizes relative geometric properties rather than precise physical measurements.

Taken together, these limitations reflect a deliberate effort to balance analytical depth with methodological transparency. By constraining model scope and avoiding unnecessary assumptions, the framework prioritizes interpretability, reproducibility, and clear separation between modeling layers. Reducing scope in this way strengthens the internal consistency of the methodology and facilitates meaningful comparison between different modeling approaches.

At the same time, the modular structure of the proposed framework allows for future extensions. Potential developments include the integration of trajectory geometry into predictive models, density-aware flow representations, coupling between demand and movement dynamics, and scenario-based generalization across different spatial configurations. In this context, it is important to emphasize that the final goal of the broader research effort—though not necessarily of this thesis—is to develop models capable of predicting pedestrian flow dynamics across diverse scenarios, accounting jointly for geometric and flow characteristics.

These limitations therefore define clear directions for future research rather than constraints on the validity of the results presented in this work.

5 Results

5.1 Overview of the Results Chapter

This chapter presents the results of the pedestrian Origin–Destination (OD) modeling framework introduced in Chapter 4. The results follow the methodological sequence: empirical OD representation, Monte Carlo modeling, neural network modeling, comparative analysis, and descriptive trajectory-level characterization.

All analyses are based on 418 pedestrian trajectories clustered into five spatial zones. A normalized empirical OD matrix constructed from the full dataset serves as the reference demand structure.

The Monte Carlo model is evaluated through repeated stochastic realizations, with performance summarized using OD-level metrics and robustness analysis. The neural network model is evaluated on held-out test data, and predicted destinations are aggregated to reconstruct OD matrices. Both approaches are assessed using correlation, mean absolute error (MAE), Kullback–Leibler divergence, and marginal flow consistency.

The chapter concludes with descriptive results on trajectory linearity, concavity, and crowd count, providing geometric and temporal context to the observed demand patterns.

5.2 Empirical Origin–Destination Structure

This section presents the empirical Origin–Destination (OD) structure derived from the full trajectory dataset. The resulting OD matrix serves as the reference demand representation for subsequent model evaluation.

5.2.1 Empirical OD Matrix

Using the five-zone clustering defined in Chapter 4, an OD matrix is constructed from all 418 trajectories. Each entry represents the proportion of trips between an origin and destination zone, and the matrix is normalized to sum to one.

Figure 5.1 presents the resulting 100% empirical OD matrix. The demand structure is clearly heterogeneous, with a small number of dominant OD pairs and several low-

probability flows, indicating that pedestrian movement is concentrated along specific spatial relations.

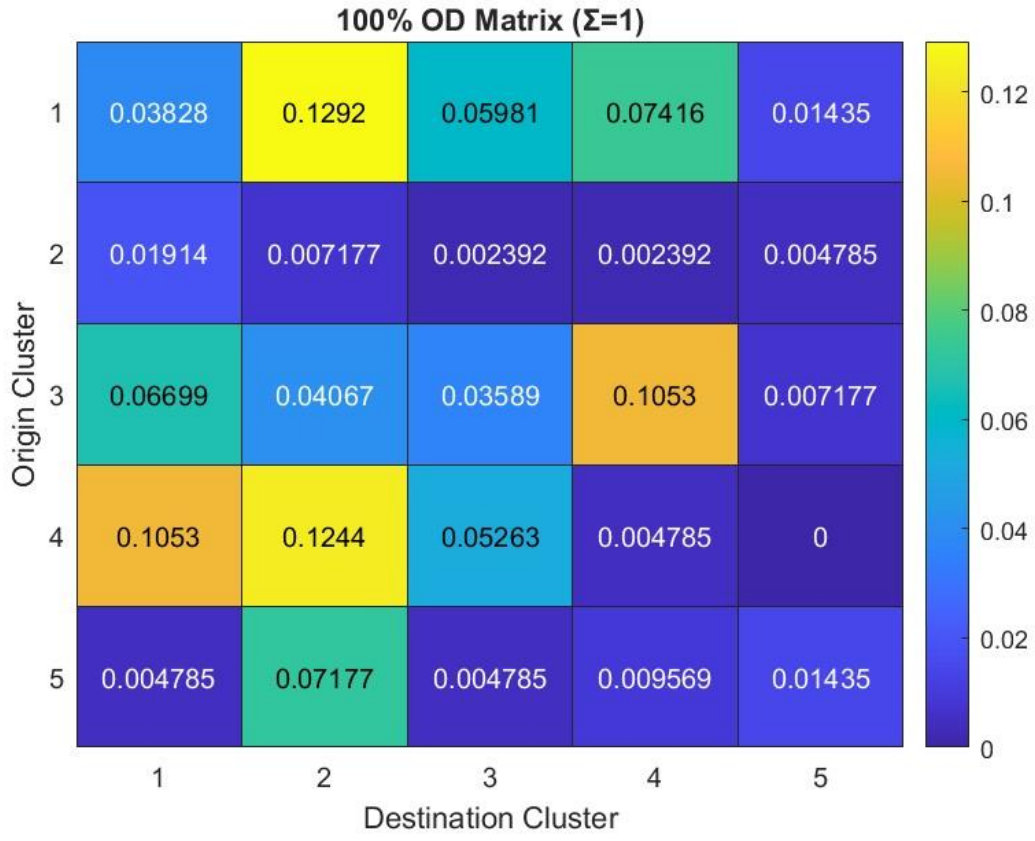

Figure 5-1 100% OD matrix.

5.2.2 Spatial OD Flow Representation

To complement the matrix-based representation, the empirical OD structure is visualized spatially through an OD flow map. Figure 5.2 displays the OD flows as arrows connecting cluster centroids, with arrow thickness and color proportional to OD probability.

This visualization highlights the dominant movement directions in physical space and provides an intuitive interpretation of the empirical OD structure.

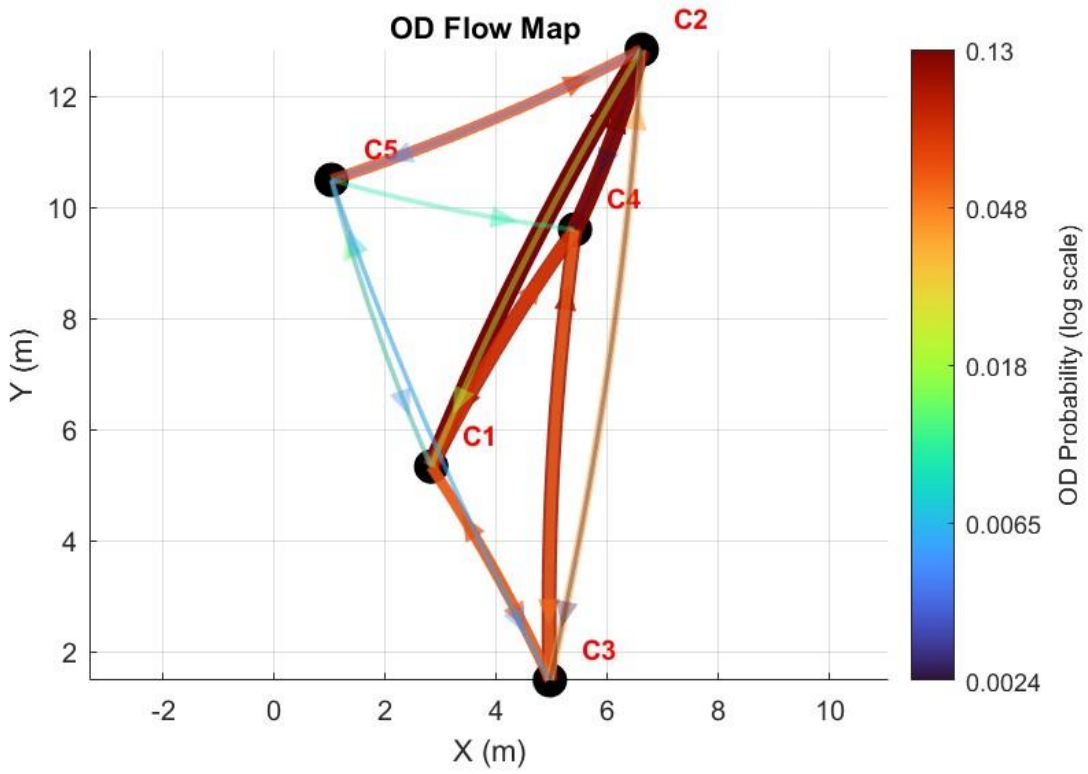

Figure 5-2 Spatial OD Flow Representation.

5.2.3 Reference Role of the Empirical OD Structure

The empirical OD matrix and flow map presented in this section define the reference demand structure used throughout the remainder of the results chapter. All Monte Carlo and neural network OD predictions reported in the following sections are evaluated against this empirical benchmark using consistent OD representations and evaluation metrics.

5.3 Monte Carlo Origin–Destination Modeling Results

5.3.1 Evaluation Setup

The Monte Carlo model generates synthetic OD matrices by sampling from the empirical OD distribution estimated on the training data. The 418 trajectories are split at the trajectory

level into 80% training and 20% test subsets. The training subset defines the sampling distribution, and the test subset provides the evaluation benchmark.

A total of 462 independent realizations are generated to quantify stochastic variability. In each realization, the number of sampled trips equals the size of the test set. Performance is evaluated by comparing simulated and observed test OD matrices using correlation, mean absolute error (MAE), and Kullback–Leibler divergence.

5.3.2 Training OD Matrix Used by the Monte Carlo Model

Figure 5.3 presents the normalized OD matrix constructed from the 80% training subset. This matrix defines the sampling distribution used by the Monte Carlo model.

OD pairs with higher probabilities correspond to more frequently observed transitions in the training data and therefore have a higher likelihood of being sampled during simulation.

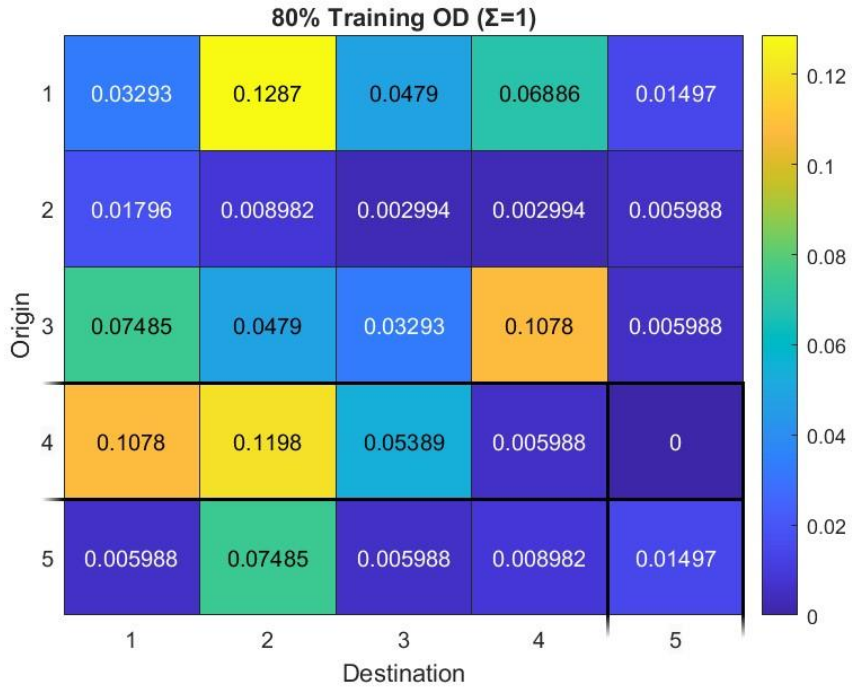

Figure 5-3 training OD Matrix (Monte Carlo)

5.3.3 Monte Carlo Performance Across Multiple Runs

The number of Monte Carlo realizations was determined through convergence analysis of performance statistics. The running mean and standard deviation of the correlation metric stabilized after approximately 400 simulations, with negligible changes observed in correlation, MAE, and KL divergence beyond this point. A total of 462 realizations was therefore retained based on convergence of performance metrics, ensuring stable estimates without unnecessary additional simulations.

Table 5.1 summarizes model performance across all realizations.

Table 5-1 Monte Carlo Performance Summary (462 Runs)

Metric	**Mean**	**Std. Dev.**
Correlation	0.768	0.083
MAE	0.0209	0.0039
KL Divergence	1.1459	0.5409

On average, the Monte Carlo model reproduces the test OD structure with moderate to high agreement. Variability across realizations reflects the inherent stochastic nature of the sampling process. Figure 5.4 presents the distribution of correlation and MAE across all runs.

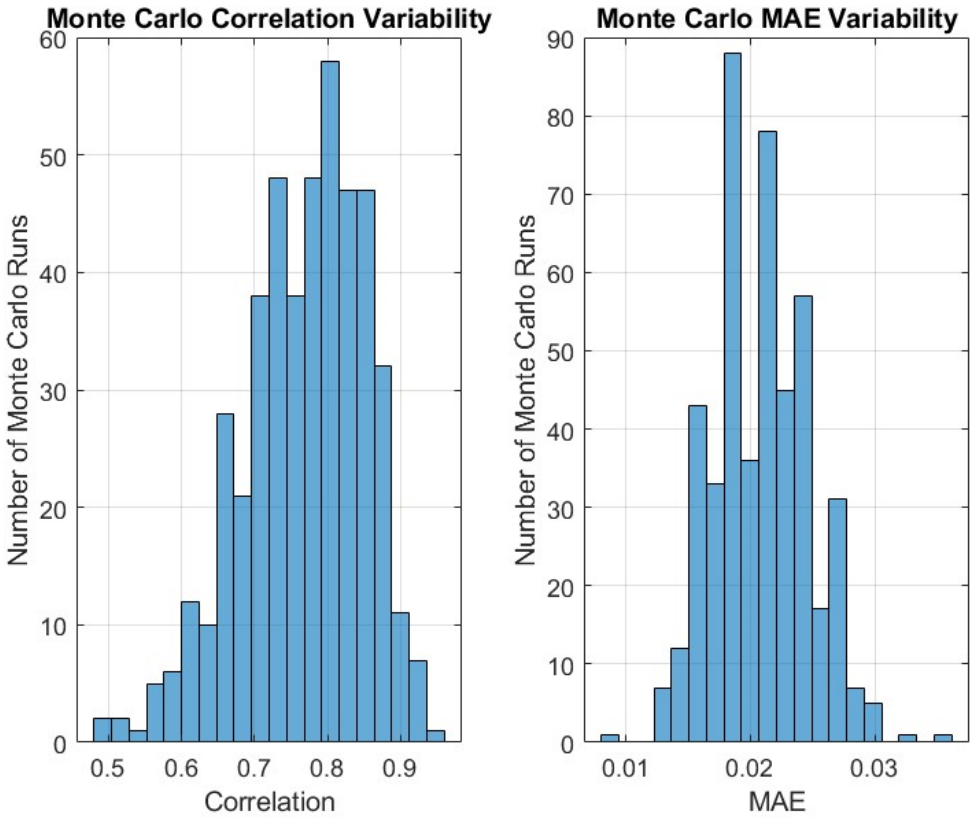

Figure 5-4 distributions of correlation and MAE across runs.

5.3.4 Best Monte Carlo Realization

Among the 462 realizations, the highest agreement with the observed test OD matrix is obtained in Run 462. Table 5.2 reports the corresponding performance metrics.

Table 5-2 Best Monte Carlo Run Performance

Metric	**Value**
Correlation	0.952
MAE	0.0086
KL Divergence	0.4088

Figures 5.5–5.7 compare the observed test OD matrix, the simulated OD matrix for this run, and their cell-wise difference. The best realization closely reproduces dominant OD flows, with small deviations across most cells.

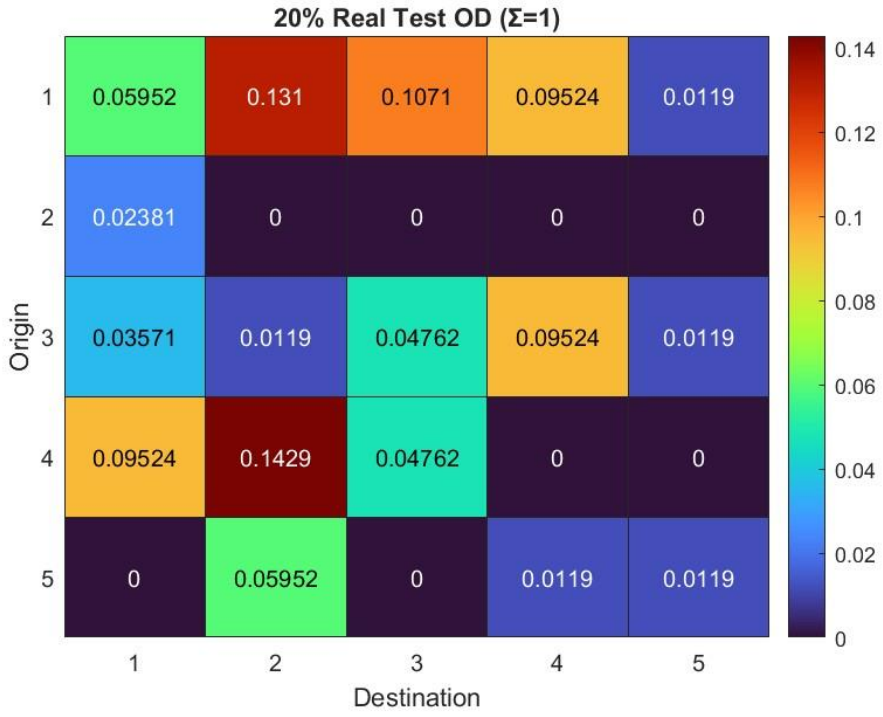

Figure 5-5 the ground-truth OD matrix computed from the test set (MONTE CARLO).

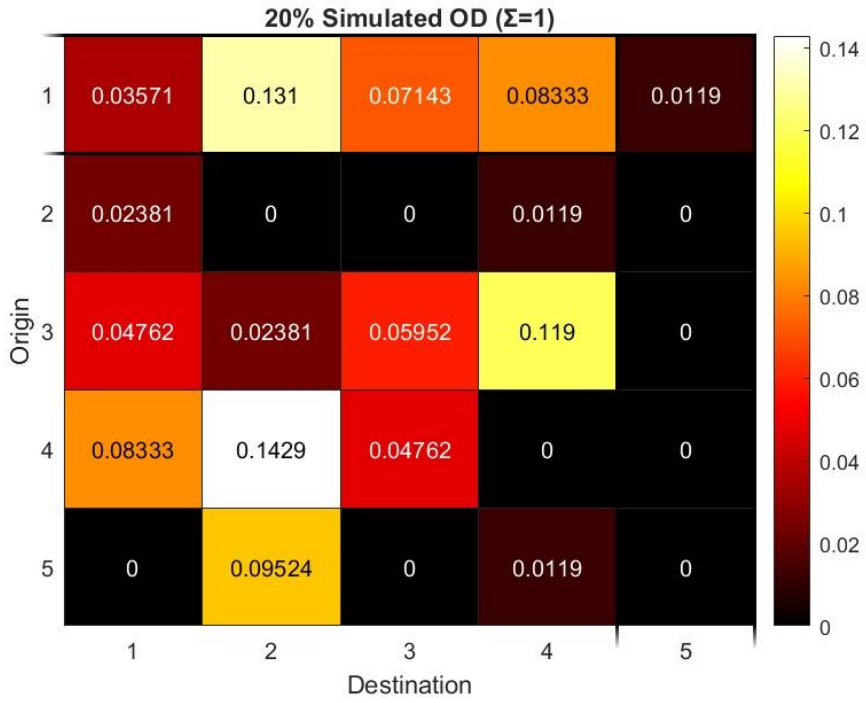

Figure 5-6 the simulated MONTE CARLO OD matrix .

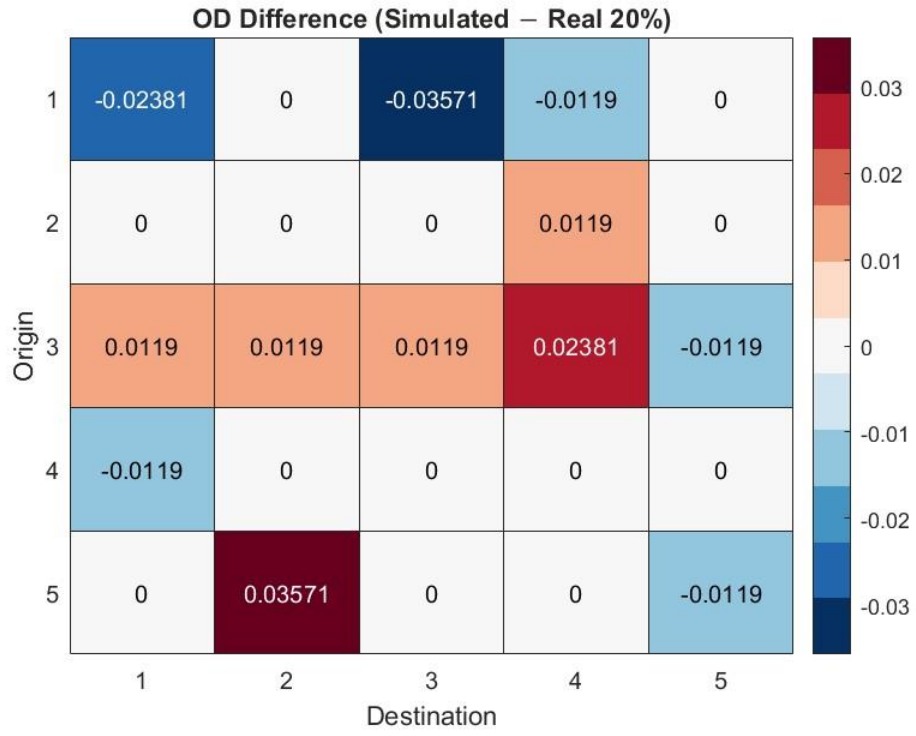

Figure 5-7 the cell-wise difference between the simulated and observed test OD matrices.

5.3.5 Marginal Flow Validation

Beyond full OD matrix comparison, marginal flow consistency is evaluated by comparing origin totals (row sums) and destination totals (column sums) between simulated and observed test OD matrices for the best Monte Carlo run.

Table 5-3 Marginal Flow Comparison (Best Run)

Marginal	Correlation	MAE	Accuracy
Origins	0.969	0.0333	83.33%
Destinations	0.985	0.0286	85.71%

Figures 5.8 and 5.9 show the corresponding marginal distributions. Aggregate origin and destination flows are well preserved.

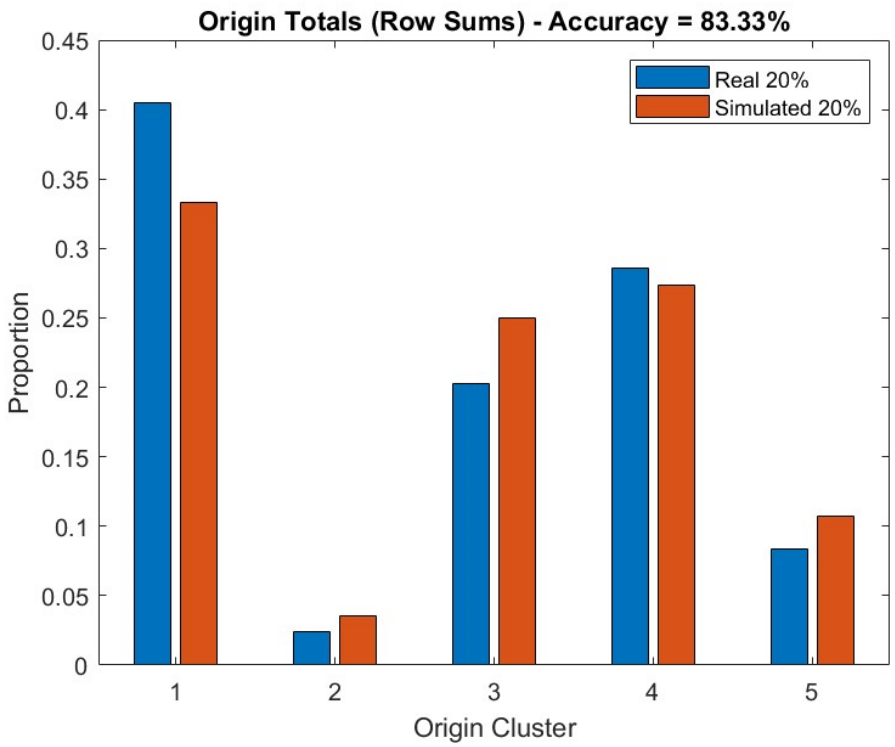

Figure 5-8 observed marginal distributions for origins.

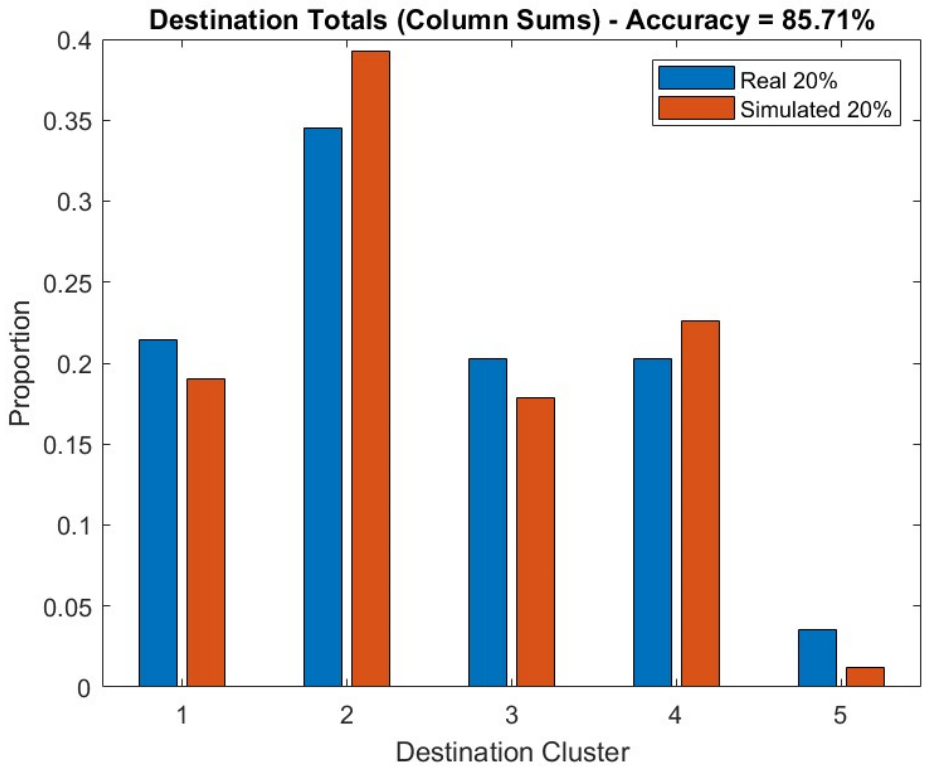

Figure 5-9 observed marginal distributions for destinations .

5.3.6 Bootstrap Robustness Analysis

To assess sensitivity to data variability, a bootstrap validation procedure is applied. Thirty bootstrap samples are generated from the original dataset, and the Monte Carlo evaluation pipeline is repeated for each sample.

The resulting performance statistics are summarized below:

Table 5-4 Bootstrap Performance Summary (30 Samples).

Metric	**Mean**	**Std. Dev.**
Correlation	0.764	0.083
MAE	0.0208	0.0041
KL Divergence	0.9477	0.3871

The bootstrap results closely match those obtained from the original data split, indicating that Monte Carlo performance is stable with respect to sampling variability.

5.3.7 Interim Interpretation

Overall, the Monte Carlo model consistently reproduces macroscopic OD demand patterns in out-of-sample evaluation, preserving global structure and marginal flows while exhibiting unavoidable stochastic variability across realizations. No comparison with the neural network model is made at this stage; these results establish the stochastic baseline against which neural network performance is assessed in the following section.

5.4 Neural Network Origin–Destination Modeling Results

5.4.1 Evaluation Setup

The neural network predicts destination zones at the trajectory level and aggregates these predictions to reconstruct OD matrices.

The dataset of 418 trajectories is split into 70% training, 15% validation, and 15% test subsets. Model training and hyperparameter selection are performed on the training and validation sets, and all reported results are computed on the held-out test set (62 trajectories).

Predicted OD matrices are normalized to sum to one and evaluated using correlation, mean absolute error (MAE), and Kullback–Leibler divergence.

5.4.2 Neural Network OD Prediction Performance

The neural network's predictive performance is evaluated at the OD-matrix level by aggregating trajectory-level predictions on the test set into a predicted OD matrix, which is compared with the empirical test OD matrix.

Table 5.5 summarizes the quantitative results. The model achieves high correlation and low absolute error, indicating strong agreement between predicted and observed OD distributions.

Table 5-5 — Neural Network OD Prediction Performance (15% Test Set).

Metric	Value
Correlation	0.985
MAE	0.0052
KL Divergence	0.7831

These results demonstrate that the neural network effectively reconstructs the global OD structure despite being trained on a limited sample.

5.4.3 OD Matrix Reconstruction and Visual Comparison

To complement the aggregate metrics, the reconstructed OD matrices are examined visually. Figure 5.10 presents the ground-truth OD matrix computed from the test set, while Figure 5.11 shows the corresponding OD matrix reconstructed from neural network predictions. Figure 5.12 illustrates the cell-wise difference between the predicted and real matrices.

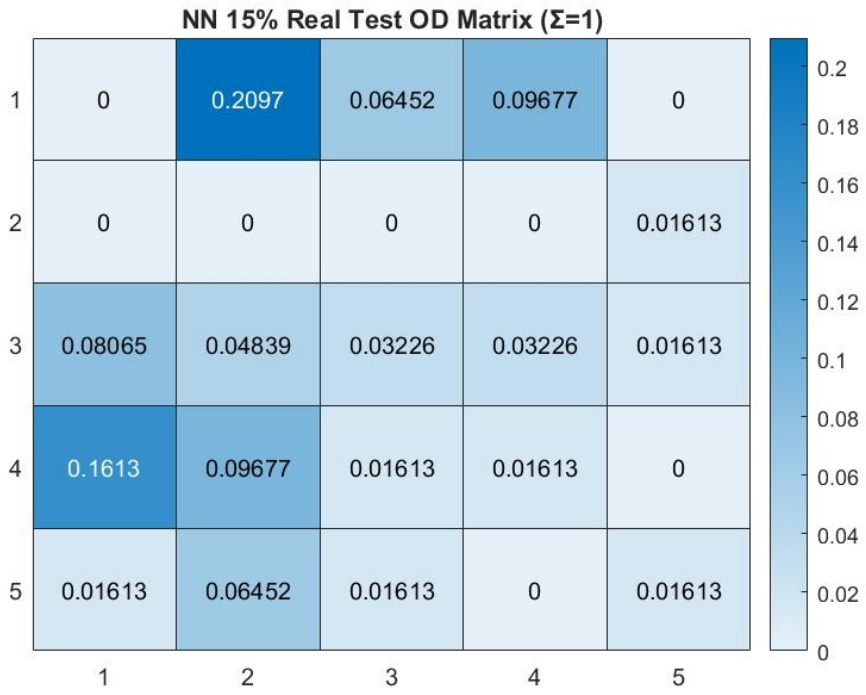

Figure 5-10 The ground-truth OD matrix computed from the test set.

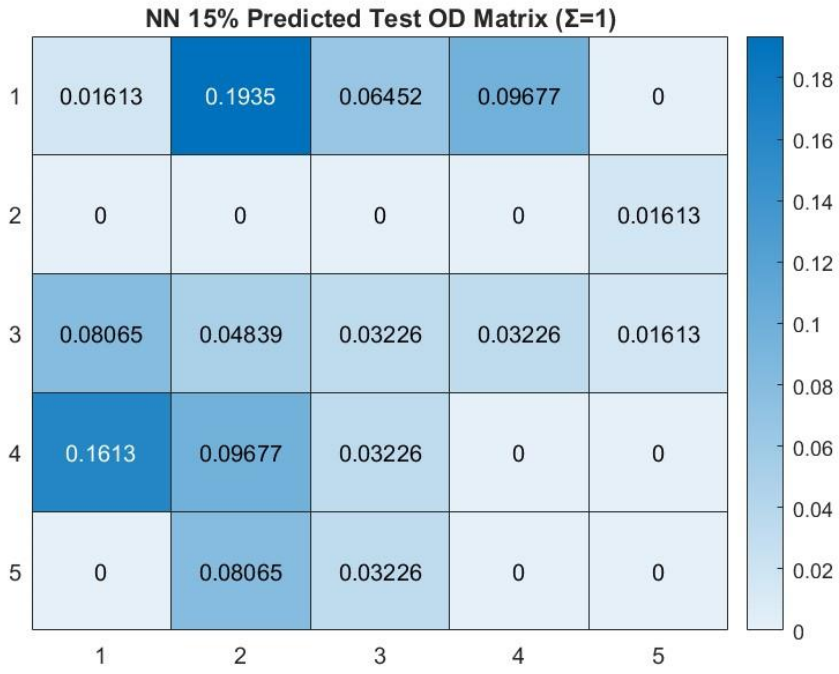

Figure 5-11 The corresponding OD matrix reconstructed from neural network predictions.

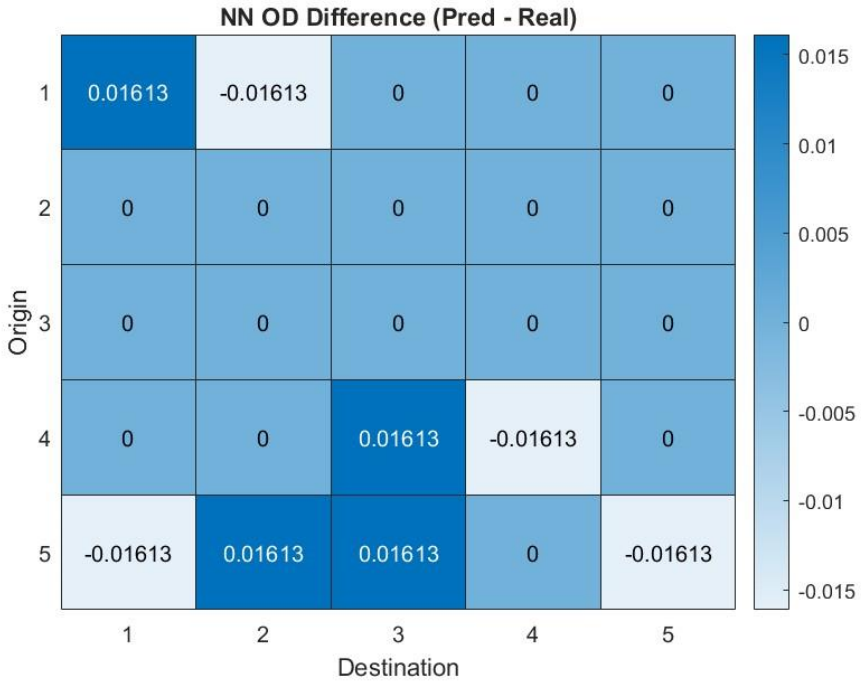

Figure 5-12 the cell-wise difference between the predicted and real matrices.

The visual comparison confirms that the neural network captures the dominant OD flows and preserves the overall spatial distribution of pedestrian demand. Deviations are generally small in magnitude and localized to a limited number of OD pairs, as highlighted in the difference matrix. No systematic bias toward over- or under-estimation of specific origins or destinations is observed.

5.4.4 Destination Marginal Flow Validation

Beyond cell-level accuracy, destination marginal totals provide an important validation of global flow allocation. Destination marginals are computed as column sums of the OD matrices and compared between predicted and observed test data.

Table 5.6 reports the destination marginal comparison metrics for the neural network model.

Table 5-6 Destination Marginal Comparison (Neural Network, 15% Test Set).

Metric	**Value**
Correlation	0.991
MAE	0.0129
Accuracy	93.55%

Figure 5.13 visualizes the destination marginals using a bar chart comparison between real and predicted flows. The results show that the neural network accurately reproduces the relative distribution of arrivals across destination clusters, with an overall accuracy exceeding 93%.

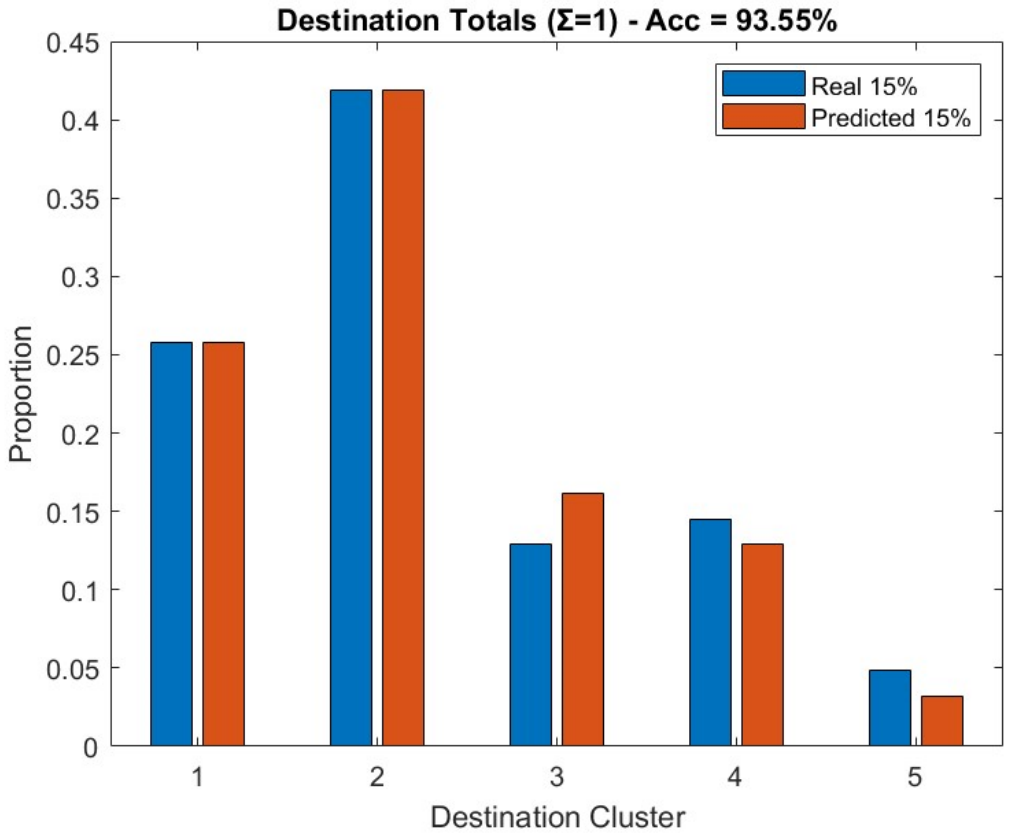

Figure 5-13 The destination marginals between real and predicted flows.

5.4.5 Trajectory-Level Classification Performance

At the trajectory level, the neural network achieves a classification accuracy of 87.10% on the test set.

Figure 5.14 presents the confusion matrix for destination prediction. Diagonal dominance indicates that most trajectories are correctly classified, while misclassifications occur primarily between neighboring destination zones. The x-axis represents predicted destination zones, and the y-axis represents true destination zones. Each cell shows the number of trajectories assigned to a predicted zone given the true zone.

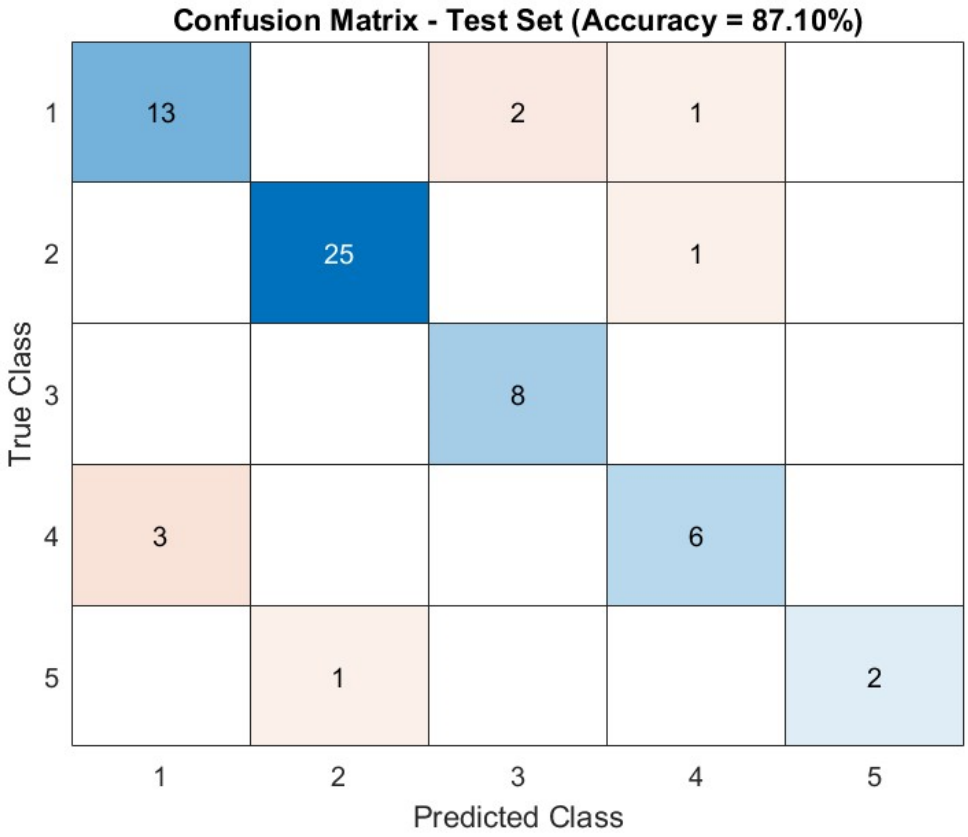

Figure 5-14 The confusion matrix for destination prediction on the test set.

5.4.6 Clarification on Origin Marginals

Because the neural network conditions on the origin cluster as an input feature, origin marginals in the reconstructed OD matrix are preserved by construction. As a result, origin marginal comparisons are not reported. Destination marginals therefore provide the relevant aggregate-level validation metric.

5.4.7 Interim Interpretation

The neural network achieves high agreement with the observed test OD matrix, low cell-wise error, and strong destination marginal consistency. A direct comparison with the Monte Carlo model is presented in the following section.

5.5 Comparative Analysis of Monte Carlo and Neural Network OD Models

Both models are evaluated using identical OD zoning and macroscopic metrics on held-out test data.

5.5.1 OD Matrix-Level Performance Comparison

Table 5.7 reports OD-level performance for both approaches. Monte Carlo values are reported as mean ± standard deviation across realizations. Neural network results correspond to the trained model evaluated on the test set.

Table 5-7 OD Matrix-Level Performance Comparison (Test Data).

Metric	**Monte Carlo**	**Neural Network**
Correlation	0.768 ± 0.083	0.985
MAE	0.0209 ± 0.0039	0.0052
KL Divergence	1.1459 ± 0.5409	0.7831

The neural network achieves higher correlation and lower error across all metrics.

5.5.2 Destination Marginal Validation

Table 5.8 compares destination marginal performance.

Table 5-8 Destination Marginal Performance (Test Data).

Model	**Correlation**	**MAE**	**Accuracy**
Monte Carlo (Best Run)	0.985	0.0286	85.71%
Neural Network	0.991	0.0129	93.55%

The neural network shows closer alignment with observed destination totals. Origin marginals are not reported for the neural network, as they are preserved by construction.

5.5.3 Model Characteristics

The Monte Carlo model generates OD matrices through stochastic sampling, producing a distribution of possible realizations. The neural network produces deterministic predictions conditioned on trajectory-level features.

5.5.4 Summary

The neural network provides higher OD reconstruction accuracy, while the Monte Carlo model offers a stochastic reference distribution. The following section complements the OD-based comparison with trajectory-level geometric and temporal analysis.

5.6 Trajectory Linearity, Concavity, and Crowd Context Results

This section reports descriptive trajectory-level results based on the geometric and temporal metrics defined in Section 4.5. The analysis is conducted on the observed trajectory dataset and examines concavity, tortuosity, and crowd context.

Figure 5.15 shows the distribution of the aligned concavity index across all trajectories. The distribution is centered near zero, indicating that most trajectories exhibit limited systematic directional curvature. However, pronounced tails are present, reflecting a subset of trajectories with substantial lateral deviation. The x-axis represents the aligned concavity value (dimensionless signed lateral deviation from the straight-line origin–destination segment), and the y-axis represents frequency (number of trajectories).

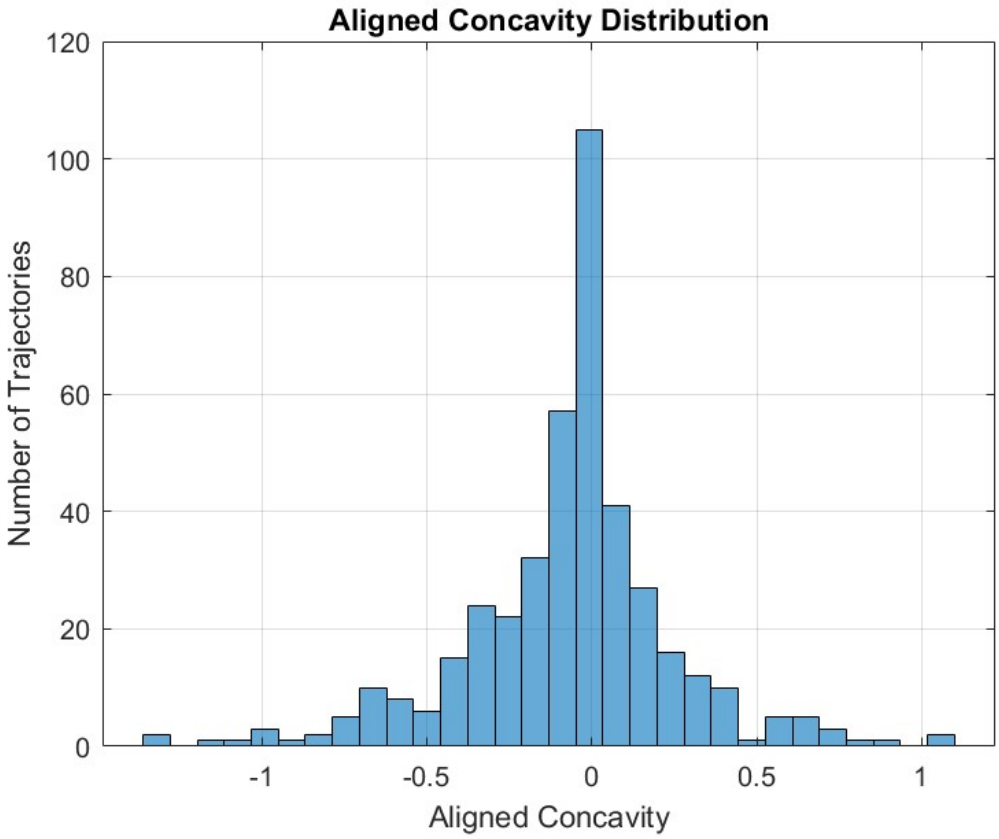

Figure 5-15 The aligned concavity index across all trajectories.

Figure 5.16 compares aligned concavity distributions by walking direction. Although both distributions remain centered near zero, their shapes differ. The reference direction exhibits negative skewness (−1.15) and high kurtosis (6.51), indicating asymmetry and heavy tails. In contrast, the opposite direction shows near-zero skewness (0.09) and moderate kurtosis (3.97), corresponding to a more symmetric but non-Gaussian distribution. The x-axis represents the aligned concavity value (dimensionless), and the y-axis represents frequency (number of trajectories).

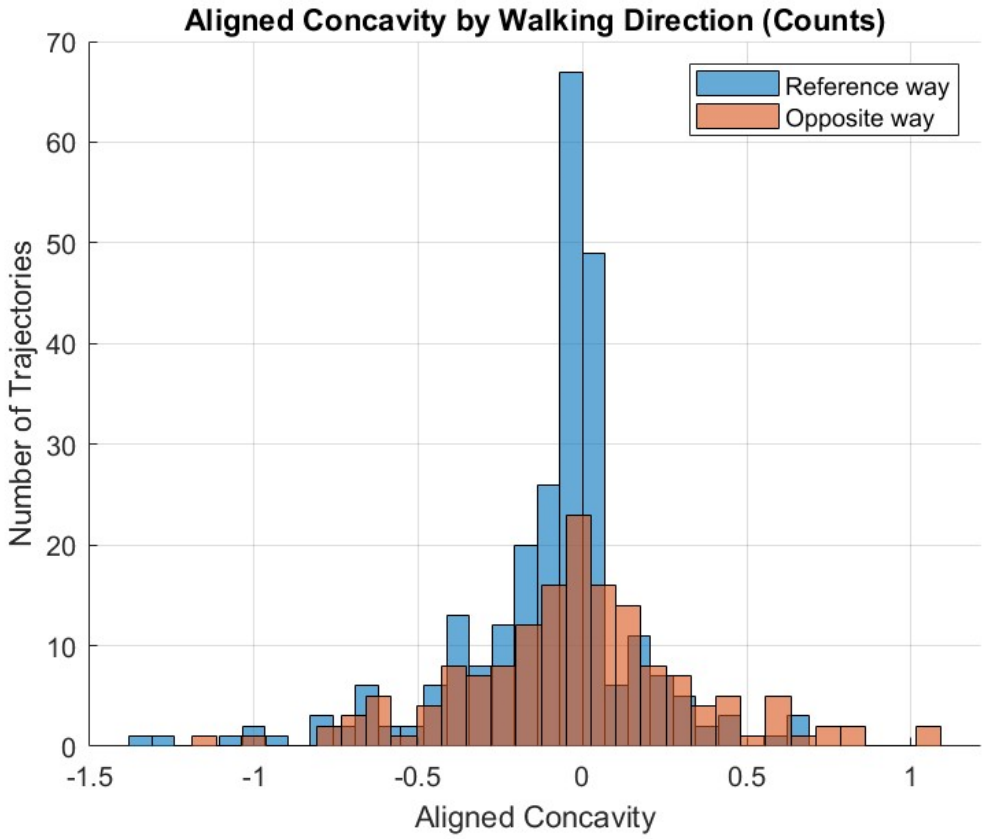

Figure 5-16 The aligned concavity distributions for the two walking directions.

Figure 5.17 presents the distribution of trajectory tortuosity. Most trajectories have values close to 1, corresponding to near-linear movement. A long right tail indicates the presence of more tortuous paths, though such cases are relatively infrequent within the dataset. The x-axis represents tortuosity (ratio of path length to straight-line distance, dimensionless), and the y-axis represents frequency (number of trajectories).

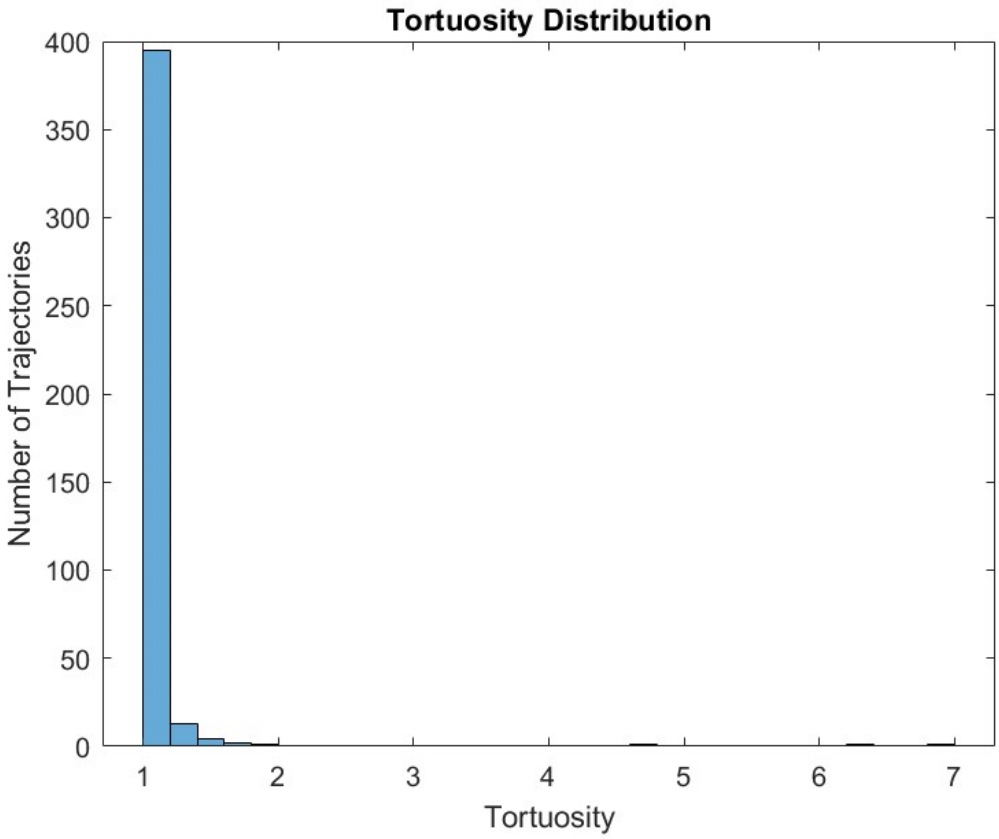

Figure 5-17 The distribution of trajectory tortuosity.

Figure 5.18 relates trajectory linearity to the mean crowd count experienced during each trajectory. The correlation between crowd count and linearity is approximately zero (corr = −0.002), indicating no observable association at the global scene level. The x-axis represents the mean number of pedestrians present during each trajectory (average count per frame), and the y-axis represents the linearity score (ratio of straight-line distance to path length, dimensionless).

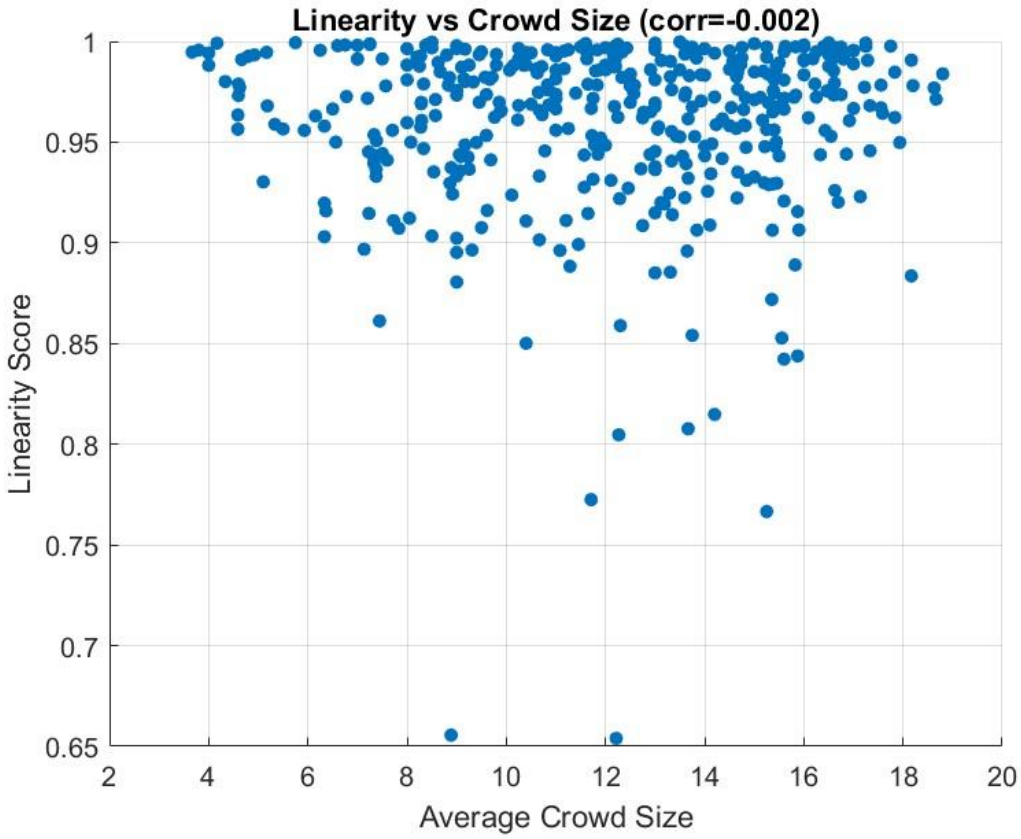

Figure 5-18 linearity score against the mean number of pedestrians.

Overall, the trajectory-level metrics reveal geometric variability and directional asymmetry within the observed pedestrian movements. While most trajectories are approximately linear, deviations occur in a subset of cases. No systematic relationship is detected between global crowd presence and trajectory linearity.

6 Discussion

6.1 Purpose and Structure of the Discussion

This chapter discusses and interprets the results presented in Chapter 5, with the objective of situating the findings of this thesis within a broader methodological and research context. No new models, metrics, or experiments are introduced. Instead, the discussion focuses on explaining observed results, clarifying their implications, and identifying how the proposed framework contributes to the long-term objective of predictive pedestrian flow modeling.

The discussion addresses three main aspects. First, the behavior and performance of the Monte Carlo Origin–Destination (OD) model are interpreted as a stochastic baseline for macroscopic demand representation. Second, the neural network OD model is discussed as a data-driven approach capable of exploiting trip-level conditioning to improve OD reconstruction accuracy. Third, the two modeling approaches are compared to highlight their complementary strengths and limitations.

In addition, the chapter reflects on the role of trajectory geometry and crowd context as descriptive elements that characterize pedestrian movement beyond OD matrices. These analyses are discussed as interpretive tools rather than predictive components and are used to motivate future research directions rather than to evaluate model performance.

6.2 Interpretation of Monte Carlo OD Modeling Results

The Monte Carlo OD model provides a probabilistic baseline for reproducing macroscopic pedestrian demand patterns. Its stochastic nature is a defining feature rather than a limitation, as it explicitly represents uncertainty in OD estimation arising from finite data and random sampling. The distribution of performance metrics observed across multiple Monte Carlo realizations reflects this inherent variability and should be interpreted as a range of plausible OD reconstructions rather than as noise around a single optimal solution.

The spread of correlation, error, and divergence measures across runs indicates that multiple OD configurations are compatible with the observed data at the macroscopic level.

This behavior is consistent with the role of Monte Carlo simulation as a generator of demand scenarios rather than as a deterministic predictor. From this perspective, the average performance across runs provides a robust indication of expected model behavior, while individual realizations illustrate variability rather than instability.

The identification of a best-performing Monte Carlo realization serves as an upper-bound reference on achievable agreement with the empirical OD matrix. However, this realization should not be interpreted as a guaranteed or reproducible outcome, but rather as an illustration of the maximum alignment attainable within the stochastic framework. This distinction is important to avoid over-interpreting isolated high-performing outcomes.

Bootstrap analysis further supports the robustness of the Monte Carlo approach by showing that performance metrics remain stable under resampling of the input data. Together, these results confirm that the Monte Carlo model successfully captures the dominant macroscopic OD structure while explicitly acknowledging uncertainty, making it a transparent and interpretable baseline for pedestrian demand modeling.

6.3 Interpretation of Neural Network OD Modeling Results

The neural network OD model differs fundamentally from the Monte Carlo approach in that it learns conditional destination probabilities based on trip-level information. By conditioning on origin location and geometric features, the neural network exploits information that is not explicitly represented in unconditional OD frequency models. This allows it to achieve higher reconstruction accuracy when evaluated on unseen test data.

It is important to distinguish between destination classification accuracy and OD matrix accuracy. While the neural network operates at the level of individual trips by predicting destination clusters, its performance is ultimately assessed through aggregated OD matrices. Strong agreement between predicted and observed OD matrices indicates that accurate trip-level inference translates into improved macroscopic demand representation, but the two evaluation levels remain conceptually distinct.

The preservation of origin marginals in the neural network results is a direct and expected consequence of the modeling setup, as origins are provided as input features. This behavior

should not be interpreted as a modeling artifact, but rather as a correct reflection of the conditional prediction task. The neural network does not predict origins or trajectories; it predicts destination probabilities given known trip attributes.

Despite operating on trip-level data, the neural network remains a macroscopic OD model in its outputs. The predicted OD matrices summarize aggregate demand patterns and do not encode route choice, path geometry, or interaction dynamics. As such, the neural network represents a data-driven enhancement of OD modeling rather than a transition toward microscopic or behavioral pedestrian simulation.

6.4 Comparative Insights: Monte Carlo and Neural Network OD Models

The comparison between the Monte Carlo and neural network models reflects fundamental differences in modeling philosophy rather than a simple ranking of performance. Both approaches aim to reproduce macroscopic Origin–Destination demand, but they do so using distinct assumptions about data usage, uncertainty, and model structure.

The Monte Carlo model relies on stochastic sampling from empirical OD frequencies, producing a distribution of plausible demand realizations rather than a single deterministic outcome. This explicit representation of variability constitutes one of its main strengths, as it allows uncertainty and robustness to be examined directly. As a result, the Monte Carlo approach serves as a transparent probabilistic baseline that captures the global structure of observed OD demand while preserving interpretability.

In contrast, the neural network model learns conditional destination probabilities by exploiting trip-level features related to origin location and geometry. This data-driven conditioning enables the model to capture nonlinear relationships and structured dependencies that are not accessible to unconditional sampling. The improved OD reconstruction accuracy observed for the neural network therefore reflects its ability to infer destination choice patterns from additional information rather than differences in OD representation.

The performance gap between the two models is thus best understood as a consequence of their conceptual foundations. The Monte Carlo model estimates unconditional OD demand and emphasizes variability, whereas the neural network learns conditional OD probabilities and emphasizes predictive accuracy. These differences arise from modeling strategy rather than implementation choices.

Importantly, the two approaches are complementary rather than competing. The Monte Carlo model provides a robust and interpretable stochastic reference, while the neural network demonstrates how conditioning on spatial and geometric features can enhance OD prediction. Together, they illustrate a range of viable modeling strategies for pedestrian demand estimation, highlighting trade-offs between simplicity, transparency, and expressiveness.

This comparison reinforces the central message of the thesis: macroscopic pedestrian OD modeling can be achieved through multiple paradigms, each offering distinct advantages depending on data availability, modeling objectives, and the desired balance between interpretability and predictive performance.

6.5 Role of Trajectory Geometry and Crowd Context

While macroscopic Origin–Destination models effectively describe aggregate pedestrian demand, they necessarily abstract away the detailed geometry of individual trajectories. The descriptive analyses of trajectory linearity, concavity, and crowd context presented in this thesis highlight the extent of geometric and temporal variability that exists within identical OD pairs and therefore cannot be captured by OD matrices alone.

The linearity and tortuosity results indicate that most pedestrian trajectories closely approximate straight-line motion between origin and destination, while a smaller subset exhibits pronounced geometric deviation. This suggests that extreme path irregularity is relatively rare but non-negligible, contributing to intra-OD variability that remains invisible at the demand-matrix level. Concavity analysis further reveals that directional curvature is not uniformly distributed across trajectories. Even after alignment by walking direction, the observed skewness and kurtosis values indicate asymmetric and heavy-tailed distributions, reflecting the presence of occasional but substantial directional deviations.

These findings confirm that trajectories sharing the same origin and destination can differ markedly in geometric structure, reinforcing the idea that OD models represent an intentional macroscopic abstraction rather than a complete description of pedestrian movement. Importantly, the concavity metrics do not imply behavioral preference or optimization, but instead provide a geometric characterization of directional variability that may arise from environmental layout, local constraints, or unobserved interactions.

The analysis of crowd context provides additional insight into the temporal environment in which trajectories occur. Crowd count varies substantially over time, reflecting changing scene occupancy. However, the absence of a strong correlation between trajectory linearity and average crowd size suggests that, at the global scene level considered here, geometric path structure is not directly driven by crowd presence alone. This result highlights the limitations of global crowd measures and suggests that local density and interaction effects—beyond the scope of this thesis—may play a more significant role in shaping pedestrian paths.

Overall, these descriptive results complement the OD modeling framework by characterizing geometric and temporal aspects of pedestrian movement that OD matrices necessarily omit. Although these metrics are not predictive and do not influence model outcomes, they provide contextual understanding that supports future research aimed at integrating demand, geometry, and flow dynamics within a unified modeling framework capable of capturing both demand and flow characteristics.

6.6 Methodological Scope and Limitations

The results presented in this thesis should be interpreted within the deliberate methodological scope adopted. The proposed framework focuses on macroscopic Origin–Destination (OD) modeling and post hoc trajectory characterization, prioritizing interpretability, robustness, and reproducibility over detailed behavioral representation.

A key limitation arises from the macroscopic abstraction of OD models, which capture aggregate demand between spatial zones without predicting route choice or detailed path geometry. While consistent with established OD modeling practice, this abstraction excludes local movement dynamics. Similarly, pedestrian interactions and density effects

are not explicitly modeled; crowd presence is represented only through a global count, providing temporal context without spatial or interaction-level detail.

The framework also does not address dynamic flow evolution. Time-dependent phenomena such as congestion formation, feedback mechanisms, and adaptive behavior are beyond the scope of this work. Trajectory geometry metrics are analyzed descriptively and are not integrated into OD prediction, ensuring conceptual separation but limiting joint demand–geometry modeling. Finally, spatial measurements rely on approximate metric conversion, though the use of normalized and ratio-based indicators mitigates sensitivity to scaling effects.

These limitations reflect conscious design choices rather than methodological shortcomings, enabling a clear and internally consistent modeling framework.

6.7 Implications for Future Pedestrian Flow Modeling

While this thesis focuses on establishing a robust Origin–Destination (OD) modeling foundation, the results naturally point toward several directions for future research. The modular structure of the proposed framework enables extensions that integrate OD demand prediction with additional dimensions of pedestrian movement, including trajectory geometry, pedestrian density, and interaction effects.

Potential developments include the incorporation of density-aware OD models, joint learning approaches that couple demand estimation with path geometry, and the integration of OD prediction with dynamic flow evolution. Extending the framework to support scenario generalization across different spatial layouts, demand levels, and operational conditions represents another important avenue for future investigation.

In this context, it is important to emphasize that the final objective of pedestrian research—though not necessarily of this thesis—is to develop models capable of predicting pedestrian flow dynamics across diverse geometrical and flow conditions. The contributions of this work are therefore best understood as providing a structured and extensible foundation upon which such predictive, geometry-aware flow models may be built in future research.

7 Conclusions

7.1 Research Objectives

This thesis investigated methods for modeling pedestrian Origin–Destination (OD) demand using observed trajectory data. The primary objective was to develop and evaluate macroscopic OD modeling approaches that are robust, interpretable, and compatible with realistic data and modeling constraints. Rather than predicting individual pedestrian paths or interactions, the focus was placed on capturing aggregate movement demand between spatial zones.

A further objective was to compare two fundamentally different modeling philosophies within a unified framework: a stochastic Monte Carlo approach and a data-driven neural network model. Both approaches were evaluated using consistent spatial zoning, normalization, and macroscopic performance metrics. In addition, the thesis explored how trajectory-level geometric and temporal characteristics—such as linearity, concavity, and crowd presence—can provide complementary insight into pedestrian movement without altering OD demand representations.

7.2 Methodological Contributions

The thesis makes several methodological contributions. First, a Monte Carlo OD modeling framework was implemented to reproduce pedestrian demand through stochastic sampling from empirical OD distributions. This approach provides a transparent probabilistic baseline and explicitly represents variability and uncertainty in aggregate flows.

Second, a neural network model was developed to predict destination zones at the trip level by conditioning on origin-related and geometric features. Aggregating predicted destinations yields OD matrices that are directly comparable to those generated by the Monte Carlo model. The use of identical spatial clustering, normalization, and evaluation metrics ensures methodological consistency and enables fair comparison between approaches.

Third, a unified evaluation framework was established to assess both models using macroscopic indicators, including correlation, mean absolute error, Kullback–Leibler divergence, and marginal flow consistency. All evaluations were conducted on held-out test data, ensuring that reported results reflect out-of-sample performance.

Finally, a set of trajectory-level geometric and temporal descriptors was introduced and computed independently from the OD models. These descriptors were used exclusively for post-hoc characterization of movement variability and contextual conditions, maintaining a clear separation between demand modeling and trajectory analysis.

7.3 Main Findings

The results show that both modeling approaches successfully reproduce the macroscopic structure of observed pedestrian OD demand. The Monte Carlo model captures global OD patterns and marginal flows, with stochastic variability that reflects the probabilistic nature of the method. Performance distributions across multiple realizations and bootstrap samples confirm the robustness of the empirical OD structure.

The neural network model achieves higher OD reconstruction accuracy by leveraging conditional information from trip-level features. While predictions are made at the individual-trip level, aggregated outputs remain fully macroscopic, preserving compatibility with OD-based demand modeling. Strong agreement between predicted and observed OD matrices demonstrates the effectiveness of feature-conditioned learning for demand estimation.

Trajectory-level analyses reveal substantial geometric variability even within identical OD pairs. Most trajectories are close to straight-line paths, while a smaller number exhibit pronounced curvature and directional asymmetry. Crowd count analysis indicates no simple relationship between global scene occupancy and trajectory geometry, highlighting the limitations of OD matrices in capturing detailed movement characteristics.

7.4 Implications and Outlook

These findings confirm that macroscopic OD modeling remains a valid and effective abstraction for pedestrian demand estimation. The comparison between stochastic and data-driven approaches illustrates how different modeling philosophies can coexist within a unified framework, each offering complementary strengths in terms of interpretability, uncertainty representation, and accuracy.

By clearly separating OD demand modeling from descriptive trajectory analysis, this thesis emphasizes the value of modular methodological design. OD matrices capture where pedestrians travel, while geometric and temporal descriptors characterize how they move. Treating these components as complementary rather than interchangeable preserves conceptual clarity and avoids overinterpretation.

While the broader objective of pedestrian research is to predict flow dynamics across diverse geometrical and operational scenarios, this thesis deliberately focuses on establishing a robust macroscopic OD modeling foundation. The results provide a clear and extensible basis for future developments toward density-aware, geometry-informed, and dynamically coupled pedestrian flow models.

References

Alahi, A., Goel, K., Ramanathan, V., Robicquet, A., Fei-Fei, L., & Savarese, S. (2016). Social LSTM: Human trajectory prediction in crowded spaces. *Proceedings of the IEEE Conference on Computer Vision and Pattern Recognition*, 961–971. https://doi.org/10.1109/CVPR.2016.110

Ben-Akiva, M., & Bierlaire, M. (2006). Discrete choice models with applications to departure time and route choice. In C. Barnhart & G. Laporte (Eds.), *Handbook of transportation science* (pp. 7–37). Springer. https://doi.org/10.1007/0-306-48058-1_2

Blue, V. J., & Adler, J. L. (2001). Cellular automata microsimulation of bidirectional pedestrian flows. *Transportation Research Record, 1678*(1), 135–141. https://doi.org/10.3141/1678-17

Burstedde, C., Klauck, K., Schadschneider, A., & Zittartz, J. (2001). Simulation of pedestrian dynamics using a two-dimensional cellular automaton. *Physica A: Statistical Mechanics and Its Applications, 295*(3–4), 507–525. https://doi.org/10.1016/S0378-4371(01)00141-8

Cao, S., Fu, L., Wang, P., Zeng, G., & Song, W. (2018). Experimental and modeling study on evacuation under good and limited visibility in a supermarket. Fire Safety Journal, 102, 27–36. https://doi.org/10.1016/j.firesaf.2018.10.003

Daamen, W., Hoogendoorn, S. P., & Bovy, P. H. L. (2003). Passenger route choice planning at large railway stations. *Transportation Research Record, 1854*(1), 25–34. https://doi.org/10.3141/1854-04

Duives, D. C., Daamen, W., & Hoogendoorn, S. P. (2021). State-of-the-art review of pedestrian simulation. *Transportation Research Part C: Emerging Technologies, 131*, 103396. https://doi.org/10.1016/j.trc.2021.103396

Fang, Z., Song, W., Zhang, J., & Wu, H. (2010). Experiment and modeling of exit-selecting behaviors during a building evacuation. *Physica A: Statistical Mechanics and Its Applications, 389*(4), 815–824. https://doi.org/10.1016/j.physa.2009.10.019

Feng, Y., Duives, D. C., & Hoogendoorn, S. P. (2021). Using virtual reality to study pedestrian exit choice behaviour during evacuations. *Safety Science, 137*, 105158. https://doi.org/10.1016/j.ssci.2021.105158

Feng, Y., Duives, D. C., & Hoogendoorn, S. P. (2022). Development and evaluation of a VR research tool to study wayfinding behaviour in a multi-story building. *Safety Science, 147*, 105573. https://doi.org/10.1016/j.ssci.2021.105573

Feng, Y., & Duives, D. C. (2023). Pedestrian wayfinding behavior in a multi-story building: A comprehensive modeling study featuring route choice, wayfinding performance, and observation behavior. *arXiv preprint arXiv:2304.11167*.

Fridolf, K., Ronchi, E., Nilsson, D., & Frantzich, H. (2013). Movement speed and exit choice in smoke-filled rail tunnels. *Fire Safety Journal, 59*, 8–21. https://doi.org/10.1016/j.firesaf.2013.03.007

Gupta, A., Johnson, J., Fei-Fei, L., Savarese, S., & Alahi, A. (2018). Social GAN: Socially acceptable trajectories with generative adversarial networks. *Proceedings of the IEEE Conference on Computer Vision and Pattern Recognition*, 2255–2264. https://doi.org/10.1109/CVPR.2018.00240

Helbing, D., & Molnár, P. (1995). Social force model for pedestrian dynamics. *Physical Review E, 51*(5), 4282–4286. https://doi.org/10.1103/PhysRevE.51.4282

Helbing, D., Farkas, I. J., Molnár, P., & Vicsek, T. (2002). Simulation of pedestrian crowds in normal and evacuation situations. In M. Schreckenberg & S. D. Sharma (Eds.), *Pedestrian and evacuation dynamics* (pp. 21–58). Springer. https://doi.org/10.1007/978-3-642-30904-3_2

Heliövaara, S., Kuusinen, J. M., Rinne, T., Korhonen, T., & Ehtamo, H. (2012). Pedestrian behavior and exit selection in evacuation of a corridor: An experimental study. *Safety Science, 50*(2), 221–227. https://doi.org/10.1016/j.ssci.2011.08.020

Hoogendoorn, S. P., & Bovy, P. H. L. (2004). Pedestrian route-choice and activity scheduling theory and models. *Transportation Research Part B: Methodological, 38*(2), 169–190. https://doi.org/10.1016/S0191-2615(03)00007-9

Hughes, R. L. (2002). A continuum theory for the flow of pedestrians. *Transportation Research Part B: Methodological, 36*(6), 507–535. https://doi.org/10.1016/S0191-2615(01)00015-7

Kobes, M., Helsloot, I., de Vries, B., & Post, J. (2010). Exit choice, (pre-)movement time and (pre-)evacuation behaviour in hotel fire evacuation. *Procedia Engineering, 3*, 37–51. https://doi.org/10.1016/j.proeng.2010.07.006

Korbmacher, J., et al. (2023). A comprehensive survey on pedestrian trajectory prediction. IEEE Transactions on Intelligent Transportation Systems. https://doi.org/10.1109/TITS.2023.3251234

Kuliga, S. F., Nelligan, B., Dalton, R. C., Marchette, S., Shelton, A. L., Carlson, L., & Hölscher, C. (2019). Exploring individual differences and building complexity in wayfinding: The case of the Seattle Central Library. *Environment and Behavior, 51*(5), 622–665. https://doi.org/10.1177/0013916519836149

Kullback, S., & Leibler, R. A. (1951). On information and sufficiency. *The Annals of Mathematical Statistics*, 22(1), 79–86. https://doi.org/10.1214/aoms/1177729694

Li, H., Thrash, T., Hölscher, C., & Schinazi, V. R. (2019). The effect of crowdedness on human wayfinding and locomotion in a multi-level virtual shopping mall. *Journal of Environmental Psychology, 65*, 101320. https://doi.org/10.1016/j.jenvp.2019.101320

Lin, J., Cao, L., & Li, N. (2019). Assessing the influence of repeated exposures and mental stress on human wayfinding performance in indoor environments using virtual reality

technology. *Advanced Engineering Informatics, 39*, 53–61. https://doi.org/10.1016/j.aei.2018.11.007

Lin, J., Zhu, R., Li, N., & Becerik-Gerber, B. (2020). Do people follow the crowd in building emergency evacuation? A cross-cultural immersive virtual reality-based study. *Advanced Engineering Informatics, 43*, 101040. https://doi.org/10.1016/j.aei.2020.101040

Lovreglio, R., Borri, D., Dell'Olio, L., & Ibeas, A. (2014). A discrete choice model based on random utilities for exit choice in emergency evacuations. *Safety Science, 62*, 418–426. https://doi.org/10.1016/j.ssci.2013.10.004

Vilar, E., Rebelo, F., Noriega, P., Duarte, E., & Mayhorn, C. B. (2014). Effects of competing environmental variables and signage on route choices in simulated everyday and emergency wayfinding situations. Ergonomics, 57(4), 511–524. https://doi.org/10.1080/00140139.2014.895054

Moussaïd, M., Helbing, D., & Theraulaz, G. (2011). How simple rules determine pedestrian behavior and crowd disasters. *Proceedings of the National Academy of Sciences, 108*(17), 6884–6888. https://doi.org/10.1073/pnas.1016507108

Nishino, T., Hanaoka, S., & Osawa, Y. (2015). Estimation of pedestrian origin–destination demand in train stations. https://www.researchgate.net/publication/279827711_Estimation_of_Pedestrian_Origin-Destination_Demand_in_Train_Stations

Robin, T., Antonini, G., Bierlaire, M., & Cruz, J. (2009). Specification, estimation and validation of a pedestrian walking behavior model. Transportation Research Part B, 43(1), 36–56. https://doi.org/10.1016/j.trb.2008.06.008

Rudenko, A., Palmieri, L., Herman, M., Kitani, K. M., Gavrila, D. M., & Arras, K. O. (2019). Human motion trajectory prediction: A survey. *The International Journal of Robotics Research, 39*(8), 895–935.https://doi.org/10.1177/0278364919857034

Tzeng, S.-Y., & Huang, J.-S. (2009). Spatial forms and signage in wayfinding decision points for hospital outpatient services. *Journal of Asian Architecture and Building Engineering, 8*(2), 453–460. https://doi.org/10.3130/jaabe.8.453

Vilar, E., Rebelo, F., Noriega, P., Duarte, E., & Mayhorn, C. B. (2014). Effects of competing environmental variables and signage on route choices in simulated everyday and emergency wayfinding situations. *Ergonomics, 57*(4), 511–524. https://doi.org/10.1080/00140139.2014.895054

von Sivers, I., Köster, G., Holl, S., & Schadschneider, A. (2014). Dynamic assignment in microscopic pedestrian simulations.Open-access PDF (arXiv preprint): https://arxiv.org/abs/1401.1308

Wang, K., Shi, X., Goh, A. P. X., & Qian, S. (2019). A machine learning based study on pedestrian movement dynamics under emergency evacuation. *Fire Safety Journal, 106*, 163–176. https://doi.org/10.1016/j.firesaf.2019.04.008

Zaier, M., Wannous, H., Drira, H., & Boonaert, J. (2025). Pedestrian trajectory prediction: A literature review and current trends. Neural Computing and Applications.

Zhao, X., Lovreglio, R., & Nilsson, D. (2020). Modelling and interpreting pre-evacuation decision-making using machine learning. *Automation in Construction, 113*, 103140. https://doi.org/10.1016/j.autcon.2020.103140